FEDERAL UNIVERSITY OF CEARA

CENTER OF SCIENCES

DEPARTMENT OF BIOCHEMISTRY AND MOLECULAR BIOLOGY

POST-GRADUATE PROGRAM IN BIOCHEMISTRY

HUMAIRA BAHADAR

ROLES OF BLUE LIGHT AND NADPH-DEPENDENT THIOREDOXIN REDUCTASE C FOR THE REGULATION OF GUARD CELL AND SINK LEAF METABOLISMS

FORTALEZA

2024

HUMAIRA BAHADAR

ROLES OF BLUE LIGHT AND NADPH-DEPENDENT THIOREDOXIN REDUCTASE C FOR THE REGULATION OF GUARD CELL AND SINK LEAF METABOLISMS

Thesis presented to the graduate program in Biochemistry of the Federal University of Ceara, as a partial requirement to obtain the title of the doctorate in Biochemistry. Concentration area: Molecular Biology.

Advisor: Prof. Dr. Danilo de Menezes Daloso.

FORTALEZA

2024

HUMAIRA BAHADAR

ROLES OF BLUE LIGHT AND NADPH-DEPENDENT THIOREDOXIN REDUCTASE C
FOR THE REGULATION OF GUARD CELL AND SINK LEAF METABOLISMS

Thesis presented to the graduate program in Biochemistry of the Federal University of Ceara, as a partial requirement to obtain the title of the doctorate in Biochemistry. Concentration area: Molecular Biology.

Approved on: 24/05/2024.

EXAMINATION BOARD

_____
Prof. Dr. Danilo de Menezes Daloso (Advisor)

Federal University of Ceara (UFC)

_____
Prof. Dr. Humberto Henrique de Carvalho

Federal University of Ceara (UFC)

_____
Prof. Dr. Marcio de Oliveira Martins

Federal University of Ceara (UFC)

_____
Dra. Valéria Freitas Lima

Federal University of Viçosa (UFV)

_____
Dra. Priscila Ariane Auler

University of São Paulo (SP)

ACKNOWLEDGMENTS

ABSTRACT

The primary metabolism is essential for plant acclimation to diverse environment conditions and involves intricate networks of biochemical pathways and regulatory mechanisms. The complexity of plant metabolism is further enhanced by the compartmentalization within plant cells and by the fact that the primary metabolism ranges substantially among cell, tissue and organ types as well as because it is highly responsive to environmental conditions, such as light and stress conditions. Recent evidence suggests that the NADPH-dependent thioredoxin reductase C (NTRC) is important for the regulation of sink leaf metabolism as well as that starch breakdown is important during the blue light (BL)-induced stomatal opening. However, the underlying mechanisms behind these responses remain unclear. Taking this into account, this PhD thesis was performed to investigate (i) the effect of the lack of the NTRC on the regulation of source and sink Arabidopsis leaf metabolism under water deficit (WD) and (ii) the role of BL for the regulation of guard cell metabolism in tobacco and cowpea. Our findings collectively demonstrated that mild WD worsens the deleterious impacts of the NTRC deficiency in Arabidopsis sink leaves, which was associated to an increased lipid peroxidation, decreased catalase activity, decreased biomass accumulation over time and stronger metabolic alterations in in sink rather than source *ntrc* leaves. We further showed that the BL-induced stomatal opening is associated to changes in primary metabolism but not to starch degradation in both cowpea and tobacco guard cells. This thesis provides important information that improve our understanding on the regulation of plant metabolism in its diverse modules, from source to sink leaves and within guard cells, highlighting that the regulation of plant metabolism is species-specific and time and scale-dependent.

Keywords: metabolic regulation; thioredoxins; NADPH-dependent thioredoxin reductases; water deficit; primary metabolism; Blue light; guard cells.

RESUMO

O metabolismo primário é essencial para a aclimatação de plantas a diversas condições ambientais e envolve redes intrincadas de vias bioquímicas e mecanismos regulatórios. A complexidade do metabolismo vegetal é ainda reforçada pela compartimentalização dentro das células vegetais e pelo fato de o metabolismo primário variar substancialmente entre tipos de células, tecidos e órgãos, bem como porque é altamente responsivo às condições ambientais, tais como condições de luz e estresse. Evidências recentes sugerem que a enzima tiorredoxina redutase C dependente de NADPH (NTRC) é importante para a regulação do metabolismo de folhas dreno, bem como que a quebra do amido é importante durante a abertura estomática induzida pela luz azul. No entanto, os mecanismos subjacentes a estas respostas permanecem obscuros. Levando isso em consideração, esta tese de doutorado foi realizada para investigar (i) o efeito da falta de NTRC na regulação do metabolismo de folhas fonte e dreno de Arabidopsis sob déficit hídrico e (ii) o papel da luz azul na regulação do metabolismo das células guarda de tabaco e feijão-caupi. Nossos resultados demonstraram que o déficit hídrico moderado exacerbou os efeitos deletérios da deficiência de NTRC nas folhas dreno de Arabidopsis, que foi associada a um aumento da peroxidação lipídica, diminuição da atividade da catalase, diminuição do acúmulo de biomassa ao longo do tempo e alterações metabólicas mais fortes nestas folhas. Nossos resultados demonstraram ainda que a abertura estomática induzida por luz azul está associada a alterações no metabolismo primário, mas não à degradação do amido das células guarda de feijão-caupi e tabaco. Esta tese fornece informações importantes que melhoram a nossa compreensão sobre a regulação do metabolismo vegetal nos seus diversos módulos, desde folhas fonte e dreno até as células guarda, destacando que a regulação do metabolismo vegetal é específica de cada espécie e dependente do tempo e da escala.

Palavras-chave: regulação metabólica; tioredoxinas; tioredoxina redutases dependentes de NADPH; déficit hídrico; metabolismo primário; Luz azul; células de guarda.

LIST OF FIGURES

LIST OF TABLES

LIST OF ABBREVIATIONS

TCA	Tricarboxylic acid cycle
NTRC	NADPH-dependent thioredoxin reductase C
ROS	Reactive oxygen species
TRX	Thioredoxins
CBC	Calvin-Benson-Bassham Cycle
WW	Well-watered
WD	Water-deficit
NPQ	Non-photochemical quenching
RWC	Relative water content
GC-MS	Gas chromatography mass spectrometry
Y (II)	Effective quantum yield of photosystem II
1-qL	Plastoquinone pool
Fv/Fm	Maximum quantum efficiency of PSII
TBARS	Thiobarbituric acid reactive substances
APX	Ascorbate Peroxidase
CAT	Catalase
SOD	Superoxide dismutase
PLS-DA	Partial least square-discriminant analysis
PCA	Principal component analysis
BL	Blue light
VIP	Variable importance in projection

CONTENTS

1. General introduction

Plants, although sessile organisms, have great capabilities to avoid or acclimate to surrounding unfavorable conditions. This is achieved by the activation of protective and adaptive resistance mechanisms. In this context, plants produce a wide range of metabolites, estimated to be between 100,000 and 1 million per plant, which play a crucial role in their resistance and tolerance against (a)biotic stresses (AFENDI; ONO; NAKAMURA; NAKAMURA *et al.*, 2013; DIXON, 2003; RAI; SAITO; YAMAZAKI, 2017; SIN'KEVICH; SELIVANOV; ANTIPINA; KROPOCHEVA *et al.*, 2016; WENG, 2014). Evidence suggests that the metabolic variation in plant species is much bigger than previously considered, both at quantitative and qualitative levels (LI; GAQUEREL, 2021; TSUGAWA; NAKABAYASHI; MORI; YAMADA *et al.*, 2019). This highlights how diverse is plant metabolism and how complex is to study and understand the regulation of plant metabolomics. The metabolome is a collective term for the endogenous and exogenous (xenobiotics) molecules carried by an organism. Endogenous metabolites has further been divided into primary/central and secondary/specialized metabolisms (ERB; KLIEBENSTEIN, 2020). Central metabolism is composed by glycolysis, the tricarboxylic acid (TCA) cycle, oxidative pentose phosphate pathway (oxPPP) among others. These pathways are involved in the main physiological activities such as the absorption and processing of the environmental resources. They comprise of a series of chemical reactions involving hexoses, organic acids and amino acids for the production of energy as ATP, carbon precursors for many compounds and reducing power such as NAD(H)/NAD(P)H (SMITH; SCHWARZLÄNDER; RATCLIFFE; KRUGER, 2021). Similarly, plant development is ruled by the interaction between phytohormones and the central metabolism via important processes such as photosynthesis, photorespiration and respiration (ARAUJO; NUNES-NESI; NIKOLOSKI; SWEETLOVE *et al.*, 2012; FERNIE; CARRARI; SWEETLOVE, 2004; PLAXTON, 1996). On the other hand, secondary metabolism accomplishes a multitude of tasks necessary for the growth and development of the plant, of which the interaction with the environment is of prime importance (SAITO; YONEKURA-SAKAKIBARA; NAKABAYASHI; HIGASHI *et al.*, 2013). Secondary metabolism is responsible for the production of an overwhelming range of high molecular weight organic molecules known as secondary metabolites having distinctive and complicated structure (KROYMANN, 2011; VERPOORTE; VAN DER HEIJDEN; MEMELINK, 2000). Primary

metabolites are common to all the plants and are essential for the growth and survival of the plant. Conversely, secondary metabolites are not necessary for the viability but contribute to the fitness of the plant (KERRIGAN, 1999).
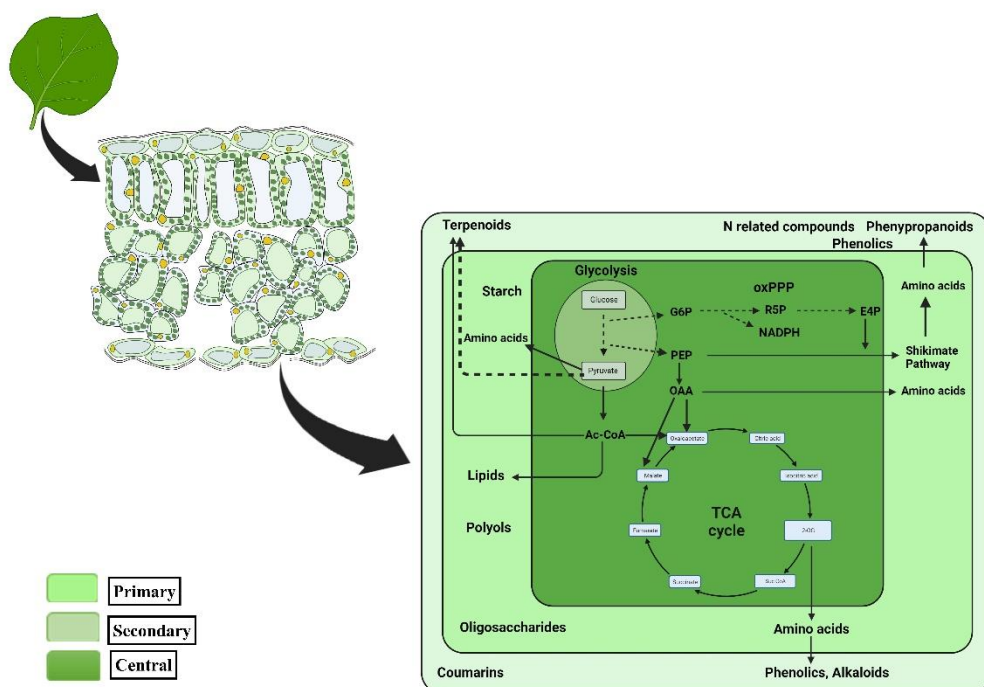
Figure 1. Simple schematics of the complex plant metabolome and the interconnection among central, primary and secondary metabolism via various biomolecules. Adapted from (Dussarrat, 2022). G6P: glucose 6 phosphate, Ac-CoA: acetyl-CoA, OAA: oxaloacetic acid, E4P: erythrose 4 phosphate, oxPPP: oxidative pentose phosphate pathway, NADPH: nicotinamide adenine dinucleotide phosphate, TCA cycle: tricarboxylic acid cycle, PEP: phosphoenol pyruvate, SucCoA: succinyl-CoA, R5P: ribulose 5 phosphate, 2 OG: 2-oxoglutarate.

1.1 On the complexity of plant metabolism

Compartmentation of metabolic reactions and other cellular activities in different organelles is a prominent feature of eukaryotic cells, but it assumes a higher degree of complexity in plant cells given the presence of cell wall, vacuoles and plastids as well as high number of isoforms and the presence of unique metabolic pathways (AP REES, 1987; SWEETLOVE; FERNIE, 2013). This compartmentation separates different enzymes and isoforms that follows different modes of regulation. Despite this division, it is noteworthy that plant metabolism operates

as a highly integrated network (SWEETLOVE; FERNIE, 2005). Thus, the organelle specific metabolism is still dependent, to lesser or greater extent, on the energy or precursor supply from other organelles. Beyond that, plant metabolism is highly dynamic and change strongly during the daily light and dark transitions (FARRÉ; WEISE, 2012; GRAF; SCHLERETH; STITT; SMITH, 2010). This awareness of time applies to both daily fluctuations and annual transitions. The synchronization between the circadian clock and environmental cycles has a prominent effect on the development of the plants such as growth, stomatal regulation and flowering control (CR, 2008; DODD; SALATHIA; HALL; KÉVEI *et al.*, 2005; GRAF; SCHLERETH; STITT; SMITH, 2010; YERUSHALMI; YAKIR; GREEN, 2011). Taken together, these characteristics make the comprehension on the regulation of plant metabolism difficult, requiring complex experimental procedures and techniques to analyze and interpret metabolic results.

One of the key feature of living organisms is their capacity to convert chemical substances and energy via various metabolic reactions and transport mechanisms (SCHWENDER; OHLROGGE; SHACHAR-HILL, 2004). Plants exhibit a complex metabolic network due to their genetic diversity and their constant exposure to a dynamic and stressful environment. The development and viability of plants relies on their ability to fine tune their metabolism serving as a buffer between the oscillating metabolic inputs and strong developmental outcomes (SWEETLOVE; RATCLIFFE, 2011). Plants possess a highly fluctuating flux through the pathways of primary metabolism due to internal requirements as well as external environmental modifications. This flexibility is achieved by constant regulation at various levels such as transporter, different regulatory proteins and enzymes which further varies among cells, tissue, developmental stage and the metabolic status (DALOSO; MORAIS; OLIVEIRA E SILVA; WILLIAMS, 2023). The metabolic regulation may be short term, achieved by allosteric modifications of a protein, alteration in protein-protein interaction and posttranslational modifications, or can be long term regulation which is obtained through *de novo* gene expression regulation at transcriptional and translation levels or at epigenetic level (BALPARDA; BOUZID; MARTINEZ; ZHENG *et al.*, 2023; FEDORIN; EPRINTSEV; IGAMBERDIEV, 2024).
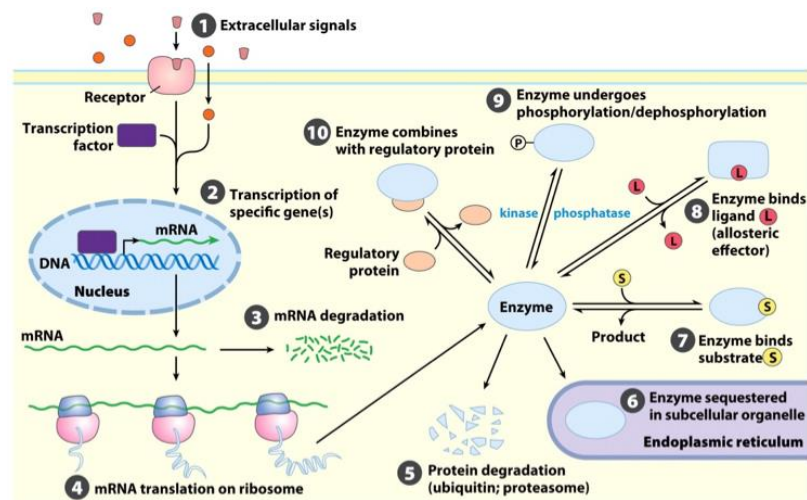
Figure 2. Schematic illustration of several factors regulating the activity of an enzyme. (Nelson and Cox).

1.2 Thioredoxin-mediated regulation of plant metabolism

Plants being aerobic organisms require oxygen for their existence. Conversely, this utilization of oxygen can generates reactive oxygen species (ROS), such as hydrogen radical, hydrogen peroxide and superoxide anion via the processes of mitochondrial respiration, photosynthesis and photorespiration, especially under stress conditions (DECROS; BALDET; BEAUVOIT; STEVENS *et al.*, 2019; RINALDUCCI; MURGIANO; ZOLLA, 2008). Photosynthesis involves the electron transfer in the presence of oxygen hence resulting in the ROS generation which can leads to oxidative damage to organic molecules and organelles/cells. Consequently, photosynthetic efficiency is intricately connected to the antioxidant and redox systems which regulate the balance of ROS in the cell. Plant growth is negatively affected by the oxidative stress arising from the imbalance between ROS production and scavenging due to different environmental stresses (ZANDALINAS; FICHMAN; DEVIREDDY; SENGUPTA *et al.*, 2020). Redox regulation is thus vital for various metabolic processes occurring in multiple subcellular compartments. Plants possess a unique redox system enabling them to quickly respond to the variations in environmental stimuli (GEIGENBERGER; FERNIE, 2014; GEIGENBERGER; THORMÄHLEN; DALOSO; FERNIE, 2017). Plants possess a number of redox regulation such as S-glutathioylation, sulfuxidation, S-nitrosylation and disulfide bond formation. There are two classes of oxidoreductases known as thioredoxins (TRXs) and Glutaredoxin (GRXs) facilitating these post-translation modifications (MICHELET; ZAFFAGNINI; MORISSE; SPARLA *et al.*, 2013).

A group of researchers found a subset of enzymes from the Calvin-Benson-Bassham Cycle (CBC) to be activated by the light which led to the discovery of the ferredoxin-thioredoxin (Fdx-TRX) system involved in the regulation of the photosynthetic electron transport. The Fdx has a close collaboration with a group of TRXs which are further divided into many classes on the basis of their primary structure including TRX f, h, m, o, x, y and z (MEYER; REICHHELD; VIGNOLS, 2005; MEYER; SIALA; BASHANDY; RIONDET *et al.*, 2008) performing different functions in different subcellular locations. The NTR-TRX system is another system transducing redox signals in various cellular compartments. In plants, three types of NTR proteins have been identified, namely NTR A, B and C (REICHHELD; MEYER; KHAFIF; BONNARD *et al.*, 2005). Additionally, plants have proteins named nucleoredoxins (NRX), composed of two or three consecutive repeats of TRX-like domains fused to a Cys-rich C-terminal domain. In *Zea mays* and *Arabidopsis*, different isoforms of NRX exhibit dual localization of nucleus and cytosol. In *Arabidopsis*, both NRX1 & 2 demonstrate disulfide reduction activities. Besides, NRX1 plays an important role in plant fertility and immunity responses.

NTRA and NTRB have been found in cytosol, mitochondria and nucleus (KNEESHAW; KEYANI; DELORME-HINOUX; IMRIE *et al.*, 2017; LAUGHNER; SEHNKE; FERL, 1998; MARCHAL; DELORME-HINOUX; BARIAT; SIALA *et al.*, 2014; REICHHELD; MEYER; KHAFIF; BONNARD *et al.*, 2005; SERRATO; PÉREZ-RUIZ; SPÍNOLA; CEJUDO, 2004). The NTRA and NTRB share 82% sequence similarity and reduce many TRXs by using NADPH. Also, these proteins confer resistance to the plants against oxidative, UV and drought stresses (BASHANDY; TACONNAT; RENOU; MEYER *et al.*, 2009; CHA; KIM; JUNG; KIM *et al.*, 2014; REICHHELD; KHAFIF; RIONDET; DROUX *et al.*, 2007; TROTTER; GRANT, 2005). The NTRC is localized to the chloroplasts and plastids and is the unique NTR having both NTR and TRX domains in a single polypeptide, which fine-tune several target proteins through disulfide linking at the expense of NADPH (GEIGENBERGER; THORMÄHLEN; DALOSO; FERNIE, 2017; SERRATO; PÉREZ-RUIZ; SPÍNOLA; CEJUDO, 2004; SPÍNOLA; PÉREZ-RUIZ; PULIDO; KIRCHSTEIGER *et al.*, 2008). Examples of NTRC-regulated enzymes include 2-Cys peroxiredoxin (2-Cys Prxs), ADP-Glc pyrophosphorylase (AGPase) and several enzymes of the Calvin-Benson-Bassham cycle. Furthermore, crosstalk between NTRC and Fdx-TRX system

enhances plant photosynthesis by i) helping the plant to lose excess light energy via non-photochemical quenching (NPQ), ii) regulation of Calvin-Benson Cycle (CBC) enzymes and iii) synthesis of ATP, chlorophyll and auxin (CARRILLO; FROEHLICH; CRUZ; SAVAGE *et al.*, 2016; KIRCHSTEIGER; PULIDO; GONZÁLEZ; CEJUDO, 2009; LEPISTÖ; PAKULA; TOIVOLA; KRIEGER-LISZKAY *et al.*, 2013; NARANJO; DIAZ-ESPEJO; LINDAHL; CEJUDO, 2016; NIKKANEN; TOIVOLA; RINTAMÄKI, 2016; PÉREZ-RUIZ; CEJUDO, 2009; RICHTER; PETER; ROTHBART; SCHLICKE *et al.*, 2013; THORMÄHLEN; ZUPOK; RESCHER; LEGER *et al.*, 2017; YOSHIDA; HISABORI, 2016).

The NTRC is involved in the acclimation of plants to high CO_2 as *ntrc* mutant exhibits a small diameter and lesser number of leaves when grown under high CO_2. This mutant also has a higher Gly/Ser ratio in sink leaves as compared to their source leaves, which is a good indicative of high photorespiration rate in these leaves, which might be associated to a higher level of stress in sink leaves of the *ntrc* mutant (SOUZA; HOU; SUN; POEKER *et al.*, 2023; TIMM; FLORIAN; ARRIVAULT; STITT *et al.*, 2012). This idea is further supported by the fact that *ntrc* mutant did not acclimate to high CO_2 due to a compromised photosynthetic activity and an elevated levels of the metabolites from the stress-related pathways such as His, Arg, Asn and branched chain amino acids in their sink leaves. These findings highlights the potential significance of NTRC protein in playing a role in the acclimation of plants amid the contemporary climate change scenario (SOUZA; HOU; SUN; POEKER *et al.*, 2023). Moreover, NTRC is involved in the metabolism of carbohydrates and organic acids and in sustaining the NAD(P)(H) redox state of the tomato fruit, indicating that the role of NTRC is not limited to source leaves but may include sink tissues (HOU; LEHMANN; GEIGENBERGER, 2021; MICHALSKA; ZAUBER; BUCHANAN; CEJUDO *et al.*, 2009). Although the role of source leaves driving plant growth and plant yield is largely documented, recent studies highlight that plant growth is mutually governed by both source and sink leaves (BURNETT; ROGERS; REES; OSBORNE, 2016; FERNIE; BACHEM; HELARIUTTA; NEUHAUS *et al.*, 2020; FETTKE; FERNIE, 2015; KAMBHAMPATI; AJEWOLE; MARSOLAIS, 2018; LEA; SODEK; PARRY; SHEWRY *et al.*, 2007; MODDE; TIMM; FLORIAN; MICHL *et al.*, 2017; TA; JOY, 1986). Therefore, understanding how the metabolism of sink leaves is regulated is important to improve plant yield.

1.3 Particularities of the guard cell metabolism

The adaptation of plants to terrestrial environment, where water is not much abundant, was made possible by the evolution of stomata. Stomata are adjustable microscopic apertures on the surface of leaves (EDWARDS; KERP; HASS, 1998). A single stomata is composed of two kidney or dumbbell shaped guard cells capable of regulating the pore size due to the changes in their volume, thereby allowing the uptake of CO_2 and the loss of water from the plant simultaneously. The gas exchange through stomata is crucial for photosynthesis and transpiration consequently governing plant water use efficiency (WUE) and plant yield (LAWSON; BLATT, 2014). The anatomy of the stomatal valve is simple but the surrounding guard cells are highly specialized due to the presence of high transport capacity for ions, complex signal transduction networks and metabolic pathways that seems to be differentially regulated as compared to the surrounding epidermal and mesophyll cells (DALOSO; MORAIS; OLIVEIRA E SILVA; WILLIAMS, 2023; DAUBERMANN; LIMA; ERBAN; KOPKA *et al.*, 2024). Collectively, all these features contribute to the changes in guard cell turgor in response to internal and external stimuli, regulating the stomatal movements in a time scale from seconds to hours (ASSMANN; WANG, 2001).

In 1856, Hugo von Mohl suggested that changes in the turgor were responsible for the osmolytic regulation of guard cells. He put forward the hypothesis according to which the photosynthesis within the guard cells was a source for the osmolytes regulating the stomatal movements via turgor. With the advent of 20th century, Lloyd further elaborated this by presenting the starch-sugar theory. According to this theory, starch granules are present at night in the guard cells which are mobilized at dawn to produce sugars required for the increased osmotic potential, while the sugars are condensed back to starch at the dusk (LLOYD, 1908; MOHL, 1856). During the following years, starch-sugar theory went into the background due to the emergence of the ion theory, reporting the surge up of the potassium (K^+) ion during stomatal opening which was coupled to the high osmolarity (HUMBLE; RASCHKE, 1971). Further studies in this line confirmed Cl^- ion as the counter ion to compensate the positive charge of the K^+ accumulation. However, further analysis suggests the presence of an additional anion rather than solely Cl^-. Malate, besides Cl- was then suggested as the organic anion to equilibrate the K^+ accumulation (OUTLAW JR; LOWRY, 1977; RASCHKE; SCHNABL, 1978). Several researchers proposed that

the source for malate is the starch present in the guard cells which is degraded to synthesize malate hence building up the required turgor for stomatal opening (OUTLAW JR; MANCHESTER, 1979; VAVASSEUR; RAGHAVENDRA, 2005).

Guard cells chloroplasts are few in number with less developed thylakoids and loose stacking of the grana. Despite of all these limitations, functional photosystem I and II, linear electron transport, O_2 release and phosphorylation have been reported. Due to the existence of the photosynthetic machinery, there is consensus that photosynthesis takes place in guard cells (LAWSON; OXBOROUGH; MORISON; BAKER, 2003; OUTLAW JR; MAYNE; ZENGER; MANCHESTER, 1981; TSIONSKY; CARDON; BARD; JACKSON, 1997; WILLMER; FRICKER, 1996). Stomata are responsive to blue and red light. Red light activates stomatal opening through photosynthesis in the chloroplast of mesophyll and guard cells while both blue and red light serves as a signal for stomatal movements through activation of H+-ATPase at the guard cell plasma membrane (ANDO; KINOSHITA, 2018; KINOSHITA; DOI; SUETSUGU; KAGAWA *et al.*, 2001). Plasma membrane associated photoreceptors, called phototropins (PHOT), are highly expressed in guard cells, the major receptors of the blue light and activated via auto-phosphorylation. Blue light activates plasma membrane H+ ATPase in the guard cells which drives K^+ influx and consequently the stomatal opening (ASSMANN; SIMONCINI; SCHROEDER, 1985; INOUE; KINOSHITA; MATSUMOTO; NAKAYAMA *et al.*, 2008; SHIMAZAKI; IINO; ZEIGER, 1986).

Although the signaling pathway triggered by blue light has been revealed in the last decades, the metabolic changes triggered by this stimulus remain unclear. In this context, it has been hypothesized that the carbon skeleton needed for generating energy and/or for malate and sugar accumulation during blue-light induced stomatal opening is derived from the breakdown of starch within guard cells . This idea comes from experiments using the double mutant of the α-amylase 3 (AMY3) and β-amylase 1 (BAM1) in *Arabidopsis,* which show inhibition of the starch degradation in guard cells and a compromised stomatal opening. These results emphasize that starch mobilization upon light perception plays an important role for rapid and efficient stomatal opening (FLÜTSCH; WANG; TAKEMIYA; VIALET-CHABRAND *et al.*, 2020; HORRER; FLÜTSCH; PAZMINO; MATTHEWS *et al.*, 2016). However, the fate of the carbons derived from starch breakdown within guard cells is still uncertain.

In summary, it is clear that the metabolism in source and sink tissues and its understanding is a field of great interest, given that it can provide new avenues to improve crop yield and introduce new varieties resistant to environmental stresses. Similarly, the comprehension of the metabolism-mediated mechanisms of stomatal movement regulation is another milestone, yet to be achieved. Considering these aspects, we aim to improve our understanding on the role of NTRC in the regulation of primary metabolism in source and sink leaves as well as the metabolic aspects underpinning the regulation of the light-induced stomatal opening. The first chapter of this thesis is based on the experiments conducted using *Arabidopsis* WT and the *ntrc* mutant under drought stress, whilst the second chapter is based on experiments using isolated guard cells to investigate the effect of the blue light on the stomatal aperture and primary metabolism.

2. Hypotheses

1) *Arabidopsis* water deficit acclimation involves a NTRC-mediated regulation of both source and sink leaf metabolisms.

2) The blue light-induced starch breakdown induces a reprograming of primary metabolism in tobacco and cowpea guard cells, providing substrates for the osmotic and energetic regulation of stomatal opening.

3. Objectives

3.1 General:

3.1.1 To investigate the role of NTRC in the regulation of the metabolism of source and sink leaves in *Arabidopsis thaliana* under water deficit stress.

3.1.2 To analyze the dynamic of guard cell primary metabolism during the blue light-induced stomatal opening.

3.2 Specific: 3.2.1

i)   To compare the metabolic changes in source and sink leaves of WT and *ntrc* mutant of *Arabidopsis thaliana* L. under irrigated and water deficit stress conditions;

ii)   To analyse the level of stress-related markers such as the relative water content; TBARS and activity of antioxidant enzymes in source and sink leaves from WT and *ntrc* mutant under irrigated and water deficit stress conditions;

iii) To investigate the photosynthetic performance of source and sink leaves from WT and *ntrc* mutant under irrigated and water deficit stress conditions.

3.2.2

i)   To measure the stomatal aperture under blue light illumination via light microscopy;

ii) To quantify and compare the amount of degraded starch in the guard cell enriched epidermal fragments;

iii) To analyse the metabolite profiling of guard cell enriched epidermal fragments via GC-MS;

iv) To correlate stomatal aperture and metabolite measurements.

4. CHAPTER 1:

Manuscript not submitted

Plant growth and acclimation to water deficit depends on a NTRC-mediated regulation of sink leaf metabolism

Humaira Bahadar[1], Paulo V.L. Souza[1], Murilo S. Alves[1], Joaquim Albenisio G. Silveira[1], Danilo M. Daloso[1*]

[1]LabPlant, Departamento de Bioquímica e Biologia Molecular, Universidade Federal do Ceará, Fortaleza 60451-970, Brasil.

* Correspondent author: daloso@ufc.br

Abstract

Plant metabolism diverge substantially between source and sink organs. However, little attention has been given to sink leaves, that co-limit plant growth with source leaves. Recent evidence demonstrated that plants lacking the NADPH-dependent thioredoxin reductase C (NTRC) have stronger photosynthetic and metabolic alterations in sink than source leaves. This suggests that the regulation of photosynthesis and metabolism of sink leaves is mediated by NTRC. Here, we aimed to obtain further insights on how NTRC regulates sink leaf metabolism and how this influence water deficit (WD) acclimation. 8-week-old Arabidopsis wild type (WT) and the *ntrc* mutant were subjected to well-watered (WW) and a mild WD for 0, 5 and 11 days. Source and sink leaves were separately evaluated at biochemical, metabolic and physiological levels. Our results collectively demonstrated that WD exacerbates the deleterious effects of the lack of NTRC in Arabidopsis sink leaves. This is evidenced by the higher lipid peroxidation and lower catalase activity, which culminates in a lack of increase in sink leaf biomass over the period under WD. Source leaf growth was the most affected by WD, while no difference in the biomass was observed between WW and WD sink leaves in WT plants. This leads to an increased percentage of sink leaves in WT under WD. Metabolite profiling results indicate that sink *ntrc* leaves were the most affected by WD imposition, which was associated to strong alterations in the level of certain sugars, organic acids and amino acids, especially fructose, beta-alanine, and asparagine. Our results collectively highlight that plant growth is co-limited by sink leaves, especially under WD, and that NTRC plays an important role to maintain the homeostasis between carbon and nitrogen metabolisms as well as the photochemical performance of sink leaves.

Keywords: Metabolic regulation, redox metabolism, sink leaves, source leaves, thioredoxin reductases.

4.1 Introduction

Plants are sessile organisms and thus frequently subjected to different types of biotic and abiotic stress conditions (GULL; LONE; WANI, 2019; SHABBIR; SINGHAL; MISHRA; CHAUHAN *et al.*, 2022). Stress periods in general disturb plant metabolic homeostasis and trigger plant stress responses to eliminate toxic products such as the excess of reactive oxygen species (ROS) produced (FOYER; NOCTOR, 2012; ZANDALINAS; FICHMAN; DEVIREDDY; SENGUPTA *et al.*, 2020). The ability of the plant to acclimate to such perturbations and achieve a new metabolic homeostasis is determinant to maintain growth and development under unfavourable conditions (RIVERO; MITTLER; BLUMWALD; ZANDALINAS, 2022). Discovering the genetic and metabolic mechanisms underpinning plant stress acclimation is thus of great interest and of paramount importance given the current climate change scenario. In this context, plants have a highly complex and spatially distributed redox system, which aid them to quickly respond to suboptimal environmental conditions and avoid oxidative stress caused by the overaccumulation of ROS (CLAEYS; INZÉ, 2013; GEIGENBERGER; THORMÄHLEN; DALOSO; FERNIE, 2017; MHAMDI; VAN BREUSEGEM, 2018).

It is well established that drought and other abiotic stress conditions culminate in oxidative stress in plant tissues, which is due in part to imbalances in the cellular redox homeostasis (XIE; ZHENG; ZHOU; KANWAR *et al.*, 2022). Beyond their role as oxidative stressors, ROS are important oxidants that regulate gene expression and enzyme activity through post-translational regulation of proteins and transcription factors (FOYER; BAKER; WRIGHT; SPARKES *et al.*, 2020). The role of ROS as oxidant of proteins is counter-balanced by redoxins. For instance, plants have several thioredoxins (TRXs) isoforms, small ubiquitous proteins that regulate the redox status of several enzymes and thus participate in the regulation of redox metabolism in different cell compartments (DA FONSECA-PEREIRA; SOUZA; FERNIE; TIMM *et al.*, 2021). TRXs reduce disulfide bonds formed between two reactive cysteines in the target proteins using reducing power from TRX reductases, which in turn use NADPH (NTR) or reduced ferredoxin (FTR) as electron donors (KÖNIG; MUTHURAMALINGAM; DIETZ, 2012; LÁZARO; JIMÉNEZ; CAMEJO; IGLESIAS-BAENA *et al.*, 2013; MEYER; BUCHANAN; VIGNOLS; REICHHELD, 2009; NOCTOR; MHAMDI; FOYER, 2014).

Whilst the FTR system is restricted to the chloroplasts, plants have three NTR isoforms distributed in different cell compartments. NTRC is located exclusively to the chloroplast, while both NTRs A and B have been found in cytosol, mitochondria and nucleus (LALOI; RAYAPURAM; CHARTIER; GRIENENBERGER *et al.*, 2001; REICHHELD; KHAFIF; RIONDET; DROUX *et al.*, 2007; REICHHELD; MEYER; KHAFIF; BONNARD *et al.*, 2005; RICHTER; PÉREZ-RUIZ; CEJUDO; GRIMM, 2018). These NTRs are encoded by different genes in *Arabidopsis thaliana.* Beyond been the only plastidial NTR, the NTRC is the unique that contains a TRX domain in its structure, which makes this isoform the only NTR to have both reductase and redoxin activities (LALOI; RAYAPURAM; CHARTIER; GRIENENBERGER *et al.*, 2001; REICHHELD; MEYER; KHAFIF; BONNARD *et al.*, 2005; SERRATO; PÉREZ-RUIZ; SPÍNOLA; CEJUDO, 2004). The presence of these NTR proteins in different subcellular compartments makes the NTR/TRX system an important redox regulator of several TRX target proteins in the respective organelles. It has been shown that several physiological process such as photosynthesis and starch synthesis in the chloroplast and photorespiration and respiration outside the chloroplast are directly or indirectly regulated by the NTR/TRX system (CEJUDO; GONZÁLEZ; PÉREZ-RUIZ, 2021; MARTÍ; JIMÉNEZ; SEVILLA, 2020). Thus, beyond its role to the regulation of redox metabolism, the NTR/TRX systems is important for the regulation of primary metabolism.

NTRC has been described as an important protein for the regulation of enzymes related to the Calvin-Benson-Bassham cycle and proteins from the photochemical reactions in the chloroplast (HOU; EHRLICH; THORMÄHLEN; LEHMANN *et al.*, 2019; TEH; LEITZ; HOLZER; NEUSIUS *et al.*, 2023; YOSHIDA; HISABORI, 2016). Therefore, the function of NTRC has been mainly attributed to the regulation of leaf photosynthesis. In fact, plants lacking NTRC has severe deleterious effects on the photosynthetic rate and growth (THORMÄHLEN; MEITZEL; GROYSMAN; ÖCHSNER *et al.*, 2015). However, evidence highlights that NTRC is also an important regulator of the metabolism of Arabidopsis roots and tomato fruits (FERRÁNDEZ; GONZÁLEZ; CEJUDO, 2012; HOU; EHRLICH; THORMÄHLEN; LEHMANN *et al.*, 2019). Furthermore, recent study demonstrated that NTRC mutation has stronger effects on photosynthesis and primary metabolism in sink than source Arabidopsis leaves, including under high CO_2 conditions, in which the *ntrc* mutant was unable to increase their biomass (SOUZA; HOU; SUN; POEKER *et al.*, 2023). This indicates that the acclimation of plants to the predicted

climate change scenario, which includes high atmospheric CO_2 concentration, depends on the role of NTRC in sink leaves. However, it is unclear how NTRC regulates sink leaf metabolism and how stress periods such as drought can affect it. Furthermore, given that plant growth seems to be co-limited by both source and sink leaves (FERNIE; BACHEM; HELARIUTTA; NEUHAUS *et al.*, 2020), it is thus important to understand how sink leaf metabolism is regulated. Thus, the aim of this work was to investigate the role of NTRC in the regulation of the metabolism of source and sink leaves in *Arabidopsis thaliana* under water deficit stress.

4.2 Material and Methods

Plant material and growth conditions

The experiments were carried out using wild type *Arabidopsis thaliana* (L.), ecotype Columbia-0 (Col-0) and the *ntrc* mutant, which correspond a T-DNA insertion mutant (SALK_012208) from SALK collection (http://signal.salk.edu/), previously characterized (DALOSO; MÜLLER; OBATA; FLORIAN *et al.*, 2015; REICHHELD; KHAFIF; RIONDET; DROUX *et al.*, 2007; SERRATO; PÉREZ-RUIZ; SPÍNOLA; CEJUDO, 2004; THORMÄHLEN; MEITZEL; GROYSMAN; ÖCHSNER *et al.*, 2015). Homozygous lines were identified by genotyping *ntrc* plants using specific primers (Supplemental Table 1). PCR products were fractionated on 1.2 % (w/v) agarose gels and visualized by ethidium bromide staining (Supplemental Fig. 1). The absence of the transcripts of *ntrc* in the leaves was confirmed by reverse transcription PCR analysis (Supplemental Fig. 1).

The seeds were disinfected with 70% alcohol and stratified for 3 days at 4°C. After that, the seeds were sown in soil mixed with vermiculite (1:1) in pots with a 0.1 L capacity and placed in a control room under short-day conditions (8/16 light/dark), daily average temperature 20-22°C and artificial white light (160 μmol photons m^{-2} s^{-1}). 8-week-old plants were subjected to a progressive water deficit (WD) by suspension of irrigation. The whole rosette was harvested at the beginning of the day after 0, 5 and 11 days under WD. A set of plants were maintained well-watered (WW) and used as control.

Relative water content measurement

Leaf relative water content (RWC) was assessed to monitor the status of leaf hydration in WW and WD plants. In brief, two disks of 1 cm^2 were taken from two different source leaves per and weighed separately to get the fresh weight (FW). Subsequently, leaf discs were hydrated in petri dishes containing distilled water and after 2 hours weighed to obtain the turgid weight (TW). Leaf discs were then dried at 72 ⁰C for 72 h. Finally, the disks were weighed to obtain the dry weight (DW). The RWC was calculated as following:

$$RWC\ (\%) = \frac{FW - DW}{TW - DW}$$

Metabolite profiling analysis

Source and sink leaves from six independent biological replicates per genotype and/or treatment were harvested in the light at the start of the photoperiod and rapidly snap-frozen by dipping into the liquid nitrogen. These frozen leaves were subsequently homogenized to a fine powder using a liquid nitrogen-cooled mortar and pestle. After grinding, samples were aliquoted and stored at -80°C until further use. The extraction of polar metabolites was performed by using approximately 50 mg of the frozen material. The frozen sample was shaken for 15 min at 350 rpm and 70 °C with methanol containing 0.2 mg ml^{-1} of ribitol as internal quantitative standard and was centrifuged for 10 min at 11000 g. The supernatant was collected in a fresh tube containing chloroform with water and was centrifuged at 11,000 g for 15 min. 500 µl of the upper (polar phase) was collected and dried in a vacuum concentrator. The derivatization and gas chromatography coupled to time of flight mass spectrometry (GC-TOF-MS) analysis were carried out using a well-established protocol (LISEC; SCHAUER; KOPKA; WILLMITZER *et al.*, 2006). The resultant chromatograms and mass spectra were analysed by using Xcalibur 2.1 software (Thermo Fisher Scientific, https://www.thermofisher.com/) and metabolites identified using the Golm Metabolome Database (KOPKA; SCHAUER; KRUEGER; BIRKEMEYER *et al.*, 2005).

Chlorophyll *a* fluorescence analysis

Chlorophyll *a* fluorescence analysis was carried out using a Dual-PAM-100 system (MAXI version WALZ) as described earlier (CARVALHO; RIBEIRO; MARTINS; BONIFACIO *et al.*, 2014). Plants were dark acclimated for 30 minutes and then transferred to PAM, where leaves were exposed to a light pulse intensity of 0.5 mmol m^{-2} s^{-1} (1Hz) to establish minimum fluorescence (F0)

followed by a saturating pulse of actinic light (470 nm) delivered for 0.8 s to get maximum fluorescence (Fm). The emission of fluorescence was recorded by the PAM and used to calculate the effective quantum yield of photosystem II [Y (II)], non-photochemical quenching (NPQ) and the reduction of plastoquinone pool (1-qL). The maximum quantum efficiency of PSII was calculated using Fv/Fm = (Fm – F0)/Fm equation. These measurements were taken in four biological replicates per genotype/ treatment.

Lipid peroxidation

Fresh leaf samples (0.05 g) were powdered using liquid nitrogen and extracted in a 5% (w/v) trichloroacetic acid (TCA) solution with subsequent centrifugation at 10,000 g for 30 min at 4°C. Lipid peroxidation was determined based on the formation of thiobarbituric acid reactive substances (TBARS) as described earlier (HEATH; PACKER, 1968). The reaction contained 0.5 mL of the extract, 2.0 mL of the 20% TCA solution and 0.5% thiobarbituric acid (TBA). The mixture was heated in a water bath at 95°C in sealed glass tubes for 1 h. The reaction was stopped by placing the tubes on ice. The absorbance of was measured in a spectrophotometer at 532 and 600 nm and used for estimation of TBARS content, using an extinction coefficient of 155 mM^{-1} cm^{-1}. Results are expressed as nmol TBARS g^{-1} FW.

Protein extraction and enzyme activity analyses

Total proteins were extracted from 0.05g of the crushed, frozen leaf material by adding 1 ml of potassium phosphate buffer (100 mM; pH 7.0) containing EDTA (final concentration of 1 mM). The homogenate was centrifuged at 15,000 g at 4°C for 15 min. The supernatant was collected and was used for the enzymatic analyses. The total content of soluble proteins was determined according to Bradford with bovine serum albumin (BSA) as standard (BRADFORD, 1976). The activity of superoxide dismutase (SOD) was determined based on the inhibition of tetrazolium chloride (NBT) nitro blue chloride photoreduction (GIANNOPOLITIS; RIES, 1977). The SOD activity unit (U) was defined as the quantity of enzyme required to inhibit 50% of NBT photoreduction, expressed as U mg^{-1} FW min^{-1}. The activity of catalase (CAT) was determined by reduction of H_2O_2 (BEERS; SIZER, 1952; HAVIR; MCHALE, 1987), calculated from the molar extinction coefficient of H_2O_2 (40 mM cm^{-1}) and expressed as mmol H_2O_2 g^{-1} of FW min^{-1}. The ascorbate peroxidase (APX) activity was measured based on the oxidation of ascorbate (ASC). The reaction mixture contains 0.45 mM of ASC, 3 mM of H_2O_2, 50 μl protein extract and 100 mM

potassium phosphate buffer (pH 7.0) containing 1 mM EDTA in a total volume of 1.5 ml (NAKANO; ASADA, 1981). APX activity was expressed as µmol ASC mg^{-1} FW min^{-1}. All enzymatic activities were determined spectrophotometrically.

Starch analysis

Starch was quantified spectrophotometrically using the pellet from the methanolic extraction of the metabolite profiling analysis. The pellet was rinsed three times with ethanol (80%) at 70 °C to remove the remaining glucose of the material. Starch was then solubilized using 400 µL of KOH (0.2M) at 90 °C for 1 hour. The solution was neutralized by adding 70 µL of acetic acid (1M). A 100 µL of this reaction mixture was used for starch digestion using citrate buffer (0.3M) (pH 5.0) and amyloglucosidase (1 U reaction^{-1}) at 55 °C for 1 hour in a final volume of 300 µL. The starch concentration was then determined as glucose released from starch by amyloglucosidase. The level of glucose was determined by following the formation of NADH (340 nm) and quantified according to standard curves of glucose (1 mM) (TRETHEWEY; RIESMEIER; WILLMITZER; STITT *et al.*, 1999).

Statistical analyses

All experiments were conducted using at least 4 biological replicates per genotype and treatment. All graphs were made using GraphPad prism 8.3.4. Heat maps were created using the MeV 4.9.0 software. Student's *t*-test or one-way ANOVA followed by Tukey's test ($P < 0.05$) were used to compare treatments and/or genotypes, as indicated in the legend of each figure. Metabolite profiling data was also analysed by partial least square discriminant analysis (PLS-DA) using the Metaboanalyst platform (CHONG; SOUFAN; LI; CARAUS *et al.*, 2018).

4.3 Results

Analysis of stress-related parameters highlights that the water deficit imposed to the plants were mild and that sink *ntrc* leaves are more sensible to this condition

No difference in the relative water content (RWC) between WT and the *ntrc* mutant was observed at the days 0 and 11 in either well-watered or water deficit (WD) plants as well as in WD plants at the day 5. The RWC was slightly higher in WT than *ntrc* in WW plants at the day 5. No

difference between WD and WW plants was observed within each genotype. However, the RWC was lower in *ntrc* under WD than WT under WW (Fig. 1a-c). To investigate whether the WD differentially affected source and sink leaves, our next analyses were carried out in these leaves separately. No changes in the effective quantum yield of the photosystem II (Fv/Fm) were observed among treatments, leaves and genotypes (Fig. S1). Similarly, no difference in TBARS, an indicator of lipid peroxidation, was observed between the genotypes and source and sink leaves under WW conditions (Figs. 2 a-b). However, the level of TBARS was higher in *ntrc* sink than *ntrc* source leaves and both source and sink WT leaves under WD (Fig. 2c). These analyses highlight that the level of WD imposed to the plants was minor, as evidenced by the minor differences in RWC and Fv/Fm between WW and WD plants, but that sink *ntrc* leaves are more sensible to the stress, as indicated by the higher TBARS values under this condition.

Water deficit affected mainly sink rather than source leaves photosynthetic performance

Plants lacking NTRC have compromised photochemical capacity (THORMÄHLEN; MEITZEL; GROYSMAN; ÖCHSNER *et al.*, 2015), including in their sink leaves (SOUZA; HOU; SUN; POEKER *et al.*, 2023). We then investigated the photosynthetic capacity of both WT and *ntrc* plants under WW and WD conditions using a pulse-amplitude modulation (PAM) chlorophyll *a* fluorescence analysis. Before the start of the WD period (i.e. day 0), no differences between the genotypes and source and sink leaves were observed in Y(I), Y(II), Y(NA), Y(NO), ETR(I) and ETR(II) (Figs. 3, 4, S5, S4, S2 and S3). By contrast, *ntrc* source leaves have higher Y(NPQ) and qN and lower qP than source WT leaves (Figs. S6, 5 and 6). Both Y(I) and ETR(I) were lower in both source and sink *ntrc* leaves under WD, when compared to these leaves in WT under WD at the day 5 (Figs. 3b-c; S2b-c). After 11 days of WD, both Y(I) and ETR(I) of *ntrc* sink leaves was lower than WT sink leaves under both WW and WD conditions, whereas no difference was observed in these parameters between genotypes and treatments in source leaves (Figs. 3d-e; S2d-e). No difference among genotypes and treatments was observed in both Y(II) and ETR(II) in source leaves (Figs. 4a-c; S3a-c). However, the values of these parameters were lower in sink *ntrc* WD-stressed leaves and in sink WW *ntrc* leaves, when compared to their respective WW and WD WT controls (Figs. 4d-e; S3d-e).

No differences in Y(NO) and Y(NA) were observed among genotypes, treatments and leaf types (Figs. S4 and S5), with exception of the high Y(NA) that was higher in source *ntrc* than

source WT leaves under WD (Fig. S5b). By contrast, both Y(NPQ) and qN were higher in sink *ntrc* than sink WT leaves under WW or WD conditions after 5 or 11 days of WD. These differences were not noticed in source leaves (Fig. S6b-e; 5b-e). The qP values showed the opposite trend of the non-photochemical quenching, in which qP was lower in sink *ntrc* than sink WT leaves under WW or WD conditions after 5 or 11 days of WD, while no difference was observed in source leaves (Fig. 6b-e).

Sink *ntrc* leaves have the lowest antioxidant capacity, as compared to sink WT leaves and the source leaves of both genotypes

It is well-established that WD can induce the accumulation of reactive oxygen species (ROS) in plant tissues, which trigger the activity of antioxidant enzymes to avoid redox imbalance in plants (KNEESHAW; KEYANI; DELORME-HINOUX; IMRIE *et al.*, 2017). We then analysed the activities of ascorbate peroxidase (APX), catalase (CAT) and superoxide dismutase (SOD) enzymes in source and sink leaves of both WT and *ntrc* after 0 and 11 days of WD. No difference between genotypes and leaf types was observed in APX, SOD and CAT activities under WW condition (Figs. S7a-b; S8a-b; 7a-b). However, several differences were observed under WD, but each enzyme had a different pattern of change in response to WD according to the leaf type and genotype. APX activity was lower in sink leaves of both WT and *ntrc*, when compared to the source leaves of these genotypes under WD (Fig. S7c). By contrast, SOD activity was lower in sink WT leaves and in both source and sink *ntrc* leaves, when compared to source WT leaves under WD (Fig. S8c). Interestingly, no difference in CAT activity was observed between leaf types in WT. However, both source and sink *ntrc* leaves had lower CAT activity than WT, in which sink *ntrc* leaves showed the lowest values under WD (Fig. 7c). These results suggest that the WD-mediated modulation of antioxidant enzymes is leaf type and NTRC dependent.

Plant growth is co-limited by sink leaves, especially under water deficit condition

To examine the effect of WD on plant growth, we measured fresh (FW) and dry (DW) weights of source and sink leaves from WT and *ntrc* in 8-week-old plants subjected to 0, 5 and 11 days of WD. No morphological stress signals were observed in plants subjected to 5 days of WD, while the bottom leaves of both WT and *ntrc* initiated the senescence process after 11 days of WD. Both FW and DW were higher in source than sink leaves in both genotypes at the day 0, but this difference is much higher between WT leaf types (Figs. S9a-b). After 5 days of WD, both FW and

DW was higher in WT source leaves, while no difference was observed among sink WT leaves and both source and sink *ntrc* leaves under WW or WD conditions (Figs. S9c-f). At day 11 of WD, the DW was higher in source WT leaves under WW and WD conditions, while the FW was higher in these leaves under WW, but no difference between WT and *ntrc* source leaves was observed under WD (Fig. S9g-j).

Given the differences in plant growth between WT and *ntrc* in the absence of stress (Fig. S9a-b), we then investigated the relative growth by normalizing the data of the days 5 and 11 according to the values of the day 0. We aimed to analyse the impact of the WD on the biomass accumulation of source and sink leaves over time. The DW of source leaves increased only in WT-WW plants, while increased DW was observed in sink leaves of *ntrc*-WW plants and in both WT-WW and WT-WD plants (see ANOVA results in Figs. 8a-d). No difference was observed between WW and WD treatments in source or sink leaves in both genotypes, with exception of source WT-WW and WT-WD plants at the days 5 and 11 (see asterisks in Fig. 8a). We next investigated the relative (%) contribution of source and sink leaves for the total rosette biomass in both genotypes under WW and WD conditions. Source leaves represented 88.6% and 84.4% of the total rosette biomass in WT and *ntrc* WW plants at the day 5, respectively. WD did not alter the % of source and sink leaves at this day (Fig. S10a-b). By contrast, the % of sink leaves were higher and lower in WT and *ntrc*, when compared to their respective WW control at the day 11, respectively (Fig. S10c-d).

Metabolite profiling analysis reveals that sink *ntrc* leaves were the most affected by WD imposition

We next investigated how the lack of NTRC coupled to water shortage condition affects starch concentration and the level of primary metabolites in source and sink leaves harvested at 09:00 am after 0 and 11 days of WD. The starch concentration did not differ among leaf types, genotypes and treatments on both days 0 and 11 (Fig. S11a-d). Partial least square-discriminant analysis (PLS-DA) highlights that the primary metabolism differs among source and sink leaves of WT and *ntrc* at the day 0, as evidenced by the separation of these groups by PC1 and/or PC2 (Fig. 9a). The discrepancies were especially observed between the genotypes and were associated

to the accumulation of 15 metabolites, that are present in the variable importance in projection (VIP) list with score higher than 1 (Fig. 9b).

Thirty-three metabolites out of the forty-five annotated were significantly different among leaf types and/or genotypes before stress imposition (Fig. 9c). Comparing with WT source leaves, several metabolites such as phosphoric acid, maleic acid, malate, salicylic acid, aspartate, pyroglutamate, glutamate, glucose anhydro, shikimic acid and cellobiose had higher levels in sink leaves from both WT and *ntrc* genotypes (Fig. 9c). Furthermore, succinate, glycerate, erythronic acid, tagatose, and glucose had lower level in both *ntrc* source and sink leaves than WT source leaves (Fig. 9c). The metabolite profiling data from WW plants at the day 11 resemble those from the day 0, in which the major separation is observed between the genotypes and is associated to a differential accumulation of certain amino acids, organic acids and sugars metabolites (Fig. 10a-c). However, WD imposition separated *ntrc* sink leaves from the other groups (Fig. 11a), which is associated to different metabolites but especially asparagine, fumarate and sucrose, that had VIP score higher than 1 and were significantly different from WT source leaves (Fig. 11b-c). Other metabolites such as glycine, oxaloacetate, glycerate, and erythronic acid had a differential accumulation in *ntrc* sink leaves, when compared to WT source leaves (Fig. 11c). These results suggest that sink *ntrc* leaves are the most affected by WD imposition.

Integrative analysis reveals the major determinants that discriminate genotypes, leaf types and soil water conditions

We next combined all data from WW and WD plants harvested at the day 11 of the experiment and carried out a principal component analysis (PCA) to investigate which parameters mostly differentiate genotypes, leaf types and water regimes. The PCA highlights that genotypes and leaf types are better separated under WD than WW conditions (Figs. 12 a-b). Under WW, both WT and *ntrc* source leaves were closely clustered, while sink leaves were clearly separated (Fig. 12 a), indicating that the major differences between the genotypes reside in sink rather than source leaves. Biplot analysis highlight that non-photochemical quenching's (qN, NPQ and Y(NPQ)), beta-alanine and asparagine are the major components that separate sink *ntrc* leaves from the other groups (Figs. 12c-d).

4.4 Discussion

Water deficit (WD) can induce oxidative stress within plant tissues, which is characterized by a disrupted cellular redox homeostasis caused by ROS overaccumulation. However, ROS is also an important signalling compound, regulating gene expression and enzyme activity through post-translational modification of proteins and transcription factors (FOYER; BAKER; WRIGHT; SPARKES *et al.*, 2020; XIE; ZHENG; ZHOU; KANWAR *et al.*, 2022). The level of ROS is thus highly regulated according to the prevailing environmental condition through a complex redox system including antioxidant enzymes and redoxins (DA FONSECA-PEREIRA; SOUZA; FERNIE; TIMM *et al.*, 2021; SOUZA; LIMA-MELO; CARVALHO; REICHHELD *et al.*, 2019). Among the redoxins, NTRC is one of the most important for plant photosynthesis and growth, as evidenced by the severe plant growth restriction observed in the *ntrc* mutant (SERRATO; PÉREZ-RUIZ; SPÍNOLA; CEJUDO, 2004; THORMÄHLEN; MEITZEL; GROYSMAN; ÖCHSNER *et al.*, 2015). NTRC is also exceptional considering that it is the unique TRX reductase with both reductase and redoxin domains in its protein structure. While the role of NTRC for photosynthesis in source leaves is well-established (PÉREZ-RUIZ; NARANJO; OJEDA; GUINEA *et al.*, 2017), only recently a study highlighted that this protein is also important for the regulation of sink leaf metabolism (SOUZA; HOU; SUN; POEKER *et al.*, 2023). However, the underlying mechanisms by which NTRC regulates photosynthesis and metabolism of sink leaves is unknown, specially under stress conditions. Taking this into account, we subjected the *ntrc* mutant to WD to understand the role of NTRC for the regulation of growth, photosynthesis and metabolism in source and sink leaves.

Plant growth is regulated by NTRC and co-limited by sink leaves, especially under WD

In multicellular organisms, growth and development are regulated by a complex network that culminates in cellular elongation, proliferation, and/or differentiation according to the nutritional status and external stimulus (ZLUHAN-MARTÍNEZ; LÓPEZ-RUÍZ; GARCÍA-GÓMEZ; GARCÍA-PONCE *et al.*, 2021). Several environmental cues are perceived by these organisms, which activate intracellular signalling pathways as well as induce the synthesis of signalling molecules that guarantee the flow of information from the perceiving cell to the entire system (FETTKE; FERNIE, 2015; GALLÉ; LAUTNER; FLEXAS; FROMM, 2015; REISSIG;

OLIVEIRA; OLIVEIRA; POSSO *et al.*, 2021; THIEME; ROJAS-TRIANA; STECYK; SCHUDOMA *et al.*, 2015). In animals, the process of cell-to-cell and organ-to-organ communication is facilitated by the nervous system, which can guide the organism to move and obtain resources to guarantee growth and development (FURIGO; DE OLIVEIRA; DE OLIVEIRA; COMOLI *et al.*, 2010). By contrast, plants neither can move nor possess a neuronal system (GALVIZ; RIBEIRO; SOUZA, 2020; TAIZ; ALKON; DRAGUHN; MURPHY *et al.*, 2019). However, plants can also perceive several environmental cues and propagate such information to the entire system as well as to neighbour plants (ALVES DE FREITAS GUEDES; MENEZES-SILVA; DAMATTA; ALVES-FERREIRA, 2019; DA SILVA; MACEDO; DANELUZZI; CAPELIN *et al.*, 2020). Therefore, plants have developed an intricate information processing system and complex intracellular signalling network that aid them to acclimate and create a new homeostasis, which guarantee growth and/or development under several environmental conditions (CHAIWANON; WANG; ZHU; OH *et al.*, 2016).

The resources acquired by the plants are usually obtained from roots and leaves and then translocated throughout the plant. Whilst water and nutrients are mostly obtained from roots, source leaves are the major producers of photoassimilates. In this context, it is generally assumed that plant growth and yield depend on the photosynthetic capacity of source leaves and the capacity of sink organs to import photoassimilates (especially sugars and amino acids) (AINSWORTH; ROGERS; NELSON; LONG, 2004; LEMOINE; CAMERA; ATANASSOVA; DÉDALDÉCHAMP *et al.*, 2013; RIBEIRO; MACHADO; HABERMANN; SANTOS *et al.*, 2012; SILVA; MAGALHÃES FILHO; SALES; PIRES *et al.*, 2018). However, recent studies highlight that plant growth is co-limited by both source and sink organs, shedding light on the importance of sink organs to improve crop growth and yield (FERNIE; BACHEM; HELARIUTTA; NEUHAUS *et al.*, 2020). In this context, previous evidence suggests that NTRC is important for both source and sink organs. The lack of NTRC compromised photosynthesis in source leaves and starch metabolism in both source and sink organs (HOU; EHRLICH; THORMÄHLEN; LEHMANN *et al.*, 2019; MICHALSKA; ZAUBER; BUCHANAN; CEJUDO *et al.*, 2009). Furthermore, a recent study revealed that plants lacking NTRC are unable to acclimate to high CO_2, which was especially attributed to a low photochemical performance and strong metabolic alteration in their sink leaves (SOUZA; HOU; SUN; POEKER *et al.*, 2023). Here, we provide further information that highlights

the importance of sink leaves for plant growth, especially under WD condition, and pinpoint NTRC as an important regulator of this process.

Although the level of water stress was mild, as evidenced by the minor alterations in RWC, TBARS and F_v/F_m in WD-stressed plants (Fig. 1-2, S1), WD imposition abolished the increase in biomass of WT source leaves over time (Fig. 8a). However, no significant change was observed between WW and WD sink WT leaves (Fig. 8b), which increased the relative (%) contribution of sink leaves to the rosette biomass in WT, while the opposite was observed in *ntrc* mutant (Fig. S10c-d). These results highlight that the WD-mediated growth restriction is mainly associated with a reduced biomass accumulation of source rather than sink leaves in WT. Additionally, the growth impairment of the *ntrc* mutant is mainly associated to a limited growth of source rather than sink leaves under WW as well as that the increased biomass accumulation of sink *ntrc* leaves over time is abolished by WD. Our findings collectively highlight that plant growth depends on NTRC and is co-limited by sink leaves, especially under WD. Previous results indicate that the Arabidopsis shoot apical meristem is preserved in carbon limiting conditions, which allow the reactivation of growth when carbon is not limiting anymore (LAUXMANN; ANNUNZIATA; BRUNOUD; WAHL *et al.*, 2016). It seems likely that Arabidopsis prioritize sink rather than source leaf growth under WD, which can be partially explained by the fact that new (sink) leaves will be morphologically and anatomically better adapted to a carbon-limiting and water restriction condition than the old (source) leaves.

On the NTRC-mediated regulation of plant photosynthesis and metabolism

The reduced growth of the *ntrc* mutant has been attributed to the fact that NTRC regulates various processes in chloroplast such as the biosynthesis of chlorophyll, starch and amino acids along with ROS metabolism and photosynthesis (LEPISTO; KANGASJARVI; LUOMALA; BRADER *et al.*, 2009; MICHALSKA; ZAUBER; BUCHANAN; CEJUDO *et al.*, 2009; PEREZ-RUIZ; SPÍNOLA; KIRCHSTEIGER; MORENO *et al.*, 2006; PULIDO; SPÍNOLA; KIRCHSTEIGER; GUINEA *et al.*, 2010; RICHTER; PETER; ROTHBART; SCHLICKE *et al.*, 2013; STENBAEK; HANSSON; WULFF; HANSSON *et al.*, 2008). Indeed, our results highlight that sink leaves were the most affected by the lack of NTRC, as indicated by the higher TBARS, lower values of photochemical parameters (Y(I), Y(II), ETR(I), ETR(II)) and greater metabolic

alterations induced by WD. Thus, our results coupled to our previous study (SOUZA; HOU; SUN; POEKER *et al.*, 2023) indicate that the reduced growth of the *ntrc* mutant is also associated to a NTRC-mediated regulation of sink leaf photosynthesis and metabolism. PCA indicates that the separation of sink *ntrc* leaves from the other leaves is mostly associated to NPQ, fructose, asparagine, beta-alanine, phosphoric acid and to a lower extent starch, salicylic acid, phenylalanine, glycine and serine (Fig. 12). This is in agreement with our previous study which showed a higher accumulation of N-related compounds such as arginine, asparagine and histidine and the stress-responsive branched chain amino acids leucine, isoleucine and valine in the *ntrc* mutant in the absence of stress (SOUZA; HOU; SUN; POEKER *et al.*, 2023). Furthermore, sink *ntrc* leaves showed a lower photochemical capacity and a lower accumulation of 3-PGA, even under high CO_2 condition (SOUZA; HOU; SUN; POEKER *et al.*, 2023). Taken together, these results suggest that sink *ntrc* leaves are constantly under stress and in a carbon limiting condition. This corroborates the fact that the *ntrc* mutant is highly susceptible to darkness and have lower growth mainly under short day or fluctuating light conditions (PÉREZ-RUIZ; NARANJO; OJEDA; GUINEA *et al.*, 2017; THORMÄHLEN; MEITZEL; GROYSMAN; ÖCHSNER *et al.*, 2015; THORMÄHLEN; ZUPOK; RESCHER; LEGER *et al.*, 2017), which might be related to an unbalance between carbon and nitrogen metabolisms. The disturbed N-metabolism could be associated to the enzyme glutamine synthetase 2 (GS2), that has been shown to interact with NTRC (GONZÁLEZ; DELGADO-REQUEREY; FERRÁNDEZ; SERNA *et al.*, 2019). In fact, the level of glutamine and glutamate is substantially altered in the *ntrc* mutant, suggesting that the GS/GOGAT cycle and likely the N assimilation might be compromised in this mutant.

Redox regulation mediated by NTRC

Our results further suggest that the reduced *ntrc* growth might be associated to a lower antioxidant capacity, given the lower activity of SOD, APX and especially catalase observed in this mutant here and in our previous study (SOUZA; HOU; SUN; POEKER *et al.*, 2023). The plant antioxidant system consists of enzymes such as SOD, catalase, APX, peroxiredoxins (PRXs), 2-Cys PRXs and those related to the ascorbate/glutathione metabolism. These antioxidant enzymes cooperatively modulate ROS levels in plant tissues (FOYER; NOCTOR, 2013). Notably, numerous plant antioxidant enzymes involved in ROS scavenging have been identified as TRX

targets (BALMER; VENSEL; TANAKA; HURKMAN *et al.*, 2004; MARCHAND; LE MARÉCHAL; MEYER; MIGINIAC-MASLOW *et al.*, 2004; WONG; BALMER; CAI; TANAKA *et al.*, 2003). However, all information currently available from Arabidopsis are derived from studies using either source leaves or the entire rosette. Further studies are now needed to unveil possible new targets and to fully understand how sink leaf metabolism is regulated by the NTRC/TRX system.

The plastidial redox network is highly orchestrated and tightly connected, in which NTRC is a major hub and compose an essential module together with ferredoxin thioredoxin reductases (FTR) (SOUZA; LIMA-MELO; CARVALHO; REICHHELD *et al.*, 2019; YOSHIDA; HISABORI, 2016). Beyond being highly co-expressed with several plastidial redox related genes, NTRC can interact directly with several proteins of the redox network, such as TRXs, peroxiredoxins (PRXs), 2-Cys PRXs, APXs, GPXs, dehydroascorbate reductase, catalase as well as with several transcription factors (GONZÁLEZ; DELGADO-REQUEREY; FERRÁNDEZ; SERNA *et al.*, 2019; SOUZA; LIMA-MELO; CARVALHO; REICHHELD *et al.*, 2019), highlighting that the role of NTRC for plant metabolic regulation is wider than initially expected. Furthermore, our previous study has surprisingly unveiled that the lack of NTRC had stronger effects on the redox metabolism in Arabidopsis rosettes harvested at night, when compared to samples harvested in the light period. For instance, the redox status of ascorbate and glutathione was substantially altered and the activity of APX, SOD and catalase were lower, which leads to an overaccumulation of H_2O_2 in *ntrc* rosettes at night, when compared to the WT (SOUZA; HOU; SUN; POEKER *et al.*, 2023). Furthermore, it has been shown that NTRC is an important regulator of starch metabolism in both source and sink tissues (GONZÁLEZ; DELGADO-REQUEREY; FERRÁNDEZ; SERNA *et al.*, 2019; HOU; EHRLICH; THORMÄHLEN; LEHMANN *et al.*, 2019; MICHALSKA; ZAUBER; BUCHANAN; CEJUDO *et al.*, 2009; THORMAEHLEN; RUBER; VON ROEPENACK-LAHAYE; EHRLICH *et al.*, 2013; THORMÄHLEN; MEITZEL; GROYSMAN; ÖCHSNER *et al.*, 2015). Although we did not find difference in starch concentration between WT and *ntrc* here (Fig. S11), it is noteworthy that Arabidopsis starch metabolism is highly influenced by the circadian rhythm and strongly vary along the day, and our analysis refers to a single time point in samples harvested at the beginning of the day. Thus, given the importance of the night period and starch metabolism for growth (APELT; BREUER; OLAS; ANNUNZIATA *et al.*, 2017; DOS ANJOS; PANDEY; MORAES; FEIL *et al.*, 2018; MARTINS;

HEJAZI; FETTKE; STEUP *et al.*, 2013; OLAS; FICHTNER; APELT, 2020), it seems likely therefore that the reduced growth of the *ntrc* mutant is also associated to a disturbed starch and redox metabolisms at night.
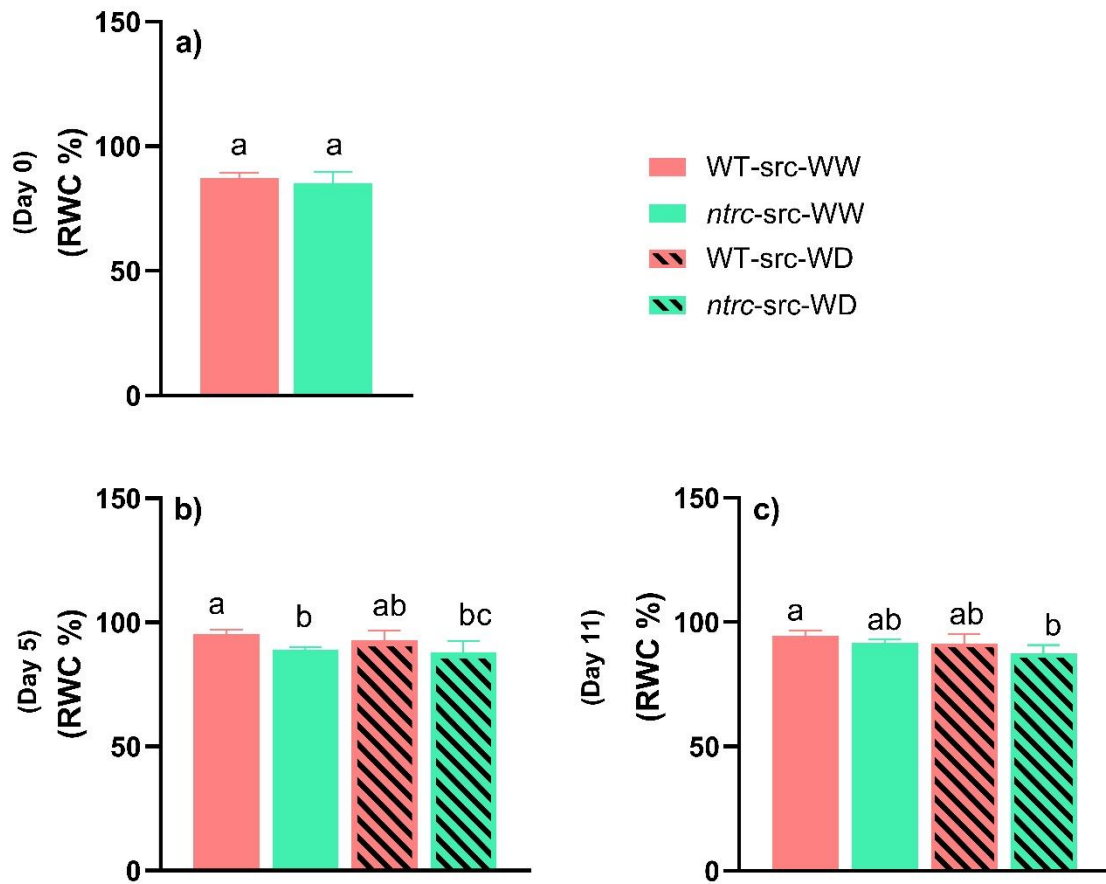
Figure 1. Relative water content (RWC) analysis in wild type (WT) and ntrc mutant subjected to well-watered (WW) or water deficit (WD) conditions for 0 (a), 5 (b) and 11 (c) days. Bars represent averages of 6 replicates ± standard deviation (SD). Different letters indicate significant difference among treatments and/or genotypes according to ANOVA and Tukey's test (P <0.05).
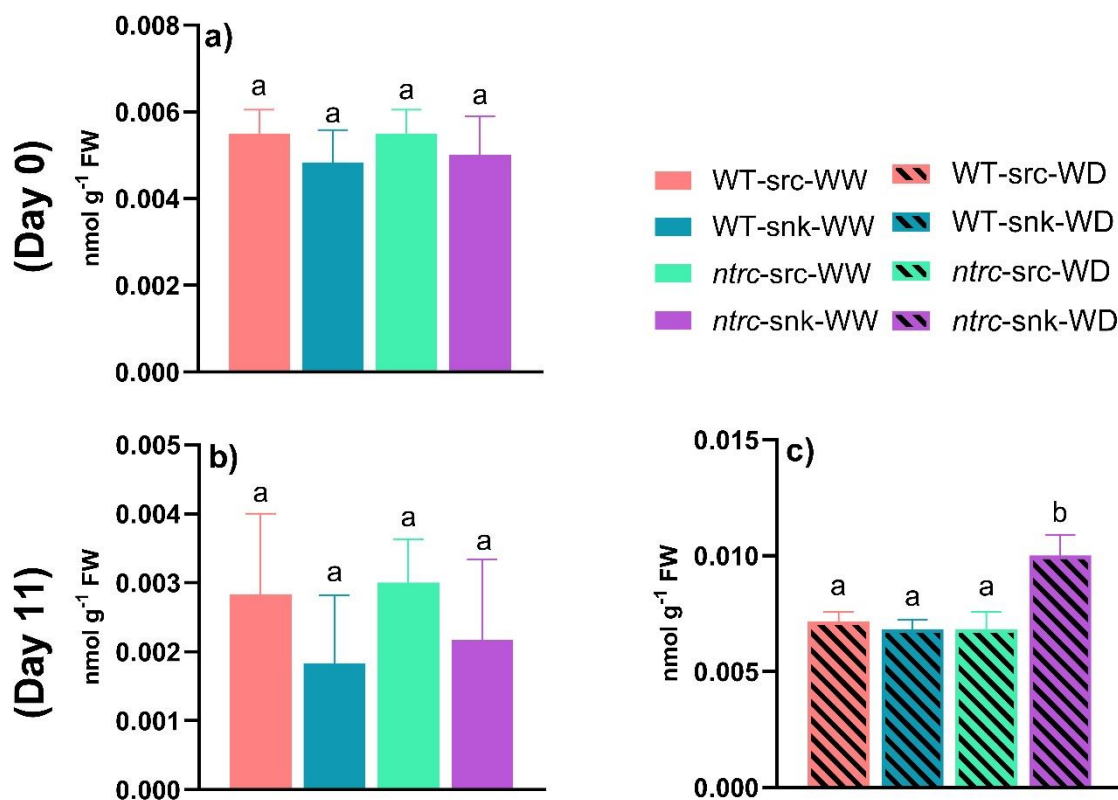
Figure 2. Content of thiobarbituric acid (TBARs) in wild type and ntrc mutant subjected to well-watered (WW) or water deficit (WD) conditions for 0 and 11 days. The TBARs was determined in source and sink leaves of both genotypes at the days 0 (a) and 11 (b-c) of the experiment. Lined graphs represent WD-treated plants. Different letters indicate significant difference among treatments and/or genotypes according to ANOVA and Tukey's test (P <0.05) (n = 6).
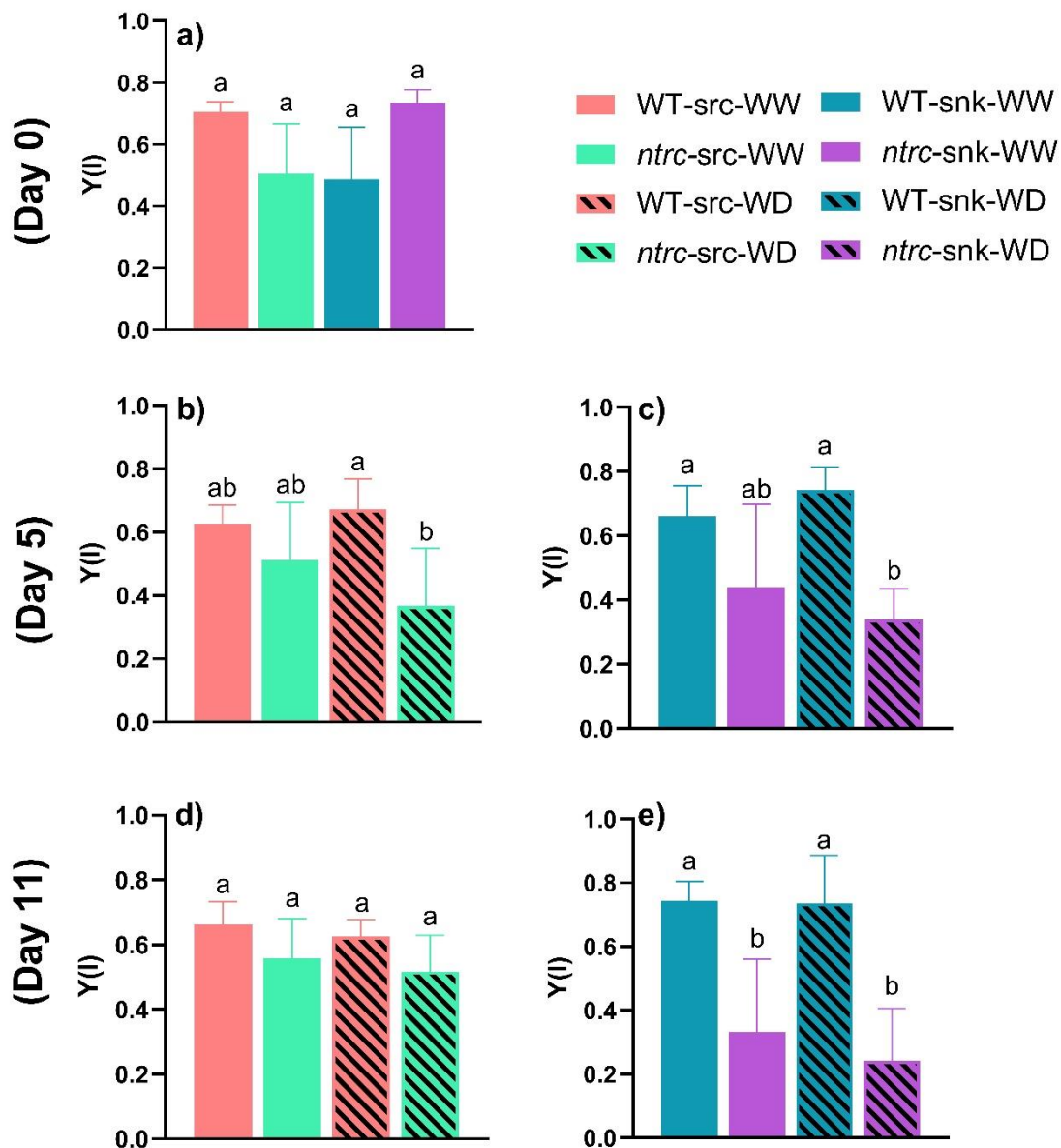
Figure 3. Chlorophyll a fluorescence analysis in wild type and ntrc mutant subjected to well-watered (WW) or water deficit (WD) conditions for 0, 5 and 11 days. Y(I), effective quantum yield of PSII (I) was determined in source and sink leaves of both genotypes at the days 0 (graph a), 5 (graph b, c) and 11 (graph d, e) of the experiment. Lined graphs represent WD-treated plants. Different letters indicate significant difference among treatments and/or genotypes according to ANOVA and Tukey's test ($P < 0.05$) ($n = 4$).
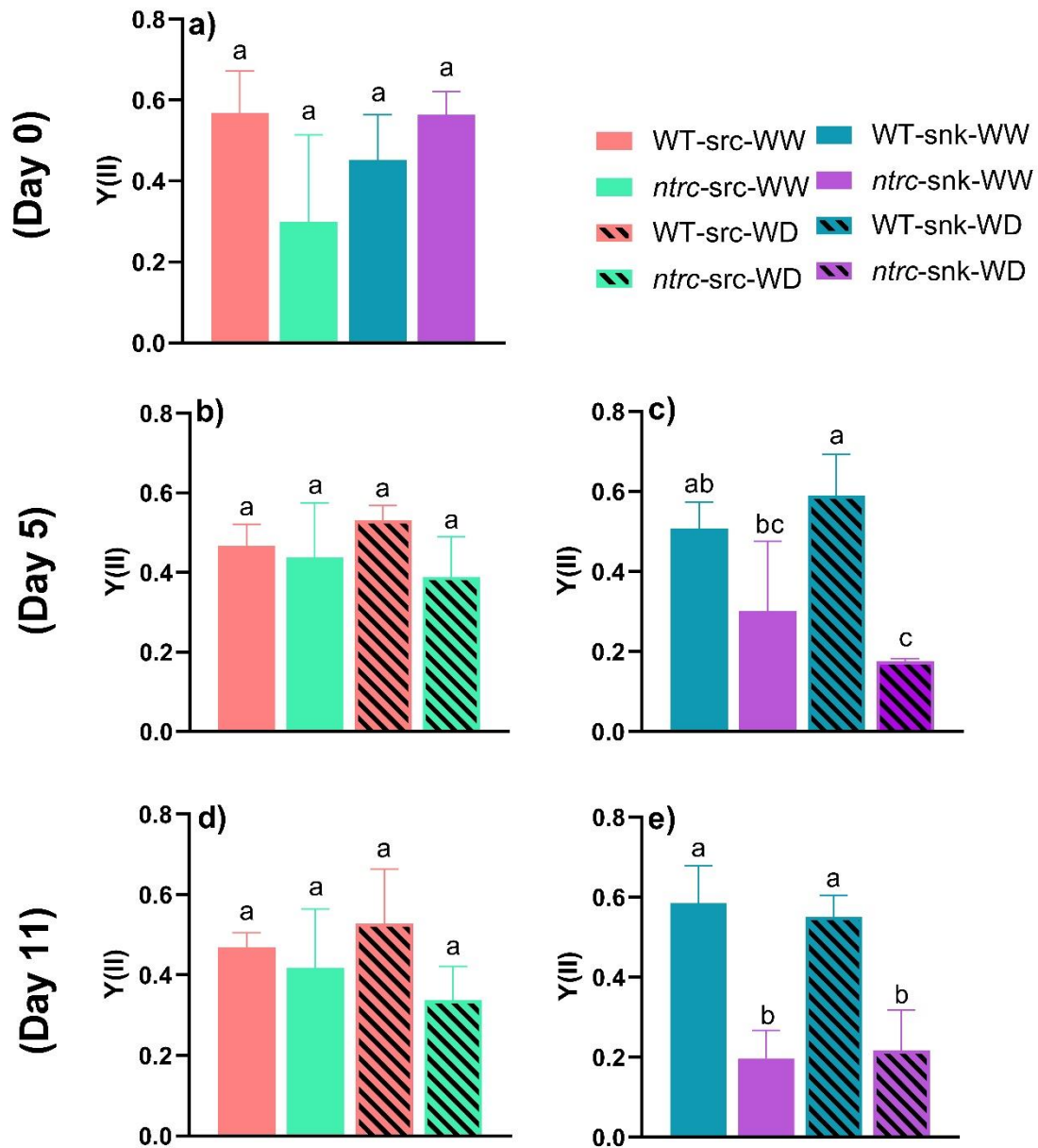
Figure 4. Chlorophyll a fluorescence analysis in wild type and ntrc mutant subjected to well-watered (WW) or water deficit (WD) conditions for 0, 5 and 11 days. The Y(II), effective quantum yield of PSII was determined in source and sink leaves of both genotypes at the days 0 (graph a), 5 (graph b, c) and 11 (graph d, e) of the experiment. Lined graphs represent WD-treated plants. Different letters indicate significant difference among treatments and/or genotypes according to ANOVA and Tukey's test (P <0.05) (n = 4).
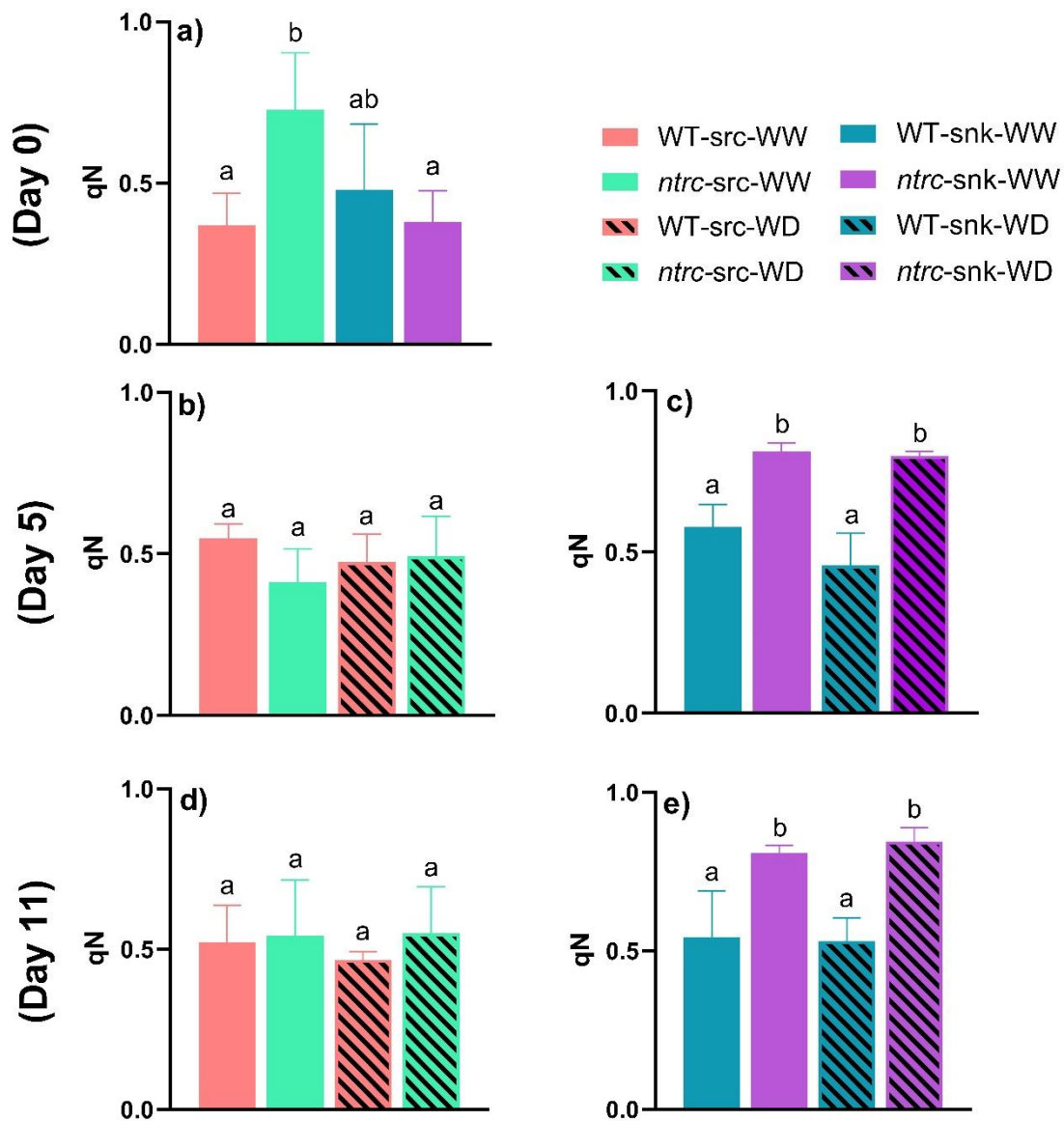
Figure 5. Chlorophyll a fluorescence analysis in wild type and ntrc mutant subjected to well-watered (WW) or water deficit (WD) conditions for 0, 5 and 11 days. qN, non-photochemical quenching of inconstant chlorophyll fluorescence was determined in source and sink leaves of both genotypes at the days 0 (graph a), 5 (graph b, c) and 11 (graph d, e) of the experiment. Lined graphs represent WD-treated plants. Different letters indicate significant difference among treatments and/or genotypes according to ANOVA and Tukey's test (P <0.05) (n = 4).
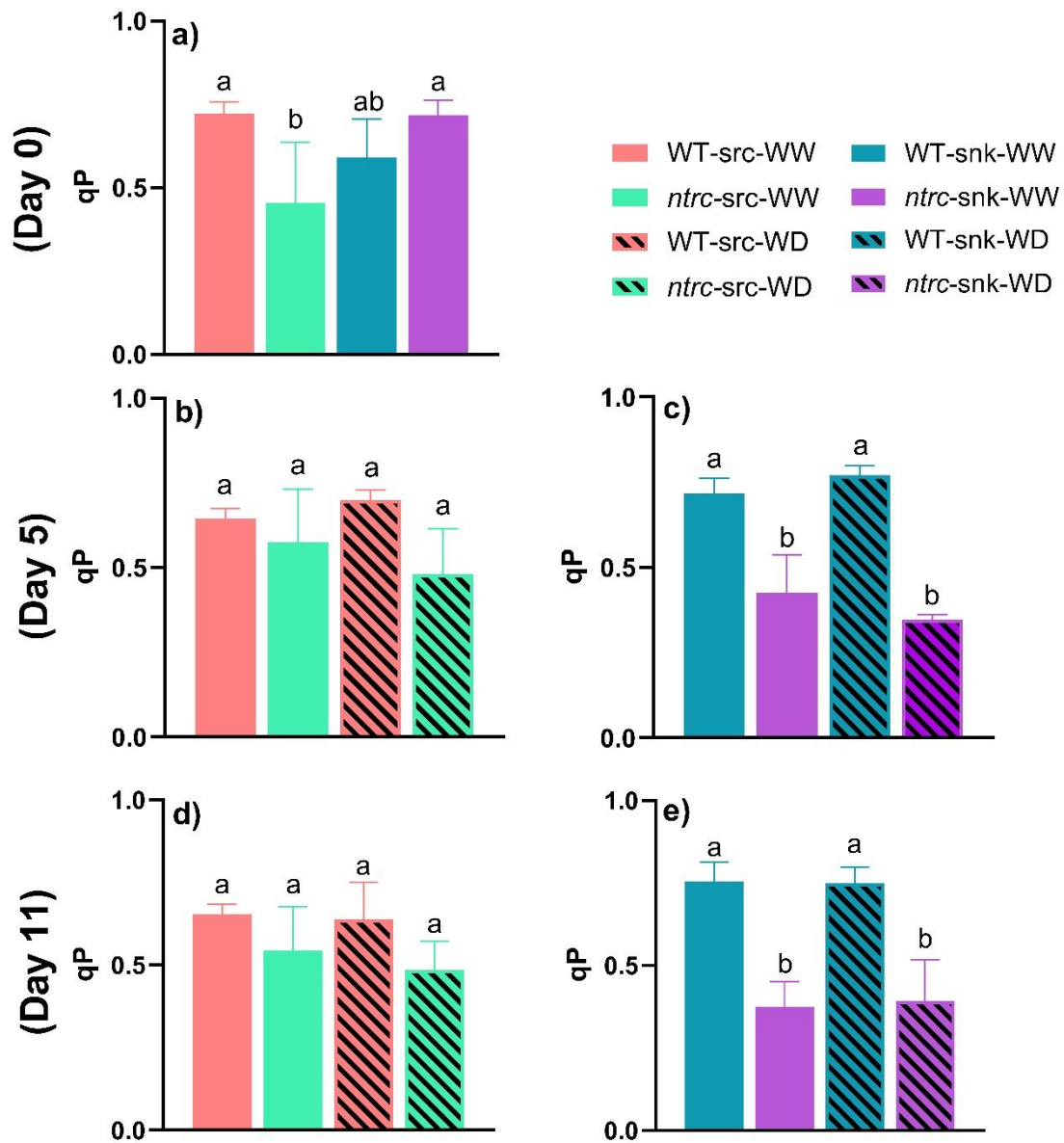
Figure 6. Chlorophyll a fluorescence analysis in wild type and ntrc mutant subjected to well-watered (WW) or water deficit (WD) conditions for 0, 5 and 11 days. qP, coefficient of photochemical quenching was determined in source and sink leaves of both genotypes at the days 0 (graph a), 5 (graph b, c) and 11 (graph d, e) of the experiment. Lined graphs represent WD-treated plants. Different letters indicate significant difference among treatments and/or genotypes according to ANOVA and Tukey's test (P <0.05) (n = 4).
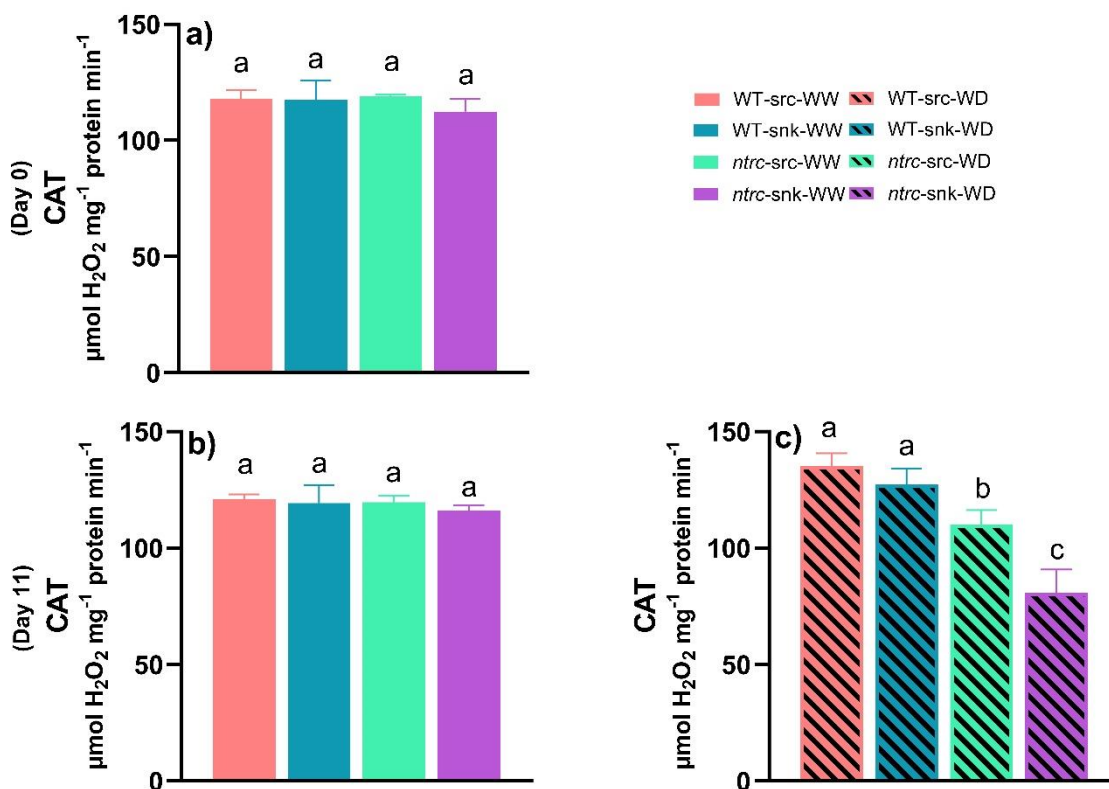
Figure 7. Catalase (CAT) activity in source and sink leaves of WT and ntrc at day 0 (a) and 11 (b-c) under WW and WD condition. Lined graphs represent WD-treated plants. Different letters indicate significant difference among treatments and/or genotypes according to ANOVA and Tukey's test (P <0.05) (n = 6).
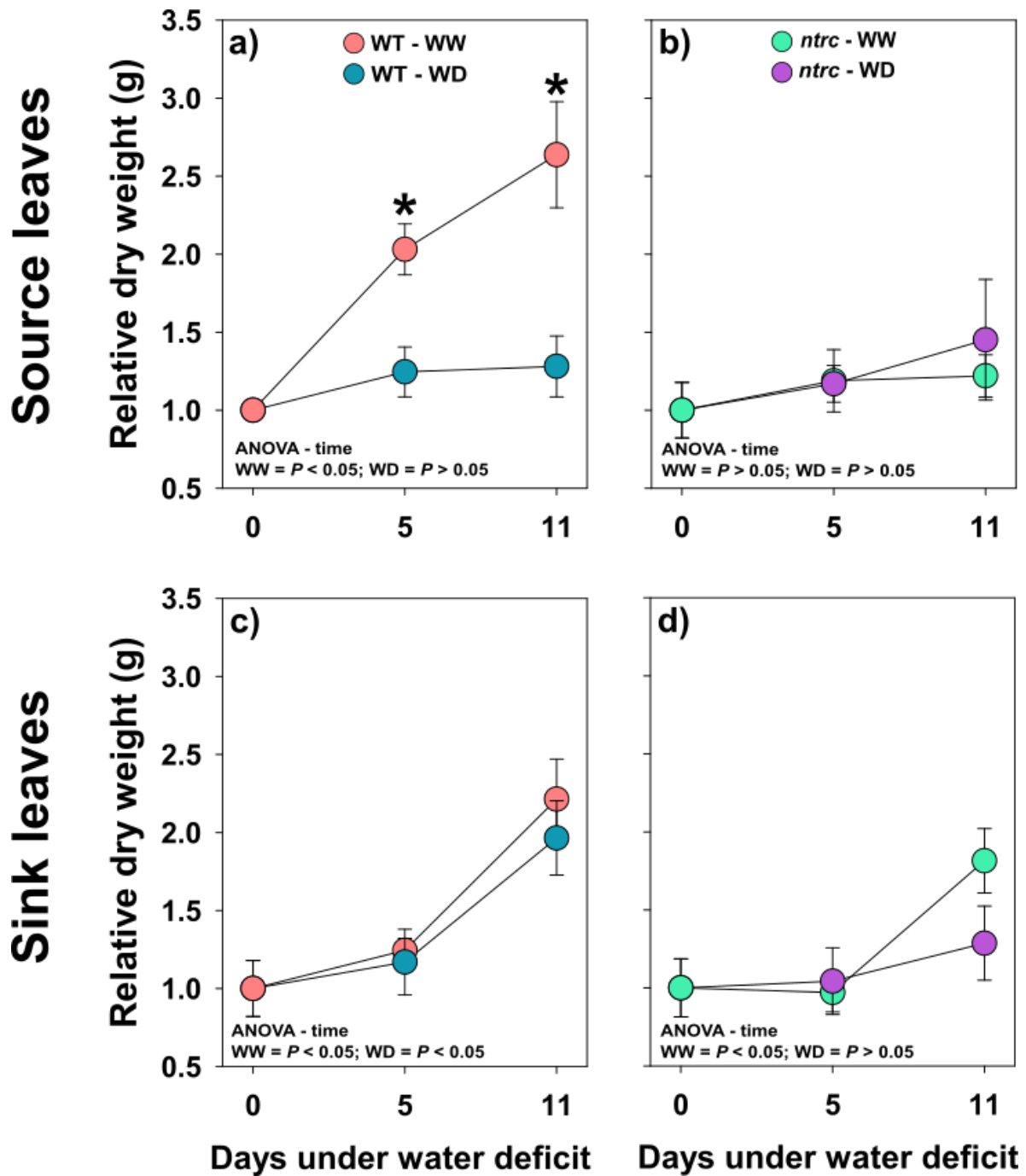
Figure 8. Relative dry weight (DW) of source and sink leaves from wild type (WT) and ntrc plants subjected to well-watered (WW) or water deficit (WD) conditions for 0, 5 and 11 days. The DW of sink and source leaves were normalized according to the values observed at the day 0 within each leaf type and genotype. The increase in DW over time was analysed by analysis of variance (ANOVA). P-values lower than 0.05 indicates significant increase in DW over the period analysed (from 0 to 11 days). Asterisks (*) indicate significant difference between WW and WD treatments in each day, genotype, and leaf type by Student's t-test ($P < 0.05$) ($n = 6$).
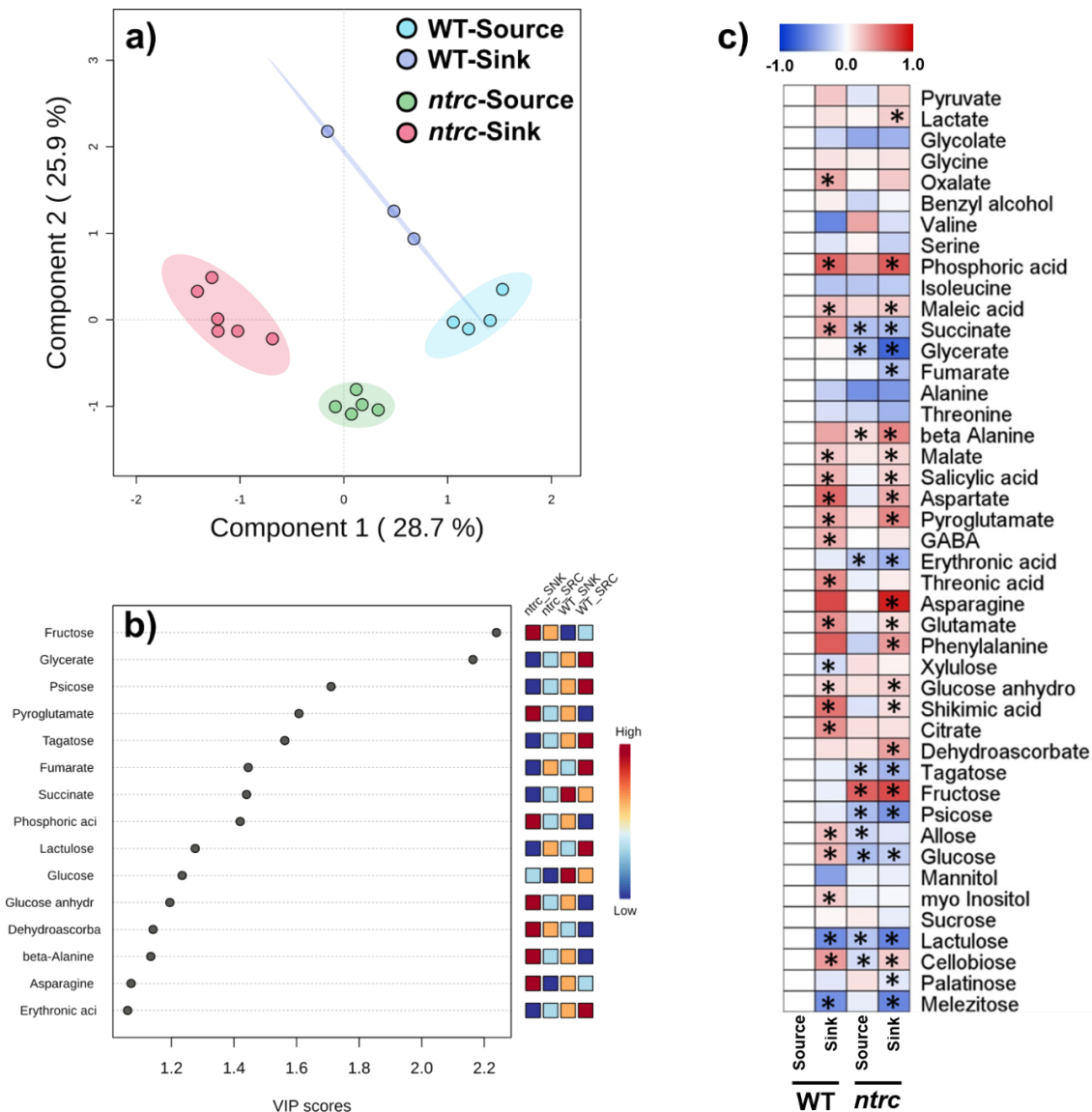
Figure 9. Partial least square-discriminant analysis (PLS-DA) and heat map representation of metabolite profiling analysis from source and sink leaves of wild type (WT) and the ntrc mutant. This data refers to well-watered (WW) plants harvested at the day 0. a) Graph representation of the PLS-DA. b) Variable importance in projection (VIP) scores of selected metabolites ranked from top to down as the most important for the PLS-DA model. c) Heat map demonstrating the level of metabolites in source and sink leaves of both genotypes. The heat map was created by normalizing the data according to the levels observed in WT source leaves followed by $\log_2$ transformation. Red and blue colors indicate increase and decrease in the level of the metabolite in comparison with WT source leaves, respectively. Asterisks (*) indicate metabolites that are significantly different from WT source leaves by Student's t-test ($P < 0.05$). Heat map was created using MEV software, while PLS-DA was carried out using the Metaboanalyst platform.

Figure 10. Partial least square-discriminant analysis (PLS-DA) and heat map representation of metabolite profiling analysis from source and sink leaves of wild type (WT) and the ntrc mutant. This data refers to well-watered (WW) plants harvested at the day 11. a) Graph representation of the PLS-DA. b) Variable importance in projection (VIP) scores of selected metabolites ranked from top to down as the most important for the PLS-DA model. c) Heat map demonstrating the level of metabolites in source and sink leaves of both genotypes. The heat map was created by normalizing the data according to the levels observed in WT source leaves followed by $\log_2$ transformation. Red and blue colors indicate increase and decrease in the level of the metabolite in comparison with WT source leaves, respectively. Asterisks (*) indicate metabolites that are significantly different from WT source leaves by Student's t-test ($P < 0.05$). Heat map was created using MEV software, while PLS-DA was carried out using the Metaboanalyst platform.

Figure 11. Partial least square-discriminant analysis (PLS-DA) and heat map representation of metabolite profiling analysis from source and sink leaves of wild type (WT) and the ntrc mutant. This data refers to water deficit (WD) plants harvested at the day 11. a) Graph representation of the PLS-DA. b) Variable importance in projection (VIP) scores of selected metabolites ranked from top to down as the most important for the PLS-DA model. c) Heat map demonstrating the level of metabolites in source and sink leaves of both genotypes. The heat map was created by normalizing the data according to the levels observed in WT source leaves followed by $\log_2$ transformation. Red and blue colors indicate increase and decrease in the level of the metabolite in comparison with WT source leaves, respectively. Asterisks (*) indicate metabolites that are significantly different from WT source leaves by Student's t-test ($P < 0.05$). Heat map was created using MEV software, while PLS-DA was carried out using the Metaboanalyst platform.

Figure 12. Principal component analysis (PCA) using all data of this work source and sink leaves of wild type (WT) and the ntrc mutant subjected to 11 days of well-watered (WW) or water deficit (WD) conditions. a-b) Graph representation of the PCA. c-d) Biplot analysis of the PCA. This analysis was carried out the Metaboanalyst platform.
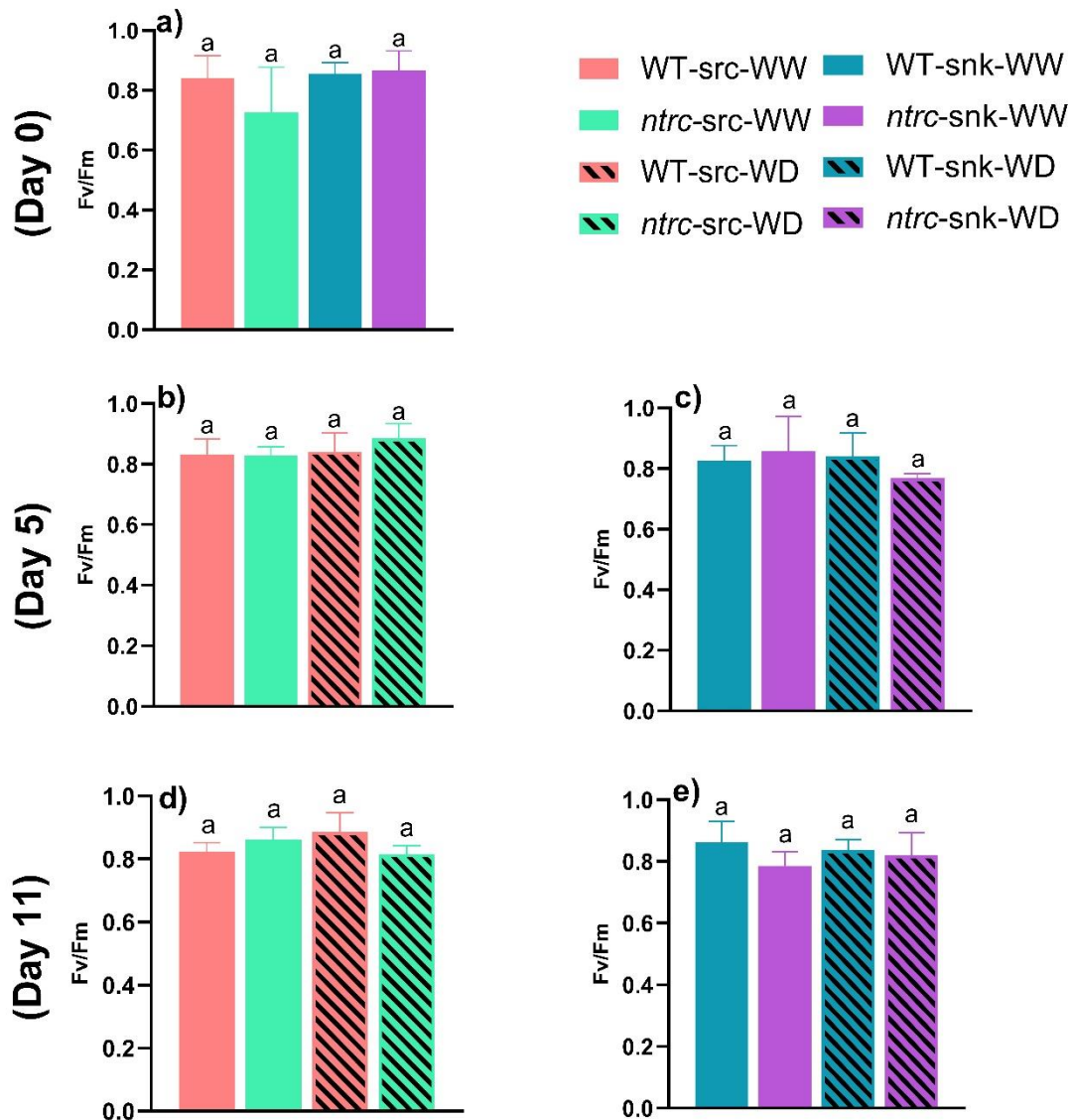
Figure S1. Chlorophyll a fluorescence analysis in wild type and ntrc mutant subjected to well-watered (WW) or water deficit (WD) conditions for 0, 5 and 11 days. The F_v/F_m, maximum quantum yield of PSII was determined in source and sink leaves of both genotypes at the days 0 (graph a), 5 (graph b, c) and 11 (graph d, e) of the experiment. Lined graphs represent WD-treated plants. Different letters indicate significant difference among treatments and/or genotypes according to ANOVA and Tukey's test (P <0.05) (n = 4).
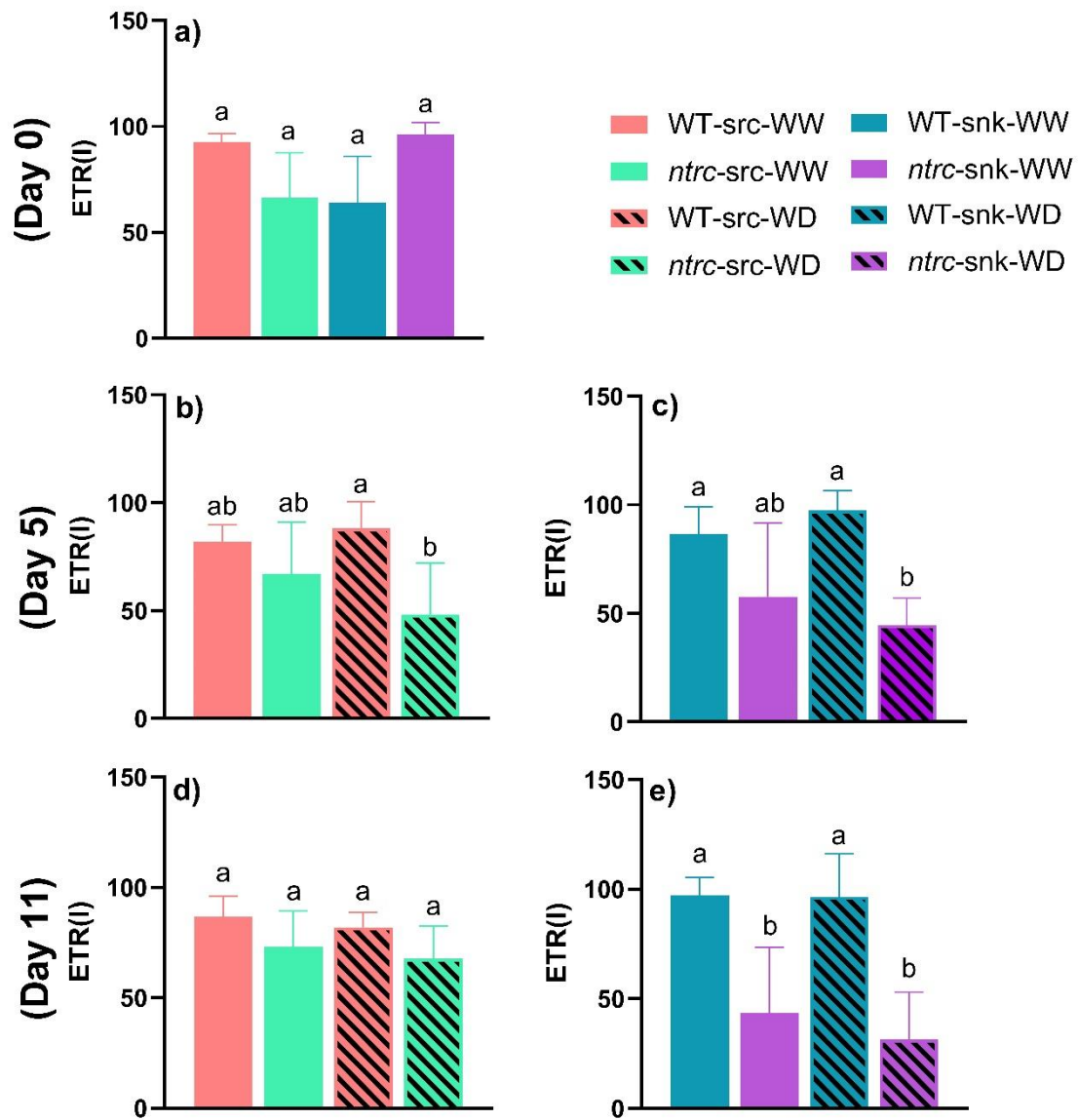
Figure S2. Chlorophyll a fluorescence analysis in wild type and ntrc mutant subjected to well-watered (WW) or water deficit (WD) conditions for 0, 5 and 11 days. ETRI, photosynthetic electron flow through PSI was determined in source and sink leaves of both genotypes at the days 0 (graph a), 5 (graph b, c) and 11 (graph d, e) of the experiment. Lined graphs represent WD-treated plants. Different letters indicate significant difference among treatments and/or genotypes according to ANOVA and Tukey's test (P <0.05) (n = 4).
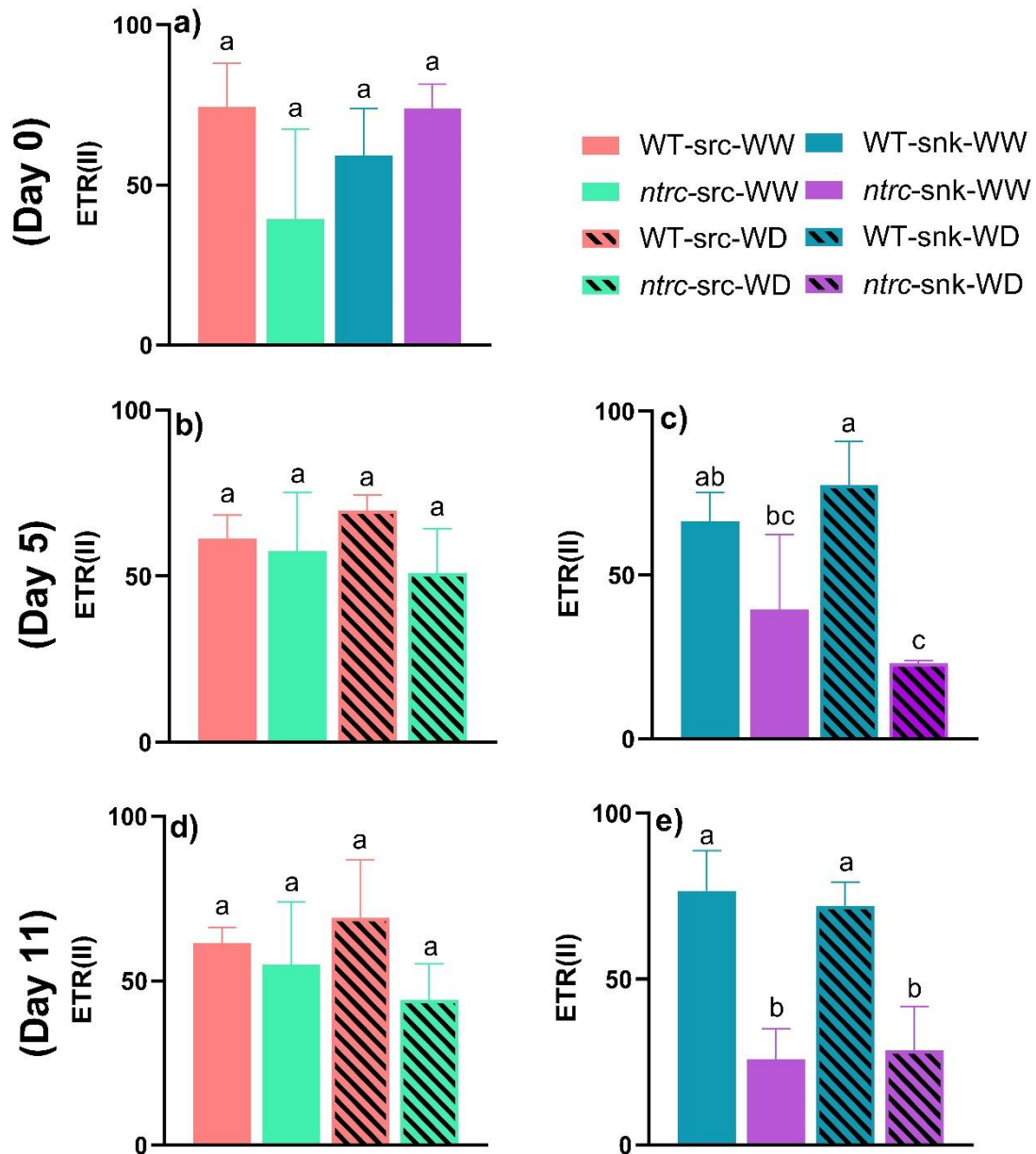
Figure S3. Chlorophyll a fluorescence analysis in wild type and ntrc mutant subjected to well-watered (WW) or water deficit (WD) conditions for 0, 5 and 11 days. ETRII, photosynthetic electron flow through PSII was determined in source and sink leaves of both genotypes at the days 0 (graph a), 5 (graph b, c) and 11 (graph d, e) of the experiment. Lined graphs represent WD-treated plants. Different letters indicate significant difference among treatments and/or genotypes according to ANOVA and Tukey's test (P <0.05) (n = 4).
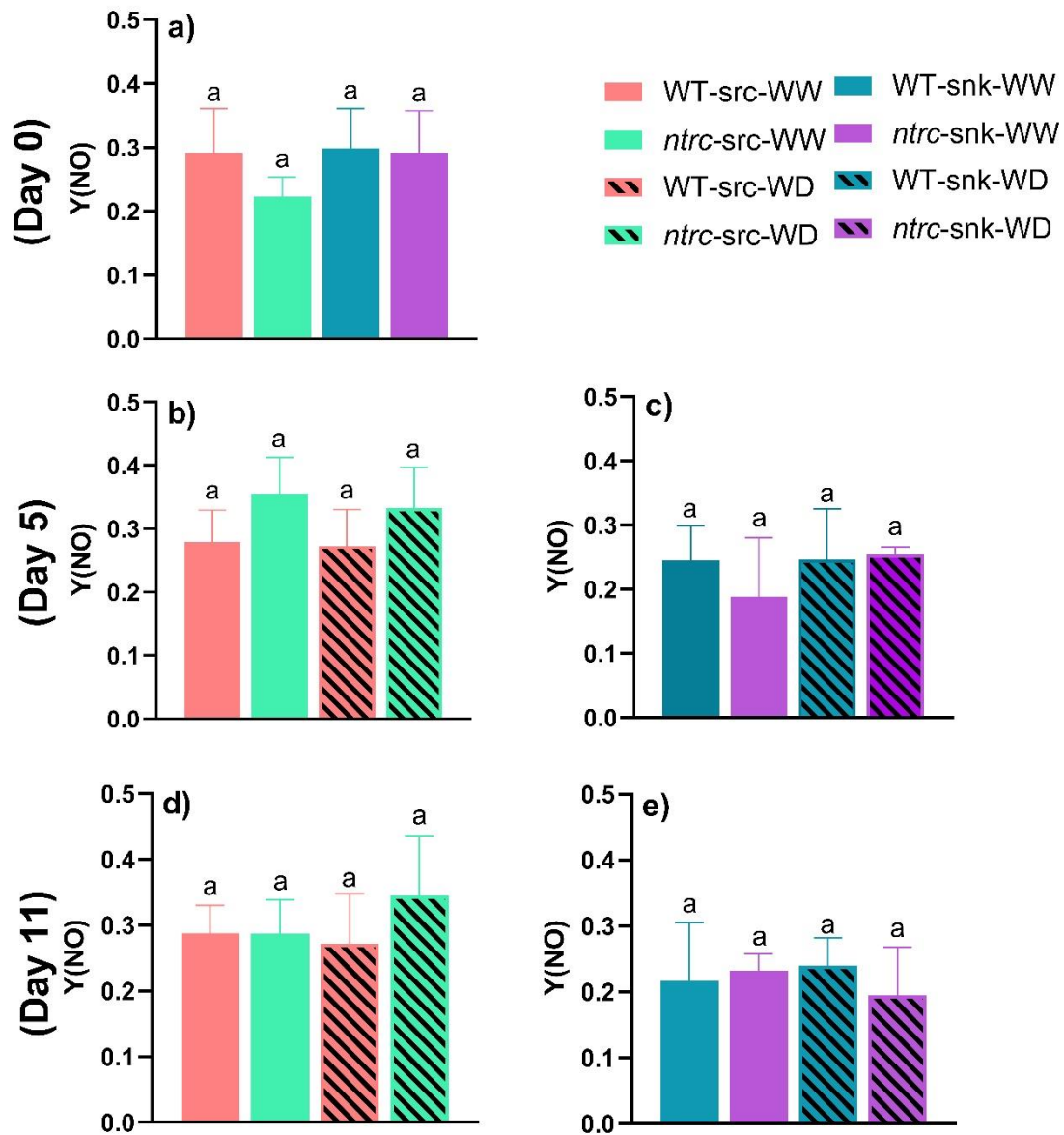
Figure S4. Chlorophyll a fluorescence analysis in wild type and ntrc mutant subjected to well-watered (WW) or water deficit (WD) conditions for 0, 5 and 11 days. Y(NO), fraction of energy that is passively dissipated in form of heat and fluorescence was determined in source and sink leaves of both genotypes at the days 0 (graph a), 5 (graph b, c) and 11 (graph d, e) of the experiment. Lined graphs represent WD-treated plants. Different letters indicate significant difference among treatments and/or genotypes according to ANOVA and Tukey's test (P <0.05) (n = 4).
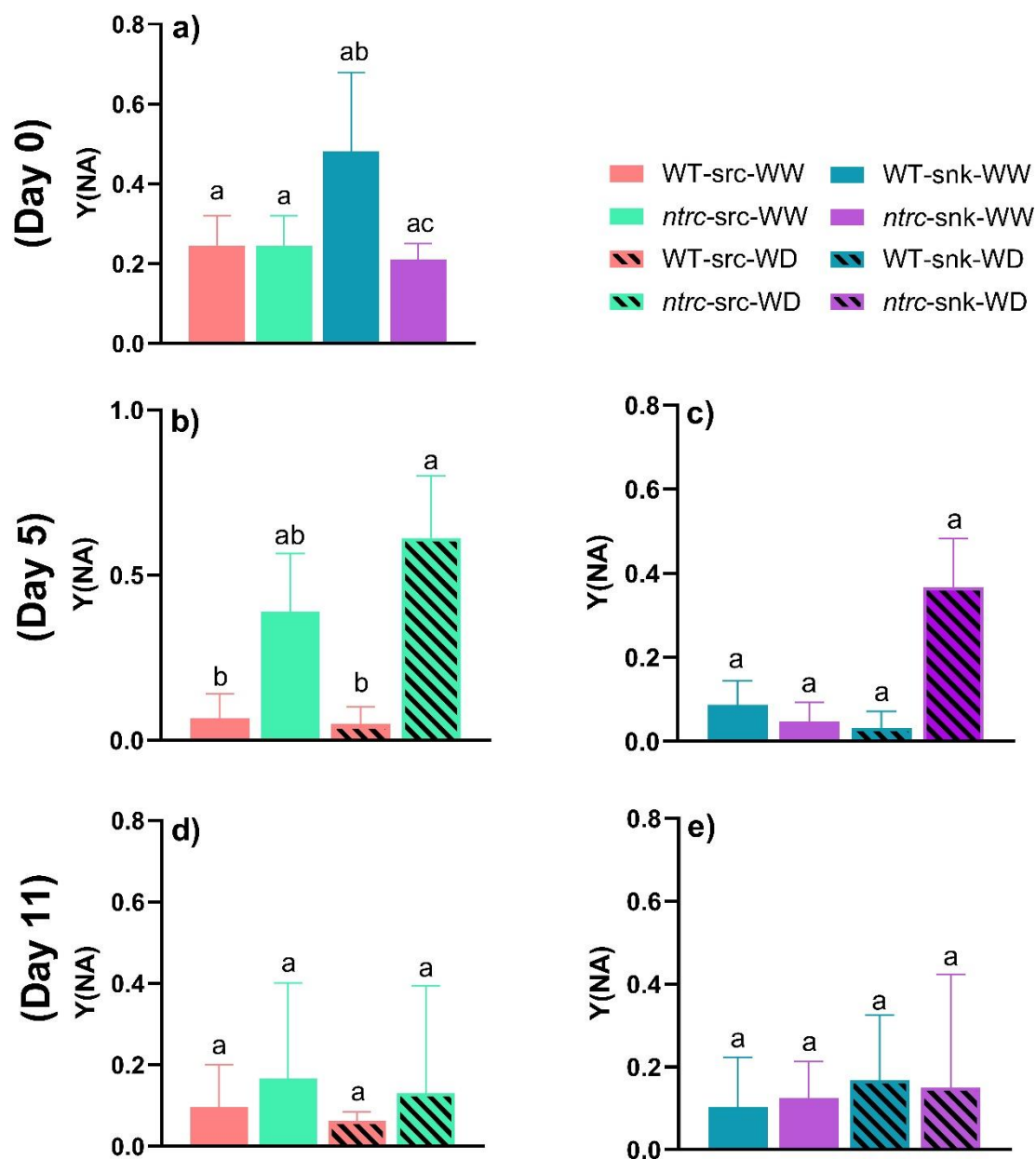
Figure S5. Chlorophyll a fluorescence analysis in wild type and ntrc mutant subjected to well-watered (WW) or water deficit (WD) conditions for 0, 5 and 11 days. Y(NA), fraction of overall P700 that cannot be oxidized in a given state was determined in source and sink leaves of both genotypes at the days 0 (graph a), 5 (graph b, c) and 11 (graph d, e) of the experiment. Lined graphs represent WD-treated plants. Different letters indicate significant difference among treatments and/or genotypes according to ANOVA and Tukey's test (P <0.05) (n = 4).
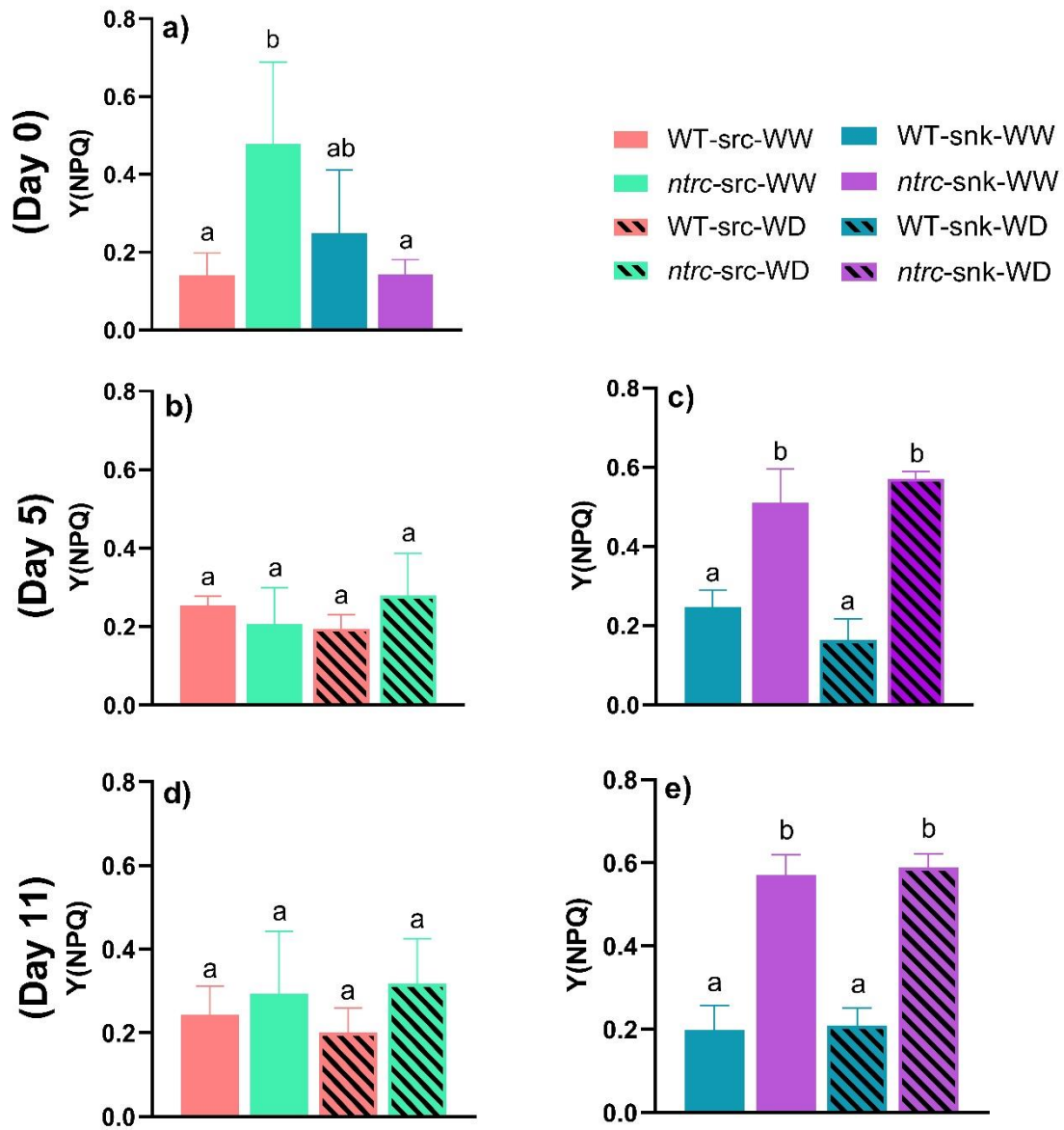
Figure S6. Chlorophyll a fluorescence analysis in wild type and ntrc mutant subjected to well-watered (WW) or water deficit (WD) conditions for 0, 5 and 11 days. Y(NPQ), fraction of energy dissipated in form of heat via the regulated non-photochemical quenching mechanism was determined in source and sink leaves of both genotypes at the days 0 (graph a), 5 (graph b, c) and 11 (graph d, e) of the experiment. Lined graphs represent WD-treated plants. Different letters indicate significant difference among treatments and/or genotypes according to ANOVA and Tukey's test (P <0.05) (n = 4).
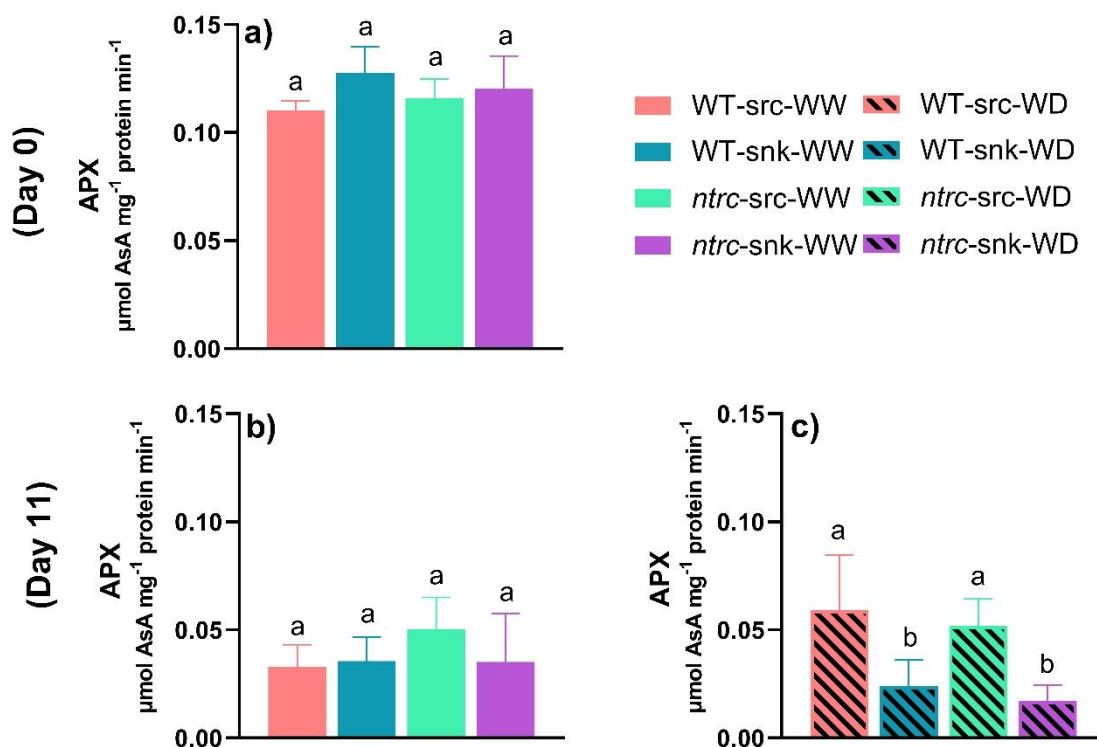
Figure S7. Ascorbate peroxidase (APX) activity in source and sink leaves of WT and ntrc at day 0 (a) and 11 (b-c) under WW and WD condition. Lined graphs represent WD-treated plants. Different letters indicate significant difference among treatments and/or genotypes according to ANOVA and Tukey's test (P <0.05) (n = 6).
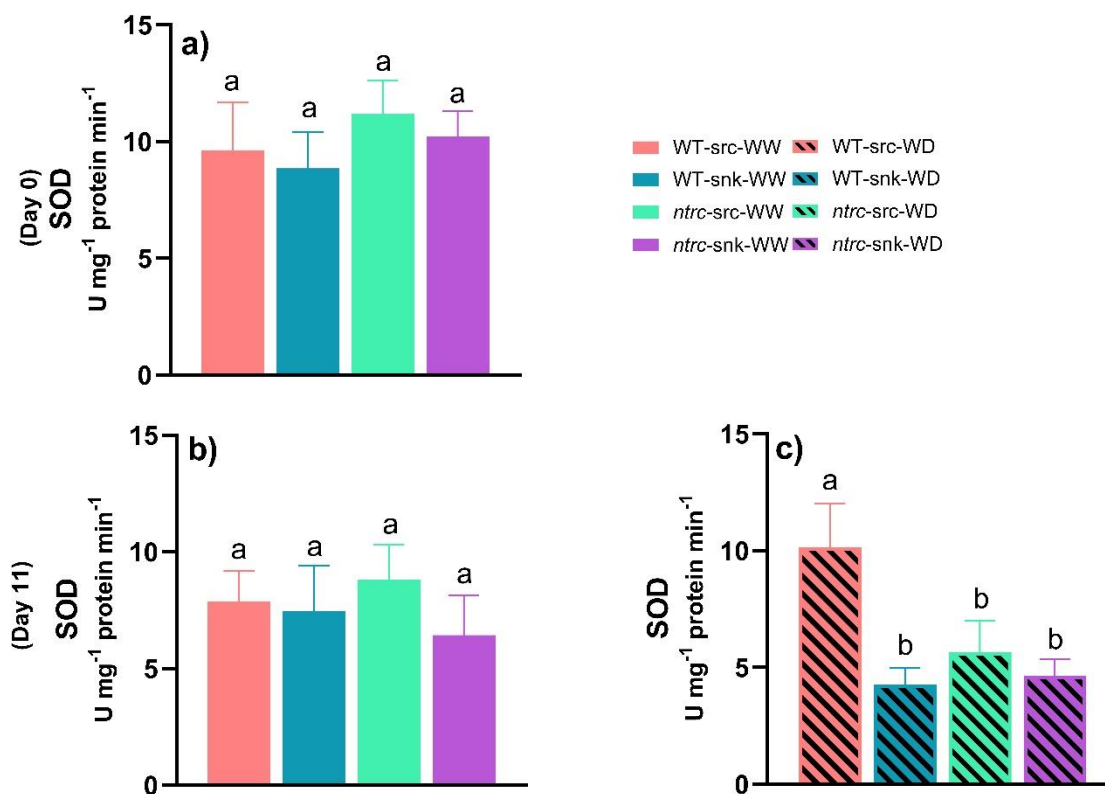
Figure S8. Superoxide dismutase (SOD) activity in source and sink leaves of WT and ntrc at day 0 (a) and 11 (b-c) under WW and WD condition. Lined graphs represent WD-treated plants. Different letters indicate significant difference among treatments and/or genotypes according to ANOVA and Tukey's test (P <0.05) (n = 6).
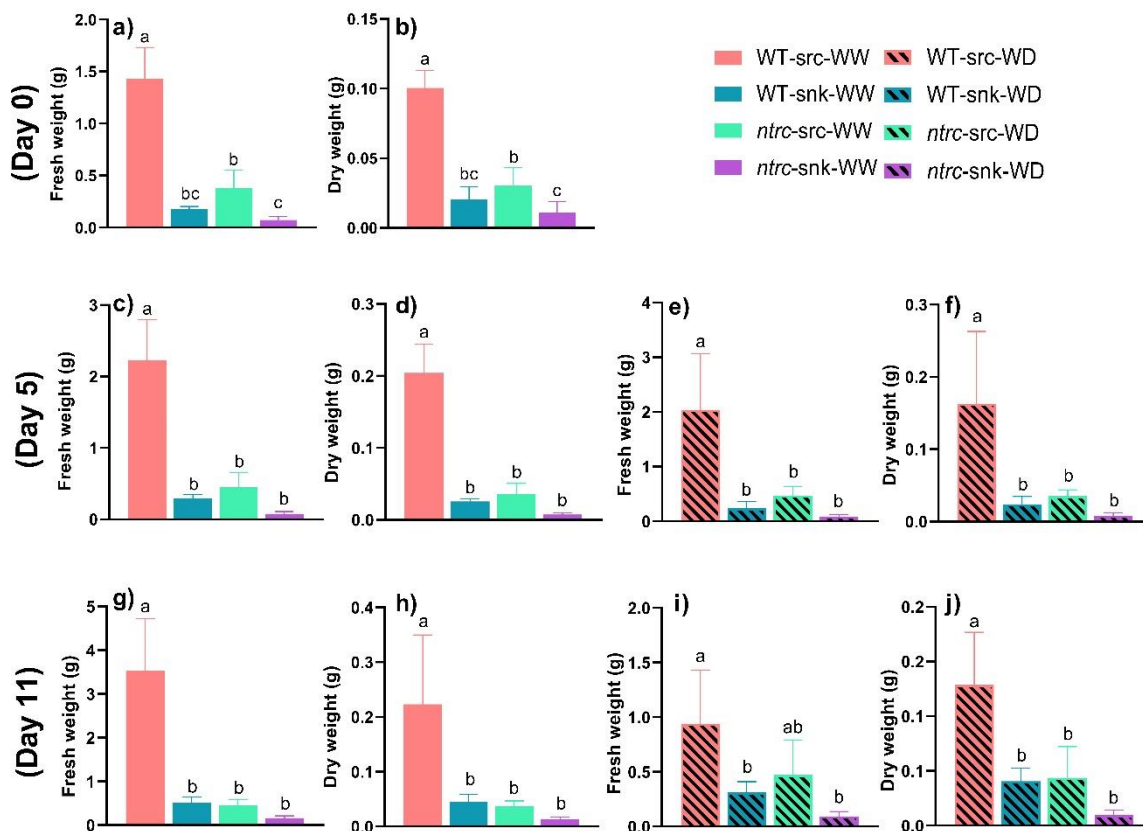
Figure S9. Growth analysis in wild type (WT) and ntrc mutant subjected to well-watered (WW) or water deficit (WD) conditions for 0, 5 and 11 days. The fresh (FW) and the dry weight (DW) of source and sink leaves were determined at the days 0 (graph a, b), 5 (graph c, d, e and f) and 11 (graph g, h, i and j) of the experiment. Lined graphs represent WD-treated plants. Different letters indicate significant difference among treatments and/or genotypes according to ANOVA and Tukey's test (P <0.05) (n = 6).
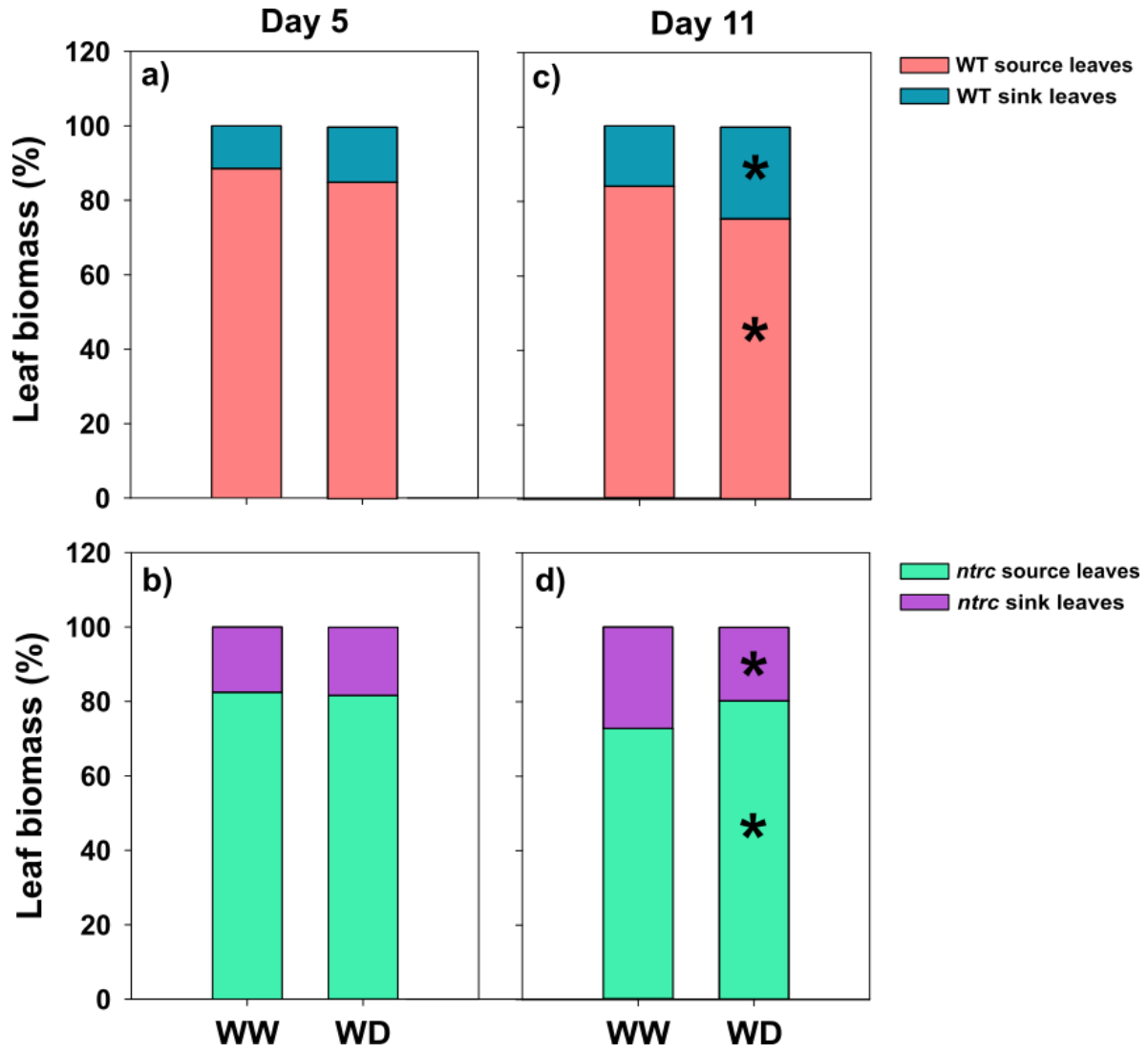
Figure S10. Relative (%) contribution of source and sink leaves for the total rosette dry weight (DW) in wild type (WT) and ntrc plants subjected to well-watered (WW) or water deficit (WD) conditions for 5 and 11 days. The total biomass (100 %) was considered as the sum of source and sink DW. Asterisks (*) indicate significant difference between WW and WD treatments in each day, genotype, and leaf type by Student's t-test (P < 0.05).
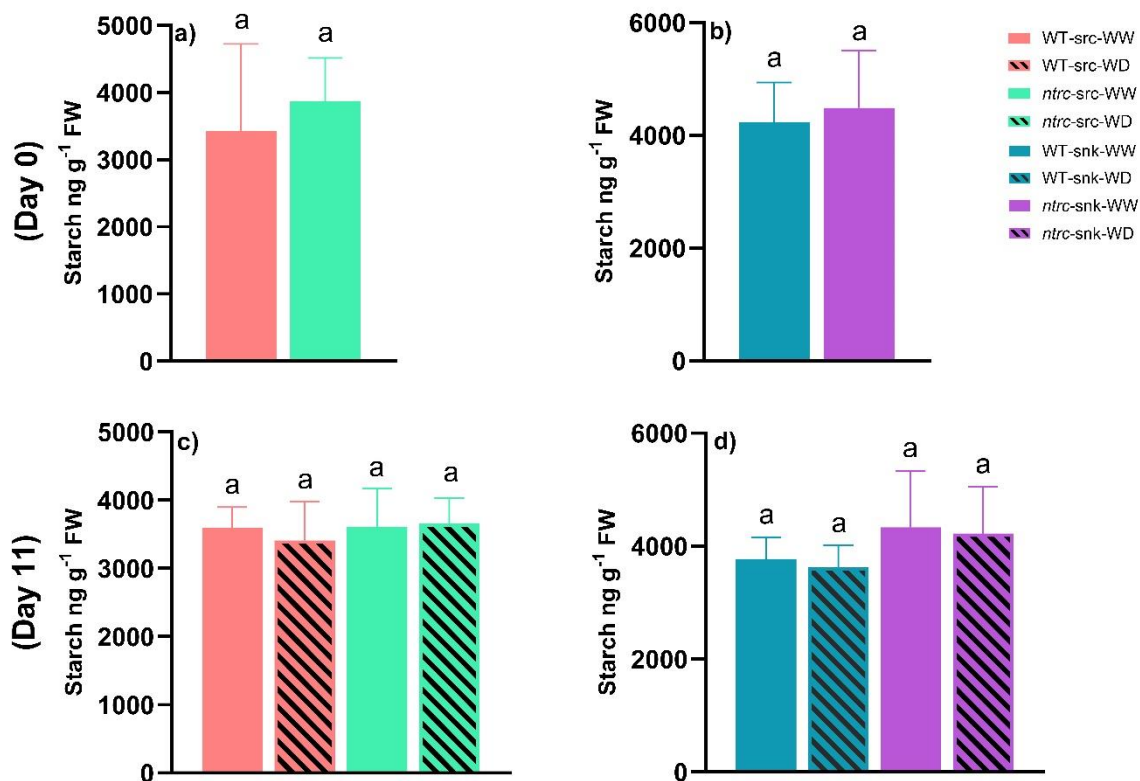
Figure S11. Concentration of starch (ng g-1 FW) in source and sink leaves of wild type (WT) and ntrc mutant subjected to well-watered (WW) or water deficit (WD) conditions for 0 (a, b) and 11 (c, d) days. Starch was determined in source and sink leaves of both genotypes at the days 0 (a, b) and 11 (c, d) of the experiment. Lined graphs represent WD-treated plants. Significant differences among the treatments are indicated by different letter, as determined by Student's t-test or ANOVA and Dunnett test ($P < 0.05$) (n=4).

Supplemental table 1

NTRC (AT2G41680)

Primer	Sequence	Reference
Forward	5'-TATTGAGCAACACCAAGGGAC-3'	(THORMÄHLEN; MEITZEL; GROYSMAN; ÖCHSNER *et al.*, 2015)
Reverse	5'-CATAATTCCAGCTGCTTCAGC-3'	
T-DNA	5'-ATTTTGCCGATTTCGGAAC-3'	

5. CHAPTER 2:

Manuscript submitted to the *New Phytologist* journal as a Letter

Letter

Blue light-induced stomatal opening is associated to changes in primary metabolism but not to starch breakdown in both cowpea and tobacco guard cells

Humaira Bahadar[1], Francisco Bruno S. Freire[1], Eva Gomes Morais[1], Valéria F. Lima[1], Leticia dos Anjos[1], Danilo M. Daloso[1]

[1]Departamento de Bioquímica e Biologia Molecular, Universidade Federal do Ceará, Fortaleza 60451-970, Brasil.

*Correspondence to: daloso@ufc.br

5.1 Introduction

Plants have many microscopic adjustable pores surrounded by two guard cells on their aerial surfaces named stomata. Changes in guard cell metabolism regulates the opening or closure of stomatal pores in response to endogenous and environmental cues (Sussmilch *et al.*, 2019). Stomatal opening allows the influx of CO_2 for photosynthesis and the efflux of water through transpiration. Thus, whilst stomatal opening is important to optimize photosynthesis and consequently plant growth, stomatal closure is key to avoid dehydration during drought periods (Lima *et al.*, 2018). Understanding the mechanisms that regulate the interplay between photosynthesis and stomatal movements has directly implications for plant metabolic engineering, especially in the current climate change scenario (Evans & Lawson, 2020). However, the regulation of stomatal movements is highly complex, involving autonomous responses of guard cell such as direct perception of light and CO_2 as well as responses triggered by stimulus from other cell types, especially subsidiary (whenever present) and mesophyll cells (Flütsch & Santelia, 2021).

Stomatal opening is induced by light, with specific mechanisms and signalling pathways that regulate responses to red (RL) and blue light (BL) (Shimazaki *et al.*, 2007). Initial studies suggested RL's role might be associated to signals derived from mesophyll photosynthetic activity (Mott *et al.*, 2008; Mott, 2009). Indeed, recent results showed that RL directly induce the phosphorylation of guard cell plasma membrane H^+-ATPases in a photosynthesis-dependent manner (Ando & Kinoshita, 2018). Similarly, BL-induced stomatal opening involves H^+-ATPases activation in guard cell plasma membrane, in a process dependent on the phototropin-mediated BL perception. This activation establishes a H^+ gradient across guard cell plasma membrane, facilitating the influx of K^+ and anions into the guard cells (Ding *et al.*, 2021). Simultaneously, metabolic changes occur within guard cells to produce osmolytes and the energy needed for (i) the metabolism, (ii) the H^+-ATPases activities and (iii) the function of several ion channels present at guard cell tonoplast and plasma membranes (Daloso *et al.*, 2017). It is expected therefore that substantial changes occur in guard cell metabolism after BL perception. However, while the BL signalling pathway is relatively well-described, the metabolic alterations triggered by this stimulus remain poorly described.

It has been long proposed that the starch breakdown within guard cells is an important mechanism during BL-induced stomatal opening (Outlaw, 2003). This idea is supported by findings showing that (i) starch content was quantitatively related to stomatal aperture in *Vicia faba*, (ii) BL-induced stomatal opening was disrupted in starch-deficient guard cells of an Arabidopsis mutant (Lasceve *et al.*, 1997), and that (iii) the Arabidopsis double mutant *amy3 bam1* (α-amylase 3, β-amylase 1) is impaired in both starch degradation within guard cells and in BL-induced stomatal opening (Horrer *et al.*, 2016; Flütsch *et al.*, 2020). These studies suggest that starch mobilization upon BL perception plays an important role for a rapid and efficient stomatal opening. However, no study to date has performed a detailed metabolic characterization of guard cells during the BL-induced stomatal opening. Furthermore, previous study showed that guard cell starch is not degraded in the first 40 min after the dark-to-white light transition in tobacco (Daloso *et al.*, 2015). It remains unclear, therefore, which metabolic pathways are activated after the BL-induced stomatal opening and starch degradation in guard cells and whether similar mechanisms occur in plant species other than Arabidopsis.

5.2 Results and discussion

Blue light-induced stomatal opening is not associated with changes in starch concentration in both cowpea and tobacco guard cells

Aiming to investigate the dynamics of guard cell metabolism during BL-induced stomatal opening, we collected a pool of guard cell enriched epidermal fragments (herein called guard cells) at pre-dawn and subjected them to BL for 0, 10, 20, 30, 40 and 60 min. Stomatal aperture increased over time under BL, while the concentration of guard cell starch did not change (Fig. 1a-d). These results do not corroborate previous findings in Arabidopsis guard cells, in which a rapid decrease in starch level (measured as starch granule area from microscopic images) was observed in the first 60 min under BL (Horrer *et al.*, 2016; Flütsch *et al.*, 2020). It is important to highlight that our starch analysis was carried out using a well-established enzymatic assay that provides the concentration of starch in the tissue (Trethewey *et al.*, 1998), in contrast to the semi-quantitative analysis performed by Horrer and colleagues. These discrepancies could be also associated to the experimental procedure used here, in which a pool of guard cell enriched epidermal fragments was obtained and stored in a hypertonic solution before the stomatal kinetic experiment, a procedure made to collect sufficient guard cells for metabolomics analysis (Daloso *et al.*, 2015). To address

this possibility, dark-adapted plants were subjected to BL and guard cells were isolated and immediately frozen after 0 and 60 min under BL, eliminating the step of pooling guard cells in a hypertonic solution. The results were consistent with the first experiment, with no difference in starch concentration between guard cells harvested at pre-dawn (0 min) and 60 min under BL (Fig. S1a-b). These findings suggest that BL-induced stomatal opening does not involve starch remobilization in cowpea and tobacco guard cells within the first 60 min upon BL. In agreement with our observations, starch degradation was also not observed in tobacco guard cells during the dark-to-white light transition (Daloso *et al.*, 2015), suggesting a species-specific mechanism in starch metabolism regulation. Alternatively, the dynamic nature of guard cell carbohydrate metabolism and a potential rapid starch turnover, with simultaneous starch synthesis and degradation in guard cells, may have masked subtle changes in starch concentration that were not detected by our analysis.

Guard cell primary metabolism is altered by blue light

We next carried out a metabolite profiling analysis to unravel the BL-induced changes in guard cell primary metabolism using a well-established gas chromatography mass spectrometry approach (Lisec *et al.*, 2006). Only three metabolites (glycerol, threonine, and 3-caffeoylquinic acid) increased over time in tobacco guard cells (Fig. 2a). By contrast, six metabolites (glycine, β-alanine, serine, aspartate, pyroglutamate and maltotriose) increased over time in cowpea guard cells, while lactate showed a lower level at 20 min compared to time 0 min (Fig. 2b). Although these results suggest minor BL-induced changes in guard cell metabolism, especially in tobacco, partial least square-discriminant analysis (PLS-DA) indicate substantial alterations in metabolism in both genotypes (Fig. 2c-d), as evidenced by the separation of certain time points from time 0 min. Notably, the separation among the time points was clearly time-dependent in cowpea, with the last time points (40 and 60 min) more separated from the time 0 min (Fig. 2d). In contrast, tobacco guard cells showed three distinct clusters (Clt) composed by the times 0 min (Clt1), 40 min (Clt2) and 20, 30 and 60 min (Clt3), with time 10 min positioned between 0 and 40 min (Fig. 2c).

The variable importance in projection (VIP) list highlights the metabolites that mostly contributed to the observed separation in PLS-DA, in which metabolites with VIP score higher than 1 are considered good representatives (Xia & Wishart, 2011). Whilst cowpea metabolites with

VIP score higher than 1 showed a pattern of continuous increase or decrease over time, tobacco metabolites showed a highly heterogenous dynamic over time (Fig. S2a-b). For instance, the level of all metabolites in the VIP score list increased from 0 to 30 min, decreased from 30 to 40 min and increased again from 40 to 60 min in tobacco (Fig. S2a). Indeed, previous results highlight that tobacco guard cell metabolism is highly dynamic (Daloso *et al.*, 2015, 2016) and substantially altered by light exposure (Lima *et al.*, 2023). Furthermore, light-triggered specific metabolic responses in guard cells appear distinct from those observed in mesophyll cells (Misra *et al.*, 2015b; Robaina-Estévez *et al.*, 2017; Daubermann *et al.*, 2024), suggesting a specific metabolic predisposition in guard cells (Misra *et al.*, 2015a; Daloso *et al.*, 2023). This highlights the particularity and complexity of guard cell metabolism, that seems to be in a constant non-steady state condition, which makes difficult to understand its functioning and modelling its metabolism.

Metabolites associated with the dynamic of the blue light-induced stomatal opening

In order to investigate which metabolites are associated with the dynamic of BL-induced stomatal opening, we employed a maximum-minimum transformation of both stomatal aperture and metabolite profiling data (Cândido-Sobrinho *et al.*, 2022) and carried out a K-means clustering analysis, which combine parameters with similar pattern of increase/decrease throughout time (Szecowka *et al.*, 2013). Seven clusters (Clt1-7) were generated for each species. The composition and the dynamics of metabolite accumulation/degradation diverged substantially between tobacco and cowpea (Figs. 3-4). In tobacco, stomatal aperture parameters (Clt3) were not clustered with any metabolite and none of the other clusters have a clear opposite dynamic than stomatal aperture. The dynamics of the Clt1, 2, 4, 5, 6 and 7 exhibited high variability over time (Fig. 3), consistent with previous results (Daloso *et al.*, 2015). By contrast, stomatal aperture parameters clustered with aspartate, maltotriose, pyroglutamate, serine and urea in cowpea (see Clt7) (Fig. 4). The maximum level of fumarate was observed at the time 0 min, decreased at 10 min, and then remained relatively constant until 60 min (Clt2). Interestingly, Clt4 showed an opposite dynamic while the clusters 1, 3, 5 and 6 showed a similar trend to Clt7 from 20 to 60 min (Fig. 4), which is exactly the time in which stomatal aperture becomes significantly different from the time 0 min in cowpea (Fig. 1b). This analysis indicates that sucrose and glutamate (Clt4) are degraded while glucose, maltotriose and pyroglutamate are synthesized during the BL-induced stomatal opening in cowpea. Further

analysis showed negative correlations between sucrose and stomatal aperture parameters in cowpea while certain sugars and amino acids were positively correlated (Fig. S3). In tobacco, 3-caffeoylquinic acid, caffeic acid, lactate, urea, proline and glycine showed positive correlations with stomatal aperture parameters (Fig. S4).

These results suggest that the dynamics of the BL-induced stomatal opening are associated with different metabolic changes in tobacco and cowpea. Interestingly, sucrose and glucose were positively correlated with metabolites of, or associated to, the tricarboxylic acid (TCA) cycle in both species (Fig. S3-4). The connection between sugars and TCA cycle-related metabolites has several precedents in the literature (Outlaw & Lowry, 1977; Tallman & Zeiger, 1988; Talbott & Zeiger, 1993; Daloso *et al.*, 2015). For instance, ^{13}C-sucrose labelling experiment showed that the carbons derived from sucrose are highly used to the synthesis of glutamine in Arabidopsis guard cells during white light-induced stomatal opening (Medeiros *et al.*, 2018). This result resembles those observed here in cowpea under BL, in which the levels of both sucrose and glutamate are reduced (Clt4) while pyroglutamate and glucose increased (Clt6-7) from 20 to 60 min (Fig. 4).

The activation of the glutamine synthetase (GS)/glutamate synthase (GOGAT) cycle toward glutamine synthesis could be a mechanism to stimulate the nitrogen assimilation and the synthesis of NO_3, an important K^+ counterion for guard cell osmoregulation (Guo *et al.*, 2003), or the activation of fumarase, given that glutamine is an allosteric activator of this enzyme (Zubimendi *et al.*, 2018). Additionally, it has been shown that glutamate can induce stomatal closure in Arabidopsis and *Vicia faba* (Yoshida *et al.*, 2016). It seems likely therefore that the degradation of glutamate is a mechanism that happens during stomatal opening conditions. Indeed, light exposure increased the photosynthetic fluxes toward this pathway in guard cells (Lima *et al.*, 2023), and this is not observed in leaves (Abadie *et al.*, 2017; Daubermann *et al.*, 2024). Further studies are needed to unveil the contribution of the GS/GOGAT pathway to the regulation of both guard cell metabolism and stomatal movements.

The blue light-induced changes in guard cell primary metabolism are species-specific and time-dependent

We next normalized the metabolite profiling data according to the control (0 min) of each genotype. PLS-DA using this relative data confirmed substantial differences in BL-induced metabolic changes between cowpea and tobacco, as evidenced by the clear separation of these

species by the component 1 in each time point (Fig. 5a-e). In cowpea, the levels of malate, citrate and fumarate was lower at 10, 20, 30 and 60 min compared to tobacco, while pyroglutamate and aspartate exhibited higher levels at 40 and 60 min (Fig. 5f-j). Several other metabolites showed lower levels in cowpea at 20, 30 and 60 min, while GABA and lactate at 10 min, glucose at 40 min and aspartate and pyroglutamate at 40 min and 60 min were higher in cowpea than tobacco (Fig. 5f-j). These results suggest that BL exposure altered guard cell primary metabolism in a species-specific and time-dependent manner.

Tobacco guard cell metabolic responses differ between blue and white light

Aiming to understand how specific are the metabolic responses to BL, we next compared our data with recent results from tobacco guard cells exposed to darkness or white light (WL) for 0, 10, 20 and 60 min (Lima *et al.*, 2023). Data from the 13 metabolites detected across all samples were normalized according to the control (0 min) of each genotype and treatment. Our analysis revealed distinct responses to BL in both cowpea and tobacco guard cells compared to tobacco under WL or darkness, as evidenced by the separation of these groups by the component 1 of the PLS-DAs (Fig. S5a-c). Interestingly, the levels of sucrose, glucose, and GABA were lower while lactate and fumarate were higher in tobacco guard cells under WL than BL (Fig. S5d). However, at 20 and 60 min, almost all 13 metabolites showed higher levels under BL than WL in tobacco, with the exception of fumarate (Fig. S5e-f). At 60 min, both cowpea and tobacco guard cells showed higher level of glycine, serine, GABA and glucose under BL than tobacco guard cells under dark or WL conditions. Furthermore, malate and fumarate preferentially accumulated in tobacco guard cells under BL and WL, respectively (Fig. S5f). These results suggest that guard cell metabolic responses depend on the light quality, which is expected given the particularities of the perception and signalling pathways associated with red, blue and green light wavelengths (Talbott *et al.*, 2006; Shimazaki *et al.*, 2007).

Our results collectively suggest that guard cell responses to BL are species-specific, time-dependent and differ from those observed under WL. Although BL-induced stomatal responses have been observed in basal lineage of plants (Doi *et al.*, 2015), evidence highlights that this is not observed in all plant species, including certain angiosperms (Matthews *et al.*, 2020). Similarly, our findings suggest that BL-induced starch degradation may not be a universal mechanism across plant species. While starch degradation has been observed in Arabidopsis guard cells upon BL

(Horrer *et al.*, 2016), this mechanism was not observed in both *Vicia faba* and *Allium cepa* under BL (Ogawa, 1981). Our results does not implicate that starch metabolism is unimportant in the regulation of cowpea and tobacco guard cell metabolism under BL, especially given potential variations in the presence of mesophyll cells and/or red light, plant growth conditions, and/or the quantity of BL imposed on guard cells (Ogawa *et al.*, 1978; Frechilla *et al.*, 2004; Loreto *et al.*, 2009). The differential BL metabolic responses observed here between cowpea and tobacco may be associated to the effectiveness of BL perception and/or intrinsic differences in guard cell metabolism between these species. A previous study showed that the stomatal aperture to low BL intensity ($10\,\mu mol\,m^{-2}\,s^{-1}$) was positively correlated with the accumulation of sucrose over 120 min and an initial increase in malate in the first 30 min followed by a decrease until 120 min in *V. faba* guard cells (Talbott & Zeiger, 1993). This response was not observed in neither of the species used here, further strengthening that the BL-induced metabolic changes may be species-specific.

5.3 Material and methods

Plant material and growth conditions

Cowpea (*Vigna unguiculata* L. *Walp.*) seeds were surface sterilized 70 % ethanol followed by washing with distilled water and sown on a germination paper, with 10 seeds per sheet. The seeds were kept inside a plastic bag for 5 days, then the seedlings were transplanted into pots (4 L) containing vermiculite and sand (1:1). Seeds of *Nicotiana tabacum* L. were surface sterilized with 70 % ethanol followed by washing with distilled water. Tobacco seeds were sown on a substrate composed of sand, vermiculite and soil (2:1:0.5) in a seed germination tray. After 1 week, the plants were transferred to bigger pots (4 L). Plants were irrigated with Hoagland's solution (Hoagland & Arnon, 1950) twice per week. Fully expanded leaves were harvested at pre-dawn for guard cell enriched epidermal fragments isolation.

Guard cell enriched epidermal fragments isolation

A pool of guard cell enriched epidermal fragments (here referred solely as guard cells) was obtained according to a protocol optimized for metabolomics analysis (Daloso *et al.*, 2015). Guard cell isolation was carried out using three leaves per replicate. Both primary and secondary veins were removed from tobacco leaves, while only the main nervure was removed from cowpea leaves. The leaves were then subjected to 1-minute pulses of blending in a blender (Philips, RI, 2044 B.V. International Philips, Amsterdam, The Netherlands) equipped with an internal filter to facilitate the

separation of guard cells from fibers, mesophyll cells, and other cell debris. After blending, guard cells were collected in a nylon membrane (200 µm) and washed with distilled water to remove contaminants. Subsequently, guard cells were transferred to a hypertonic solution (0.5 M mannitol) under dark condition to prevent stomatal opening. These steps were repeated until a sufficient pool of guard cells was obtained for subsequent stomatal aperture and metabolomics analyses.

Stomatal kinetic experiment under blue light

Guard cells harvested at pre-dawn were collected from the hypertonic solution, extensively washed with distilled water, transferred to petri dishes containing a stomatal opening solution (5mM KCl + 5mM NaOH + 50µM $CaCl_2$, pH 6.5), and then exposed to blue light (75-90 µmol photons $m^{-2} s^{-1}$). After 0, 10, 20, 30, 40 and 60 minutes under blue light, guard cells were collected on a nylon membrane, rapidly washed to remove excess buffer, and then frozen in liquid nitrogen. The samples were stored in -80^0C until further analysis.

Measurement of stomatal aperture

Stomatal aperture was determined using a light microscope with a coupled digital camera. At least 40-60 stomata were measured for each replicate of all samples. The stomatal length and width were measured using the ImageJ software (http://fiji.sc/), as described earlier (Medeiros *et al.*, 2018).

Metabolite profiling analysis via gas chromatography mass spectrometry

Approximately 500 mg of powdered samples was used for metabolite extraction. The extraction and derivatization of polar metabolite were carried out using a well-established protocol (Lisec *et al.*, 2006), however 1 mL of polar phase was collected, instead of 150 µL (Lima *et al.*, 2021). The metabolites were analysed by gas chromatography coupled to mass spectrometry (GC-MS, QP-PLUS 2010, Shimadzu, Japan) as described earlier (Lisec *et al.*, 2006). The mass spectra obtained was analysed using Xcalibur® 2.1 (Thermo Fisher Scientific, Waltham, MA, USA). Metabolites were annotated using the Golm Metabolome Database (http://gmd.mpimp-golm.mpg.de/) (Kopka *et al.*, 2005). Metabolite levels were normalized by the level of ribitol and fresh weight (FW) used for extraction.

Starch quantification

Starch levels were measured using a spectrophotometer as described (Trethewey *et al.*, 1998). Starch was quantified in the pellet remaining after metabolite extraction for metabolite profiling. The pellet was washed three times with 80% ethanol at 70 ^{0}C until a clear pellet was obtained. Starch in the pellet was then digested by the addition of 400 µL of 0.2M KOH at 90 °C for 1 h, neutralized with 210 µL of 1M acetic acid. Subsequently, 100 µL of this solution was used for starch digestion using citrate buffer (0.3M) at pH 5.0 and amyloglucosidase (1 U reaction^{-1}) at 55 °C for 1 h in a final volume of 300 µL. Starch was quantified using an enzymatic method coupled to NADH production measured at 340 nm using a commercially available kit (Glucose assay kit, Sigma-Aldrich). Starch levels were quantified based on a standard curve of glucose.

Statistical analyses

Data are presented as the mean of four replicates ± standard deviation (SD). Significant differences between different time points were determined by one-way ANOVA and Dunnett test ($P < 0.05$), using the time 0 min as control. Punctual comparisons were carried out by Student's *t*-test ($P < 0.05$). Metabolomics data were analysed using the MetaboAnalyst platform (Pang *et al.*, 2021). Pearson correlation analysis and partial least squares-discriminant analysis (PLS-DA) was performed on cube root-transformed and mean-centered data (for cowpea data) and log transformation and auto-scaling mode (for tobacco data) (Xia & Wishart, 2011). Heat maps were carried out using MeV 4.9.0 software. K-means clustering based on Euclidian distance was carried out using stomatal aperture and metabolite profiling data. The number of clusters was manually determined according to the dynamic of accumulation/degradation of the metabolites in both species. This analysis was carried out using the MetaboAnalyst platform.
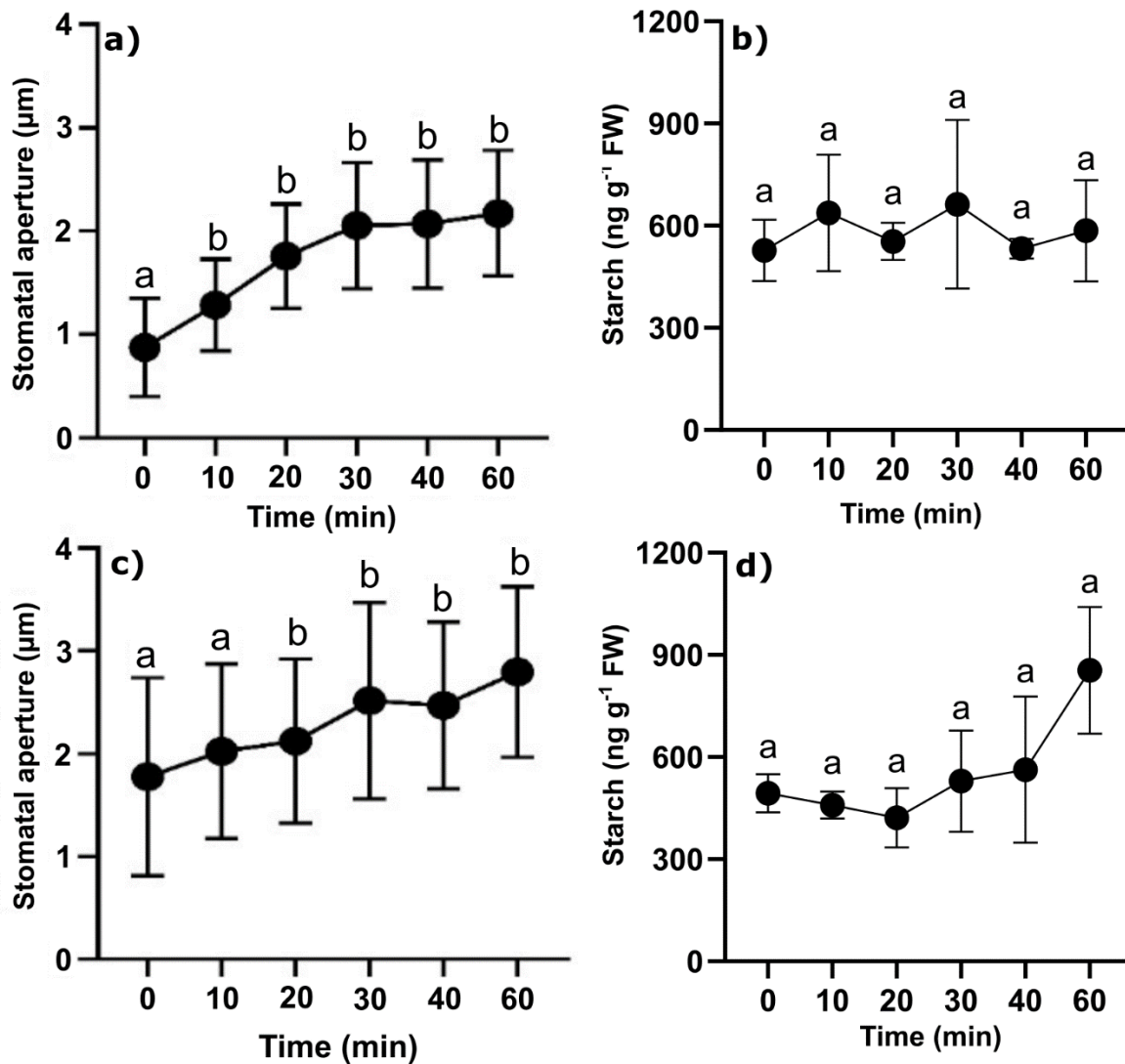
Figure 1. Stomatal aperture (a,c) and concentration of starch (b,d) in guard cells of tobacco (a-b) and cowpea (c-d) throughout time under blue light. A pool of guard cell-enriched epidermal fragments was harvested at pre-dawn, stored in a hypertonic solution to avoid stomatal opening and then transferred to blue light. After 0, 10, 20, 30, 40 and 60 minutes, the guard cells were harvested in a membrane and rapidly washed with distilled water. One set of the guard cells were immediately used to measure stomatal aperture using light microscope and another set was rapidly frozen in liquid nitrogen for starch analysis. Stomatal aperture (a-b) refers to the width of the stomatal pore (in µm). Guard cell starch concentration was determined spectrophotometrically. Significant differences throughout time are indicated by different letters, as determined by ANOVA and Dunnett test ($P < 0.05$) (n=4), in which the time 0 min was used as control.
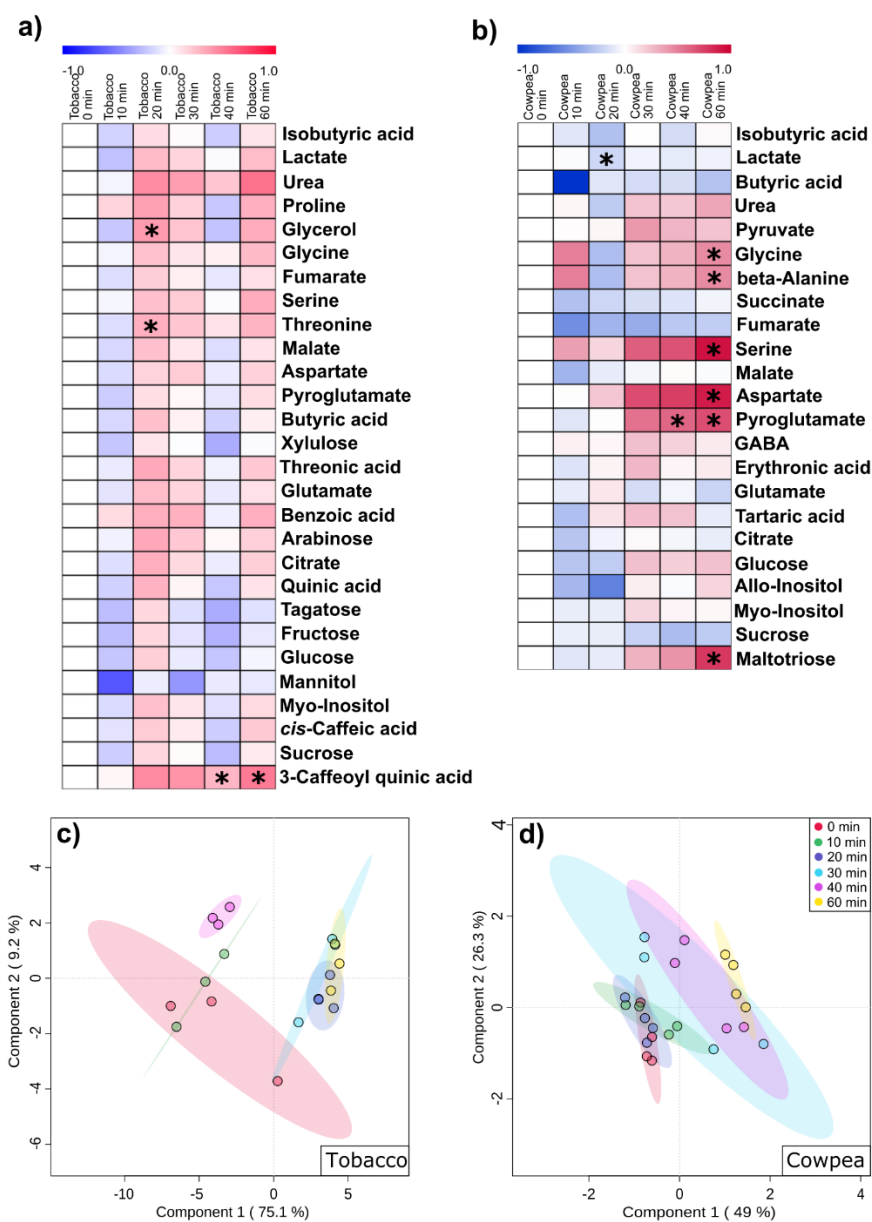
Figure 2. Changes in guard cell primary metabolites induced by blue light. a-b) Heat map representation of the changes in metabolite profiling of tobacco (a) and cowpea (b) guard cells harvested after 0, 10, 20, 30, 40 and 60 min of the dark-to-blue light. Metabolite profiling data were normalized by the average of values found at the time 0 min followed by log2 transformation for heat map representation. Asterisks (*) indicate significant differences from the control (time 0 min) by Student's t-test ($P < 0.05$) (n = 3 to 4). c-d) Partial least square-discriminant analysis (PLS-DA) using metabolite profiling data from tobacco (c) and cowpea (d) guard cells harvested after 0, 10, 20, 30, 40 and 60 minutes of the dark-to-blue light transition. The percentage variation explained by the components 1 and 2 of the PLS-DAs are represented in each axis.
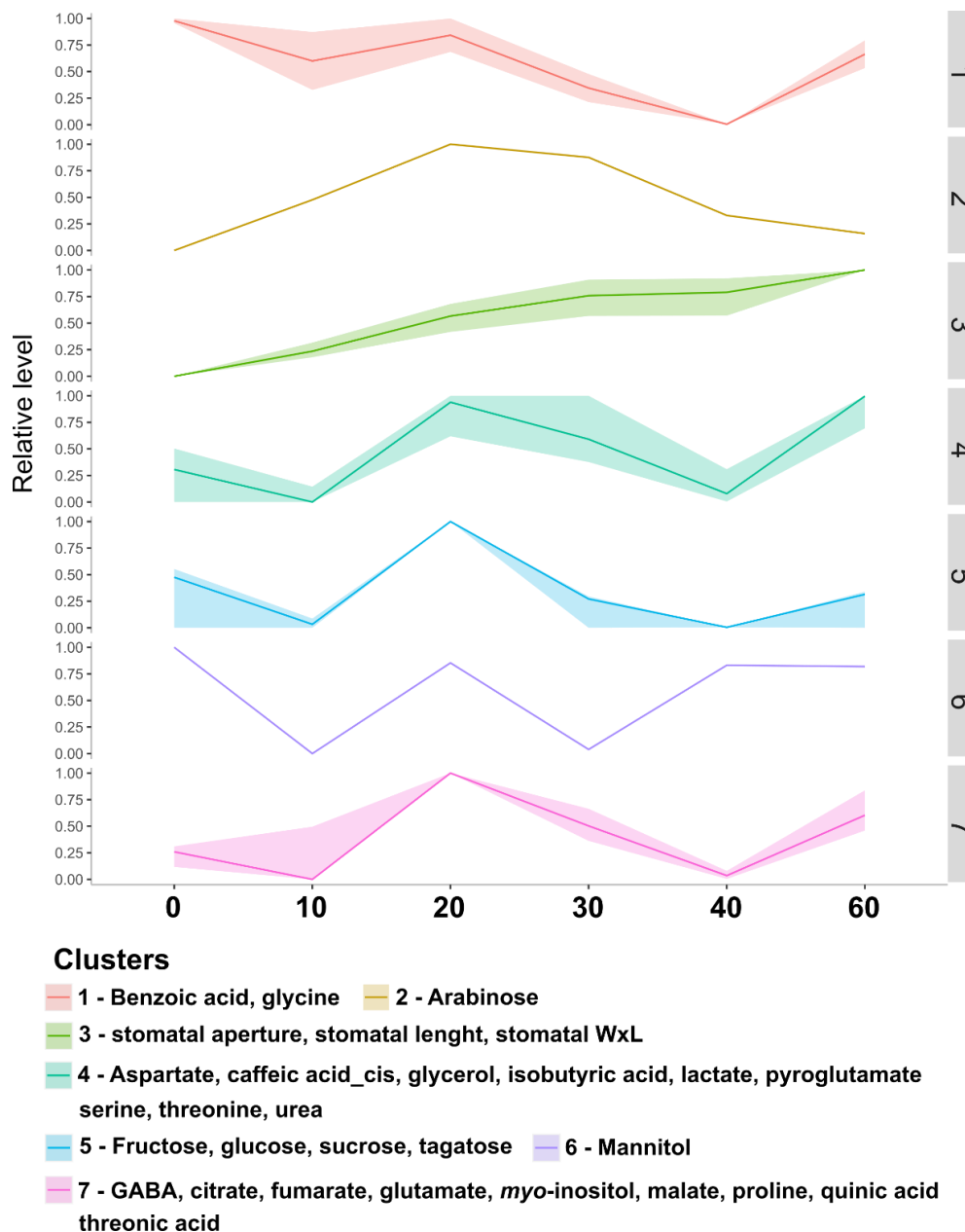
Figure 3. K-means clustering analysis using tobacco stomatal aperture and metabolite profiling data normalized using a minimum (0)- maximum (1) transformation. Seven (1-7) clusters were generated, which combine parameters with similar trend of increasing or decreasing throughout the time of the experiment (i.e. from 0 to 60 minutes). The Y axis highlight that relative level of the parameters, in which the minimum and the maximum values observed between 0 and 60 minutes were set to 0 or 1, and the values in between were then proportionally normalized between 0 and 1 throughout time. This analysis was carried out using the Metaboanalyst platform (n = 4). Abbreviation: stomatal WxL; stomatal width x length.

Clusters

- 1 - Beta-Alanine, glycine
- 2 - Fumarate
- 3 - Butyric acid_4-hydroxy, citrate, malate, succinate
- 4 - Glutamate, sucrose
- 5 - GABA, erythronic acid, *myo*-inositol, pyruvate, tartaric acid
- 6 - Glucose, lactate, isobutyric acid
- 7 - Aspartate, maltotriose, pyroglutamate, serine, urea, stomatal aperture, stomatal lenght, stomatal width x length
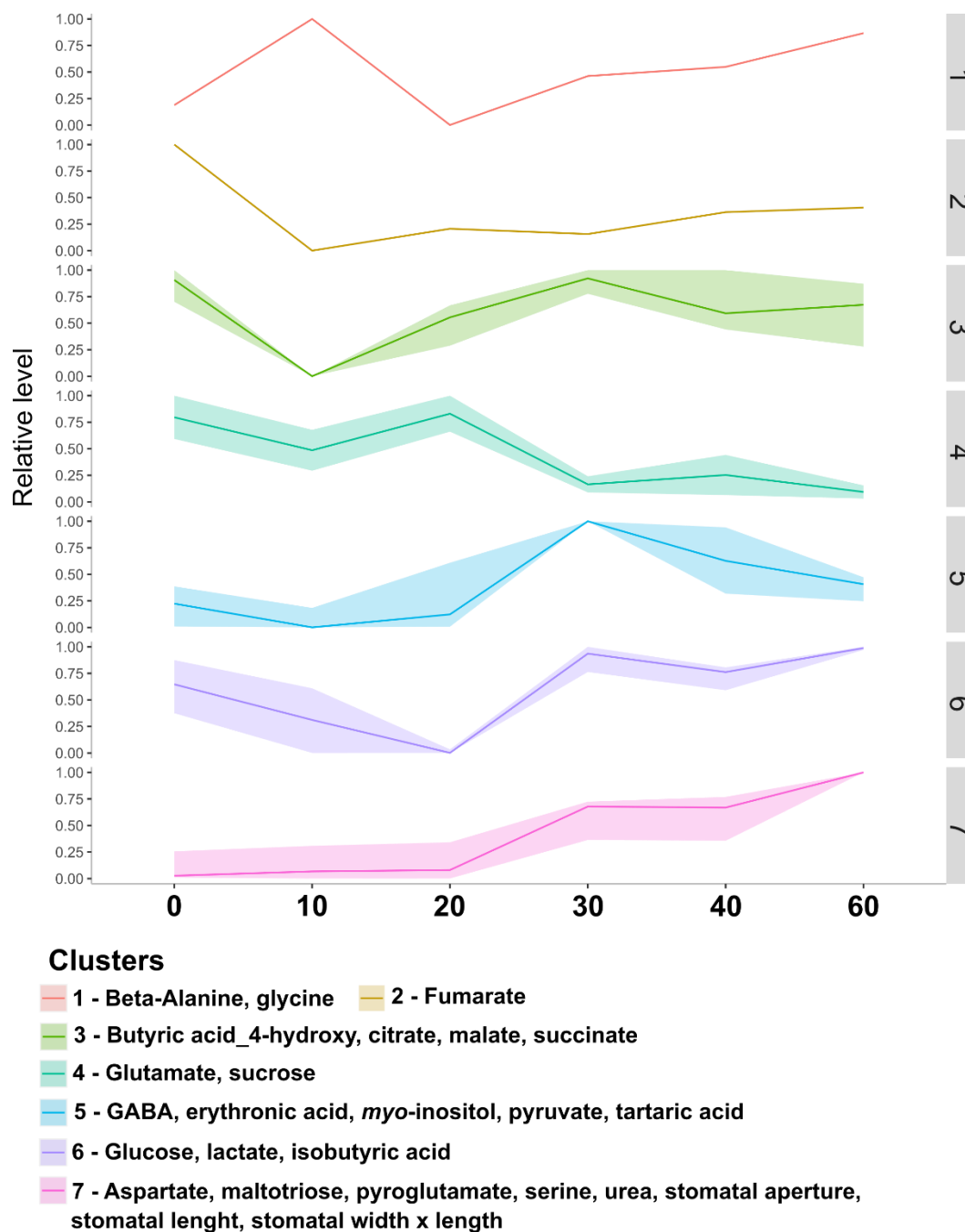
Figure 4. K-means clustering analysis using cowpea stomatal aperture and metabolite profiling data normalized using a minimum (0)- maximum (1) transformation. Seven (1-7) clusters were generated, which combine parameters with similar trend of increasing or decreasing throughout the time of the experiment (i.e. from 0 to 60 minutes). The Y axis highlight that relative level of the parameters, in which the minimum and the maximum values observed between 0 and 60 minutes were set to 0 or 1, and the values in between were then proportionally normalized between 0 and 1 throughout time. This analysis was carried out using the Metaboanalyst platform (n = 4).
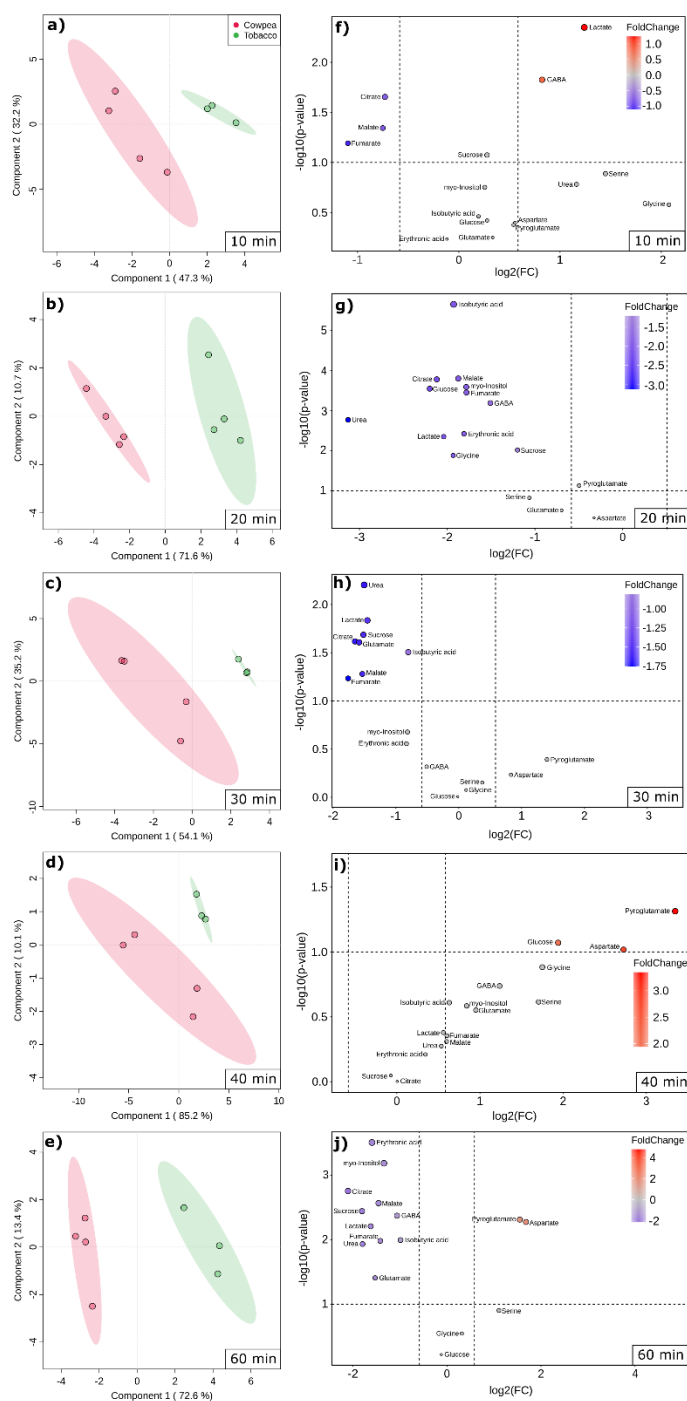
Figure 5. Partial least-square discriminant analysis (PLS-DA) (a-e) and volcano plots (f-j) comparing the relative metabolic changes between tobacco and cowpea guard cells subjected to 0, 10, 20, 30, 40 and 60 min of blue light. These analyses were carried out using the metabolite profiling data normalized according to the time 0 min within each genotype. a-e). The percentage variation explained by the components 1 and 2 are represented in each axis. f-j) Metabolites in blue and red colour have lower and higher level in cowpea than tobacco, respectively, by Student´s t test (P < 0.05). These analyses were carried out using the Metaboanalyst platform (n = 4).
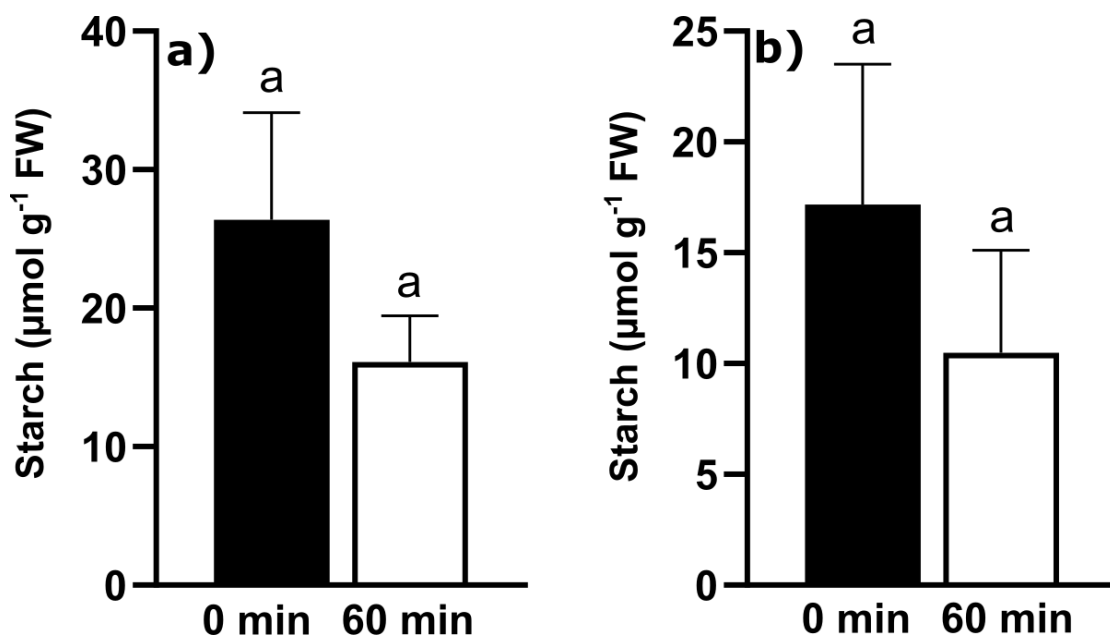
Figure S1. Concentration of starch in guard cells of tobacco (a) and cowpea (b) under blue light. Guard cell enriched epidermal fragments were harvested at pre-dawn and immediately submitted to blue light for 0 and 60 minutes. After these time points, the guard cell enriched epidermal fragments were collected in a membrane and frozen in liquid nitrogen. Significant differences among the treatments are indicated by different letter, as determined by ANOVA and Dunnett test ($P < 0.05$) (n=4).
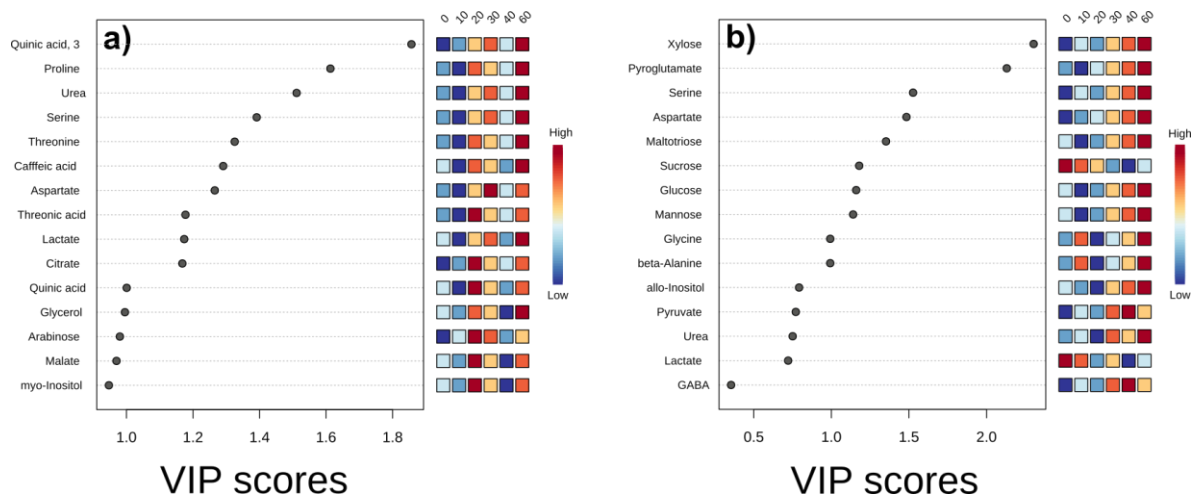
Figure S2. Variable importance in projection (VIP) scores from the partial least square-discriminant analysis (PLS-DA) using metabolite profiling data from tobacco (a) and cowpea (b) guard cells. The data refer to the changes observed from 0 min to 60 min. The metabolites of the VIP score list are ranked from top to down as the most important for each PLS-DA model. These analyses were carried out using the Metaboanalyst platform.
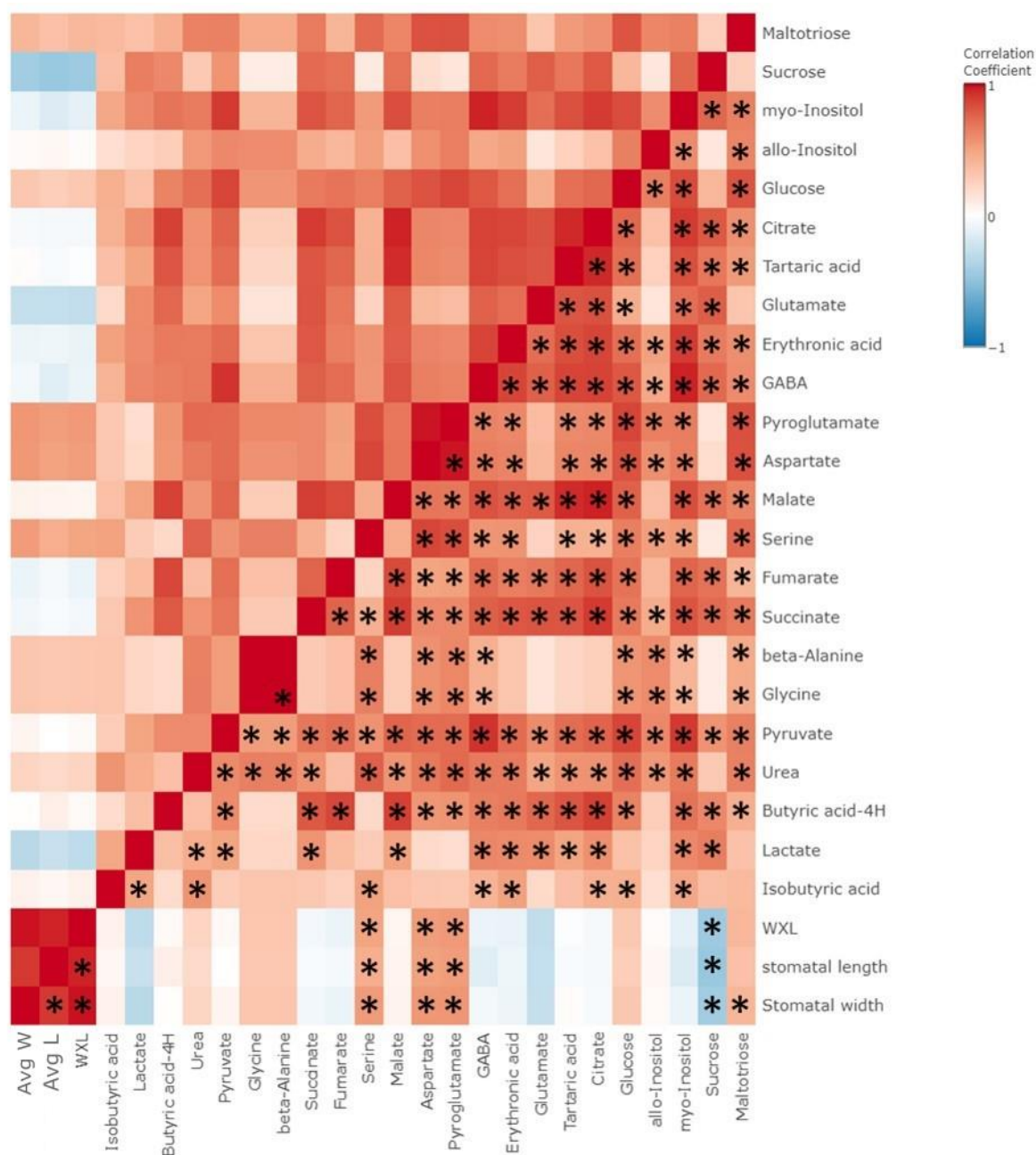
Figure S3. Heat map representation of Pearson correlation analyses carried out among stomatal aperture parameters and metabolite profiling data from cowpea guard cells. Blue and red colours indicate negative and positive correlations, respectively. Asterisks (*) indicate significant correlation ($P < 0.05$). The heat map was generated using the Metaboanalyst platform. Avg W; average stomatal width, Avg L; average stomatal length, Avg WXL; stomatal average width x stomatal average length.
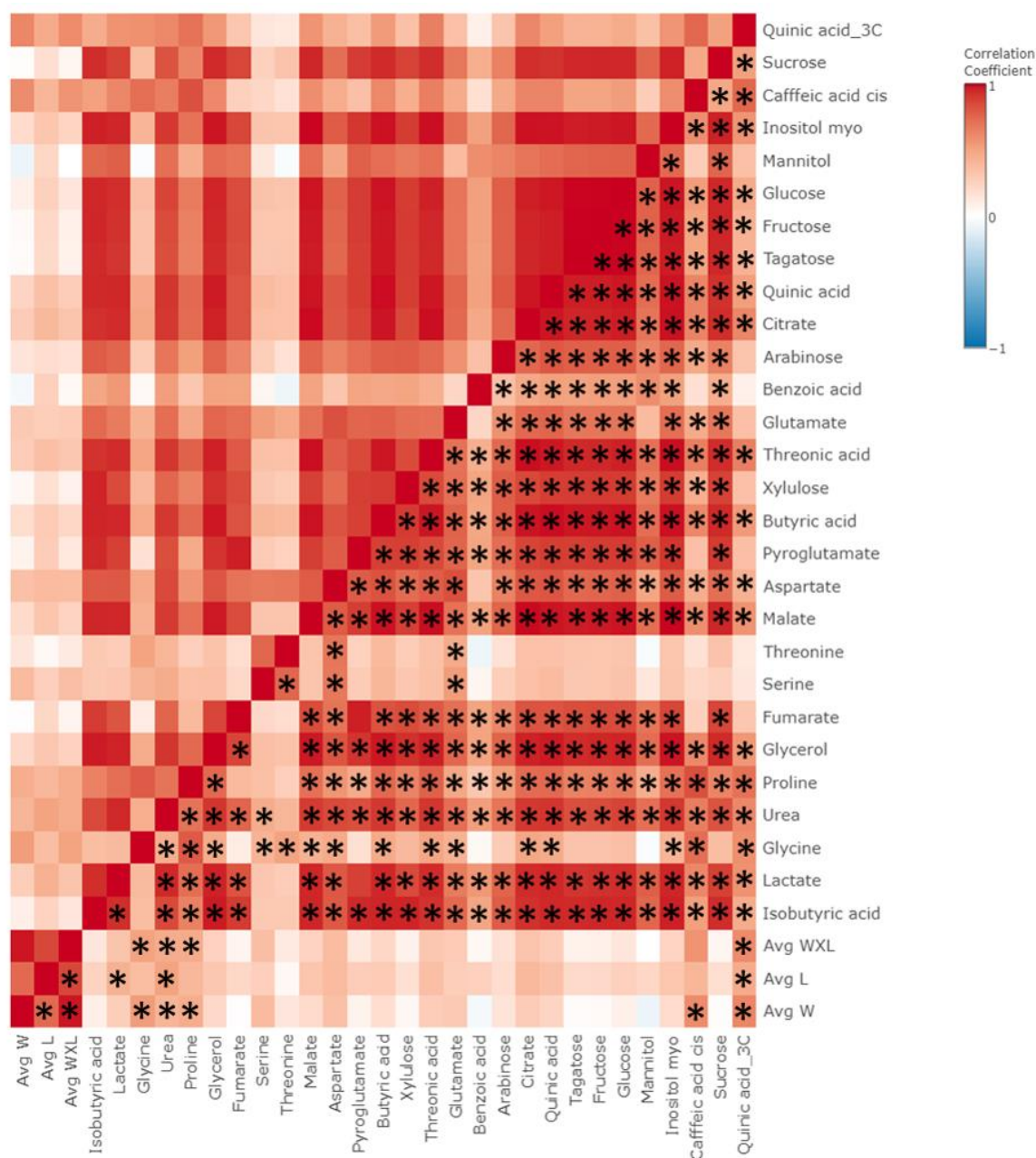
Figure S4. Heat map representation of Pearson correlation analyses carried out among stomatal aperture parameters and metabolite profiling data from tobacco guard cells. Blue and red colours indicate negative and positive correlations, respectively. Asterisks (*) indicate significant correlation ($P < 0.05$). The heat map was generated using the Metaboanalyst platform. Avg W; average stomatal width, Avg L; average stomatal length, Avg WXL; stomatal average width x stomatal average length.
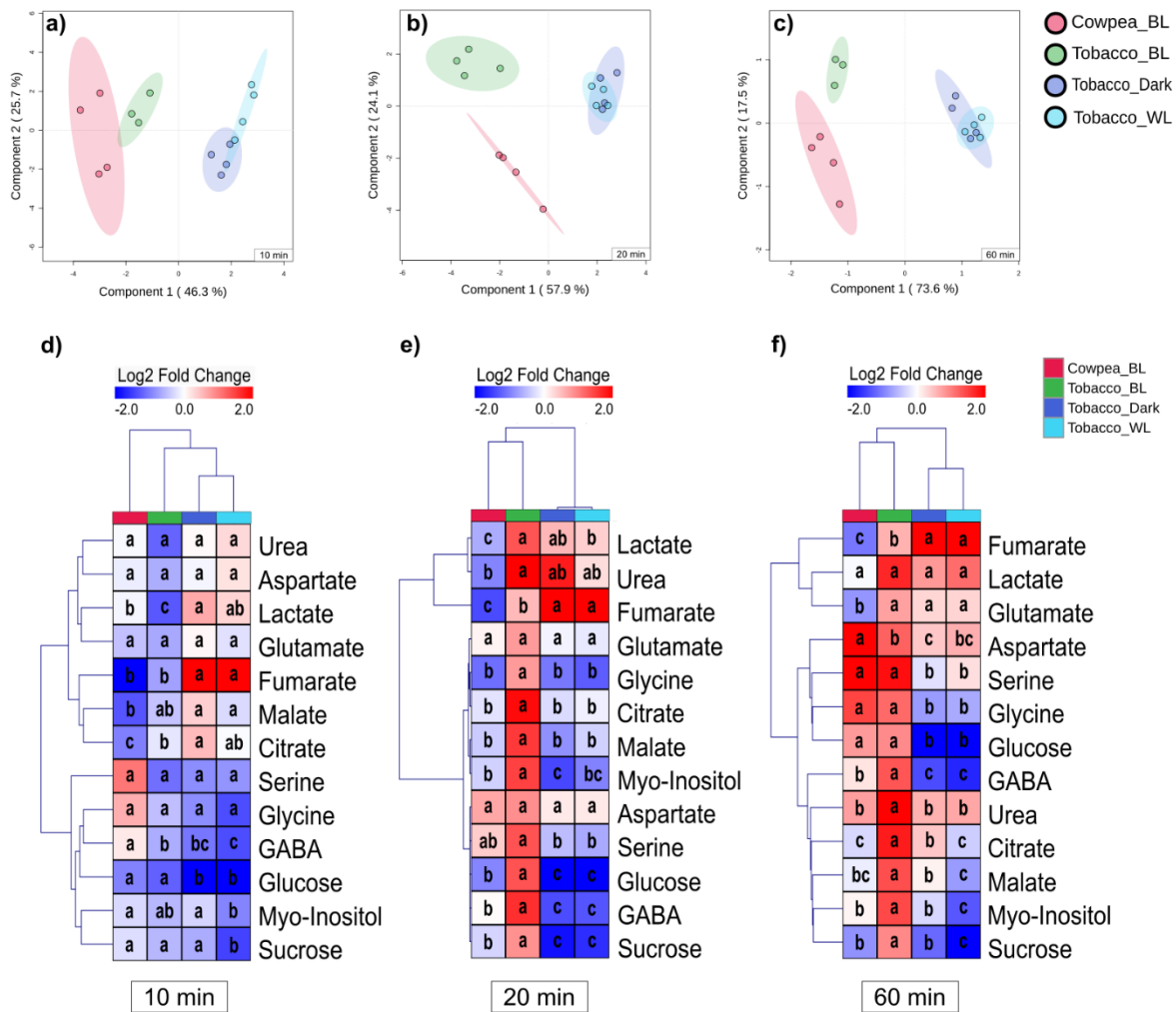
Figure S5. Partial least square-discriminant analysis (PLS-DA) (a-c) and heat map representation (d-f) comparing the guard cell metabolic changes induced by white light (WL), blue light (BL) and extended darkness (Dark). These analyses were carried out using metabolite profiling data from 10 (a,d), 20 (b,e) and 60 minutes (c,f) normalized according to the values obtained at the time 0 min within each genotype and treatment. Guard cells were collected at predawn, transferred to plates and maintained under darkness or transferred to WL (400 μmol photons m^{-2} s^{-1}) or BL (75-90 μmol photons m^{-2} s^{-1}) for 0, 10, 20 and 60 minutes. The percentage variation explained by the PC1 and PC2 of the PLS-DAs are represented in each axis. These analyses were carried out using the Metaboanalyst platform (n = 4). The data from tobacco guard cells subjected to Dark or WL are derived from Lima et al. (2023). Plant Physiology and Biochemistry 201, 107862.

REFERENCES

AFENDI, F. M.; ONO, N.; NAKAMURA, Y.; NAKAMURA, K. *et al.* Data mining methods for omics and knowledge of crude medicinal plants toward big data biology. **Computational and Structural Biotechnology Journal**, 4, n. 5, p. e201301010, 2013.

AINSWORTH, E. A.; ROGERS, A.; NELSON, R.; LONG, S. P. Testing the "source–sink" hypothesis of down-regulation of photosynthesis in elevated [CO2] in the field with single gene substitutions in Glycine max. **Agricultural and forest meteorology**, 122, n. 1-2, p. 85-94, 2004.

ALVES DE FREITAS GUEDES, F.; MENEZES-SILVA, P. E.; DAMATTA, F. M.; ALVES-FERREIRA, M. Using transcriptomics to assess plant stress memory. **Theoretical and Experimental Plant Physiology**, 31, p. 47-58, 2019.

ANDO, E.; KINOSHITA, T. Red light-induced phosphorylation of plasma membrane H+-ATPase in stomatal guard cells. **Plant Physiology**, 178, n. 2, p. 838-849, 2018.

AP REES, T. Compartmentation of plant metabolism. **The biochemistry of plants**, 12, p. 87-113, 1987.

APELT, F.; BREUER, D.; OLAS, J. J.; ANNUNZIATA, M. G. *et al.* Circadian, carbon, and light control of expansion growth and leaf movement. **Plant Physiology**, 174, n. 3, p. 1949-1968, 2017.

ARAUJO, W. L.; NUNES-NESI, A.; NIKOLOSKI, Z.; SWEETLOVE, L. J. *et al.* Metabolic control and regulation of the tricarboxylic acid cycle in photosynthetic and heterotrophic plant tissues. **Plant, cell & environment**, 35, n. 1, p. 1-21, 2012.

ASSMANN, S.; SIMONCINI, L.; SCHROEDER, J. Blue light activates electrogenic ion pumping in guard cell protoplasts of Vicia faba. **Nature**, 318, n. 6043, p. 285-287, 1985.

ASSMANN, S. M.; WANG, X.-Q. From milliseconds to millions of years: guard cells and environmental responses. **Current opinion in plant biology**, 4, n. 5, p. 421-428, 2001.

BALMER, Y.; VENSEL, W. H.; TANAKA, C. K.; HURKMAN, W. J. *et al.* Thioredoxin links redox to the regulation of fundamental processes of plant mitochondria. **Proceedings of the national academy of sciences**, 101, n. 8, p. 2642-2647, 2004.

BALPARDA, M.; BOUZID, M.; MARTINEZ, M. d. P.; ZHENG, K. *et al.* Regulation of plant carbon assimilation metabolism by post-translational modifications. **The Plant Journal**, 114, n. 5, p. 1059-1079, 2023.

BASHANDY, T.; TACONNAT, L.; RENOU, J.-P.; MEYER, Y. *et al.* Accumulation of flavonoids in an ntra ntrb mutant leads to tolerance to UV-C. **Molecular Plant**, 2, n. 2, p. 249-258, 2009.

BEERS, R. F.; SIZER, I. W. A spectrophotometric method for measuring the breakdown of hydrogen peroxide by catalase. **J Biol chem**, 195, n. 1, p. 133-140, 1952.

BRADFORD, M. M. A rapid and sensitive method for the quantitation of microgram quantities of protein utilizing the principle of protein-dye binding. **Analytical biochemistry**, 72, n. 1-2, p. 248-254, 1976.

BURNETT, A. C.; ROGERS, A.; REES, M.; OSBORNE, C. P. Carbon source–sink limitations differ between two species with contrasting growth strategies. **Plant, Cell & Environment**, 39, n. 11, p. 2460-2472, 2016.

CARRILLO, L. R.; FROEHLICH, J. E.; CRUZ, J. A.; SAVAGE, L. J. *et al.* Multi-level regulation of the chloroplast ATP synthase: the chloroplast NADPH thioredoxin reductase C (NTRC) is required for redox modulation specifically under low irradiance. **The Plant Journal**, 87, n. 6, p. 654-663, 2016.

CARVALHO, F. E.; RIBEIRO, C. W.; MARTINS, M. O.; BONIFACIO, A. *et al.* Cytosolic APX knockdown rice plants sustain photosynthesis by regulation of protein expression related to photochemistry, Calvin cycle and photorespiration. **Physiologia plantarum**, 150, n. 4, p. 632-645, 2014.

CEJUDO, F. J.; GONZÁLEZ, M.-C.; PÉREZ-RUIZ, J. M. Redox regulation of chloroplast metabolism. **Plant Physiology**, 186, n. 1, p. 9-21, 2021.

CHA, J.-Y.; KIM, J. Y.; JUNG, I. J.; KIM, M. R. *et al.* NADPH-dependent thioredoxin reductase A (NTRA) confers elevated tolerance to oxidative stress and drought. **Plant physiology and biochemistry**, 80, p. 184-191, 2014.

CHAIWANON, J.; WANG, W.; ZHU, J.-Y.; OH, E. *et al.* Information integration and communication in plant growth regulation. **Cell**, 164, n. 6, p. 1257-1268, 2016.

CHONG, J.; SOUFAN, O.; LI, C.; CARAUS, I. *et al.* MetaboAnalyst 4.0: towards more transparent and integrative metabolomics analysis. **Nucleic acids research**, 46, n. W1, p. W486-W494, 2018.

CLAEYS, H.; INZÉ, D. The agony of choice: how plants balance growth and survival under water-limiting conditions. **Plant physiology**, 162, n. 4, p. 1768-1779, 2013.

CR, M. Comes a time. **Curr Opin Plant Biol**, 11, p. 514-520, 2008.

DA FONSECA-PEREIRA, P.; SOUZA, P. V.; FERNIE, A. R.; TIMM, S. *et al.* Thioredoxin-mediated regulation of (photo) respiration and central metabolism. **Journal of Experimental Botany**, 72, n. 17, p. 5987-6002, 2021.

DA SILVA, F. B.; MACEDO, F. d. C. O.; DANELUZZI, G. S.; CAPELIN, D. *et al.* Action potential propagation effect on gas exchange of ABA-mutant microtomato after re-irrigation stimulus. **Environmental and experimental botany**, 178, p. 104149, 2020.

DALOSO, D. d. M.; MORAIS, E. G.; OLIVEIRA E SILVA, K. F.; WILLIAMS, T. C. R. Cell-type-specific metabolism in plants. **The Plant Journal**, 114, n. 5, p. 1093-1114, 2023.

DALOSO, D. M.; MÜLLER, K.; OBATA, T.; FLORIAN, A. *et al.* Thioredoxin, a master regulator of the tricarboxylic acid cycle in plant mitochondria. **Proceedings of the National Academy of Sciences**, 112, n. 11, p. E1392-E1400, 2015.

DAUBERMANN, A. G.; LIMA, V. F.; ERBAN, A.; KOPKA, J. *et al.* Novel guard cell sink characteristics revealed by a multi-species/cell-types meta-analysis of 13C-labelling experiments. **Theoretical and Experimental Plant Physiology**, p. 1-20, 2024.

DECROS, G.; BALDET, P.; BEAUVOIT, B.; STEVENS, R. *et al.* Get the balance right: ROS homeostasis and redox signalling in fruit. **Frontiers in Plant Science**, 10, p. 1091, 2019.

DIXON, R. a.; Strack, D. Phytochemistry meets genome analysis, and beyond. **Phytochemistry**, 62, n. 6, p. 815-816, 2003.

DODD, A. N.; SALATHIA, N.; HALL, A.; KÉVEI, E. *et al.* Plant circadian clocks increase photosynthesis, growth, survival, and competitive advantage. **Science**, 309, n. 5734, p. 630-633, 2005.

DOS ANJOS, L.; PANDEY, P. K.; MORAES, T. A.; FEIL, R. *et al.* Feedback regulation by trehalose 6-phosphate slows down starch mobilization below the rate that would exhaust starch reserves at dawn in Arabidopsis leaves. **Plant direct**, 2, n. 8, p. e00078, 2018.

EDWARDS, D.; KERP, H.; HASS, H. Stomata in early land plants: an anatomical and ecophysiological approach. **Journal of Experimental Botany**, p. 255-278, 1998.

ERB, M.; KLIEBENSTEIN, D. J. Plant secondary metabolites as defenses, regulators, and primary metabolites: the blurred functional trichotomy. **Plant physiology**, 184, n. 1, p. 39-52, 2020.

FARRÉ, E. M.; WEISE, S. E. The interactions between the circadian clock and primary metabolism. **Current opinion in plant biology**, 15, n. 3, p. 293-300, 2012.

FEDORIN, D. N.; EPRINTSEV, A. T.; IGAMBERDIEV, A. U. The role of promoter methylation of the genes encoding the enzymes metabolizing di-and tricarboxylic acids in the regulation of plant respiration by light. **Journal of Plant Physiology**, p. 154195, 2024.

FERNIE, A. R.; BACHEM, C. W.; HELARIUTTA, Y.; NEUHAUS, H. E. *et al.* Synchronization of developmental, molecular and metabolic aspects of source–sink interactions. **Nature plants**, 6, n. 2, p. 55-66, 2020.

FERNIE, A. R.; CARRARI, F.; SWEETLOVE, L. J. Respiratory metabolism: glycolysis, the TCA cycle and mitochondrial electron transport. **Current opinion in plant biology**, 7, n. 3, p. 254-261, 2004.

FERRÁNDEZ, J.; GONZÁLEZ, M.; CEJUDO, F. J. Chloroplast redox homeostasis is essential for lateral root formation in Arabidopsis. **Plant signaling & behavior**, 7, n. 9, p. 1177-1179, 2012.

FETTKE, J.; FERNIE, A. R. Intracellular and cell-to-apoplast compartmentation of carbohydrate metabolism. **Trends in Plant Science**, 20, n. 8, p. 490-497, 2015.

FLÜTSCH, S.; WANG, Y.; TAKEMIYA, A.; VIALET-CHABRAND, S. R. *et al.* Guard cell starch degradation yields glucose for rapid stomatal opening in Arabidopsis. **The Plant Cell**, 32, n. 7, p. 2325-2344, 2020.

FOYER, C. H.; BAKER, A.; WRIGHT, M.; SPARKES, I. A. *et al.* On the move: redox-dependent protein relocation in plants. **Journal of Experimental Botany**, 71, n. 2, p. 620-631, 2020.

FOYER, C. H.; NOCTOR, G. Managing the cellular redox hub in photosynthetic organisms. : Wiley Online Library. 35**:** 199-201 p. 2012.

FOYER, C. H.; NOCTOR, G. Redox signaling in plants. : Mary Ann Liebert, Inc. 140 Huguenot Street, 3rd Floor New Rochelle, NY 10801 USA. 18**:** 2087-2090 p. 2013.

FURIGO, I.; DE OLIVEIRA, W.; DE OLIVEIRA, A.; COMOLI, E. *et al.* The role of the superior colliculus in predatory hunting. **Neuroscience**, 165, n. 1, p. 1-15, 2010.

GALLÉ, A.; LAUTNER, S.; FLEXAS, J.; FROMM, J. Environmental stimuli and physiological responses: the current view on electrical signalling. **Environmental and Experimental Botany**, 114, p. 15-21, 2015.

GALVIZ, Y. C.; RIBEIRO, R. V.; SOUZA, G. M. Yes, plants do have memory. **Theoretical and experimental plant physiology**, 32, n. 3, p. 195-202, 2020.

GEIGENBERGER, P.; FERNIE, A. R. Metabolic control of redox and redox control of metabolism in plants. **Antioxidants & redox signaling**, 21, n. 9, p. 1389-1421, 2014.

GEIGENBERGER, P.; THORMÄHLEN, I.; DALOSO, D. M.; FERNIE, A. R. The unprecedented versatility of the plant thioredoxin system. **Trends in plant science**, 22, n. 3, p. 249-262, 2017.

GIANNOPOLITIS, C. N.; RIES, S. K. Superoxide dismutases: I. Occurrence in higher plants. **Plant physiology**, 59, n. 2, p. 309-314, 1977.

GONZÁLEZ, M.; DELGADO-REQUEREY, V.; FERRÁNDEZ, J.; SERNA, A. *et al.* Insights into the function of NADPH thioredoxin reductase C (NTRC) based on identification of NTRC-interacting proteins in vivo. **Journal of Experimental Botany**, 70, n. 20, p. 5787-5798, 2019.

GRAF, A.; SCHLERETH, A.; STITT, M.; SMITH, A. M. Circadian control of carbohydrate availability for growth in Arabidopsis plants at night. **Proceedings of the National Academy of Sciences**, 107, n. 20, p. 9458-9463, 2010.

GULL, A.; LONE, A. A.; WANI, N. U. I. Biotic and abiotic stresses in plants. **Abiotic and biotic stress in plants**, p. 1-19, 2019.

HAVIR, E. A.; MCHALE, N. A. Biochemical and developmental characterization of multiple forms of catalase in tobacco leaves. **Plant physiology**, 84, n. 2, p. 450-455, 1987.

HEATH, R. L.; PACKER, L. Photoperoxidation in isolated chloroplasts: I. Kinetics and stoichiometry of fatty acid peroxidation. **Archives of biochemistry and biophysics**, 125, n. 1, p. 189-198, 1968.

HORRER, D.; FLÜTSCH, S.; PAZMINO, D.; MATTHEWS, J. S. *et al.* Blue light induces a distinct starch degradation pathway in guard cells for stomatal opening. **Current Biology**, 26, n. 3, p. 362-370, 2016.

HOU, L.-Y.; EHRLICH, M.; THORMÄHLEN, I.; LEHMANN, M. *et al.* NTRC plays a crucial role in starch metabolism, redox balance, and tomato fruit growth. **Plant physiology**, 181, n. 3, p. 976-992, 2019.

HOU, L.-Y.; LEHMANN, M.; GEIGENBERGER, P. Thioredoxin h 2 and o 1 Show Different Subcellular Localizations and Redox-Active Functions, and Are Extrachloroplastic Factors Influencing Photosynthetic Performance in Fluctuating Light. **Antioxidants**, 10, n. 5, p. 705, 2021.

HUMBLE, G.; RASCHKE, K. Stomatal opening quantitatively related to potassium transport: evidence from electron probe analysis. **Plant Physiology**, 48, n. 4, p. 447-453, 1971.

INOUE, S.-i.; KINOSHITA, T.; MATSUMOTO, M.; NAKAYAMA, K. I. *et al.* Blue light-induced autophosphorylation of phototropin is a primary step for signaling. **Proceedings of the National Academy of Sciences**, 105, n. 14, p. 5626-5631, 2008.

KAMBHAMPATI, S.; AJEWOLE, E.; MARSOLAIS, F. Advances in asparagine metabolism. **Progress in Botany Vol. 79**, p. 49-74, 2018.

KERRIGAN, P. K. Natural product chemistry: A mechanistic, biosynthetic and ecological approach, (Torssell, Kurt BG). : ACS Publications 1999.

KINOSHITA, T.; DOI, M.; SUETSUGU, N.; KAGAWA, T. *et al.* Phot1 and phot2 mediate blue light regulation of stomatal opening. **Nature**, 414, n. 6864, p. 656-660, 2001.

KIRCHSTEIGER, K.; PULIDO, P.; GONZÁLEZ, M.; CEJUDO, F. J. NADPH thioredoxin reductase C controls the redox status of chloroplast 2-Cys peroxiredoxins in Arabidopsis thaliana. **Molecular Plant**, 2, n. 2, p. 298-307, 2009.

KNEESHAW, S.; KEYANI, R.; DELORME-HINOUX, V.; IMRIE, L. *et al.* Nucleoredoxin guards against oxidative stress by protecting antioxidant enzymes. **Proceedings of the National Academy of Sciences**, 114, n. 31, p. 8414-8419, 2017.

KÖNIG, J.; MUTHURAMALINGAM, M.; DIETZ, K.-J. Mechanisms and dynamics in the thiol/disulfide redox regulatory network: transmitters, sensors and targets. **Current opinion in plant biology**, 15, n. 3, p. 261-268, 2012.

KOPKA, J.; SCHAUER, N.; KRUEGER, S.; BIRKEMEYER, C. *et al.* GMD@ CSB. DB: the Golm metabolome database. **Bioinformatics**, 21, n. 8, p. 1635-1638, 2005.

KROYMANN, J. Natural diversity and adaptation in plant secondary metabolism. **Current opinion in plant biology**, 14, n. 3, p. 246-251, 2011.

LALOI, C.; RAYAPURAM, N.; CHARTIER, Y.; GRIENENBERGER, J.-M. *et al.* Identification and characterization of a mitochondrial thioredoxin system in plants. **Proceedings of the National Academy of Sciences**, 98, n. 24, p. 14144-14149, 2001.

LAUGHNER, B. J.; SEHNKE, P. C.; FERL, R. J. A novel nuclear member of the thioredoxin superfamily. **Plant Physiology**, 118, n. 3, p. 987-996, 1998.

LAUXMANN, M. A.; ANNUNZIATA, M. G.; BRUNOUD, G.; WAHL, V. *et al.* Reproductive failure in Arabidopsis thaliana under transient carbohydrate limitation: flowers and very young siliques are jettisoned and the meristem is maintained to allow successful resumption of reproductive growth. **Plant, cell & environment**, 39, n. 4, p. 745-767, 2016.

LAWSON, T.; BLATT, M. R. Stomatal size, speed, and responsiveness impact on photosynthesis and water use efficiency. **Plant physiology**, 164, n. 4, p. 1556-1570, 2014.

LAWSON, T.; OXBOROUGH, K.; MORISON, J. I.; BAKER, N. R. The responses of guard and mesophyll cell photosynthesis to CO2, O2, light, and water stress in a range of species are similar. **Journal of experimental botany**, 54, n. 388, p. 1743-1752, 2003.

LÁZARO, J. J.; JIMÉNEZ, A.; CAMEJO, D.; IGLESIAS-BAENA, I. *et al.* Dissecting the integrative antioxidant and redox systems in plant mitochondria. Effect of stress and S-nitrosylation. **Frontiers in plant science**, 4, p. 460, 2013.

LEA, P. J.; SODEK, L.; PARRY, M. A.; SHEWRY, P. R. *et al.* Asparagine in plants. **Annals of applied biology**, 150, n. 1, p. 1-26, 2007.

LEMOINE, R.; CAMERA, S. L.; ATANASSOVA, R.; DÉDALDÉCHAMP, F. *et al.* Source-to-sink transport of sugar and regulation by environmental factors. **Frontiers in plant science**, 4, p. 272, 2013.

LEPISTO, A.; KANGASJARVI, S.; LUOMALA, E.-M.; BRADER, G. *et al.* Chloroplast NADPH-thioredoxin reductase interacts with photoperiodic development in Arabidopsis. **Plant Physiology**, 149, n. 3, p. 1261-1276, 2009.

LEPISTÖ, A.; PAKULA, E.; TOIVOLA, J.; KRIEGER-LISZKAY, A. *et al.* Deletion of chloroplast NADPH-dependent thioredoxin reductase results in inability to regulate starch synthesis and causes stunted growth under short-day photoperiods. **Journal of experimental botany**, 64, n. 12, p. 3843-3854, 2013.

LI, D.; GAQUEREL, E. Next-generation mass spectrometry metabolomics revives the functional analysis of plant metabolic diversity. **Annual Review of Plant Biology**, 72, p. 867-891, 2021.

LISEC, J.; SCHAUER, N.; KOPKA, J.; WILLMITZER, L. *et al.* Gas chromatography mass spectrometry–based metabolite profiling in plants. **Nature protocols**, 1, n. 1, p. 387-396, 2006.

LLOYD, F. E. **The physiology of stomata**. Carnegie Institution of Washington, 1908. v. 82). 0598345760.

MARCHAL, C.; DELORME-HINOUX, V.; BARIAT, L.; SIALA, W. *et al.* NTR/NRX define a new thioredoxin system in the nucleus of Arabidopsis thaliana cells. **Molecular plant**, 7, n. 1, p. 30-44, 2014.

MARCHAND, C.; LE MARÉCHAL, P.; MEYER, Y.; MIGINIAC-MASLOW, M. *et al.* New targets of Arabidopsis thioredoxins revealed by proteomic analysis. **Proteomics**, 4, n. 9, p. 2696-2706, 2004.

MARTÍ, M. C.; JIMÉNEZ, A.; SEVILLA, F. Thioredoxin network in plant mitochondria: cysteine S-posttranslational modifications and stress conditions. **Frontiers in Plant Science**, 11, p. 571288, 2020.

MARTINS, M. C. M.; HEJAZI, M.; FETTKE, J.; STEUP, M. *et al.* Feedback inhibition of starch degradation in Arabidopsis leaves mediated by trehalose 6-phosphate. **Plant physiology**, 163, n. 3, p. 1142-1163, 2013.

MEYER, Y.; BUCHANAN, B. B.; VIGNOLS, F.; REICHHELD, J.-P. Thioredoxins and glutaredoxins: unifying elements in redox biology. **Annual review of genetics**, 43, p. 335-367, 2009.

MEYER, Y.; REICHHELD, J. P.; VIGNOLS, F. Thioredoxins in Arabidopsis and other plants. **Photosynthesis Research**, 86, n. 3, p. 419-433, 2005.

MEYER, Y.; SIALA, W.; BASHANDY, T.; RIONDET, C. *et al.* Glutaredoxins and thioredoxins in plants. **Biochimica Et biophysica acta (BBA)-molecular cell research**, 1783, n. 4, p. 589-600, 2008.

MHAMDI, A.; VAN BREUSEGEM, F. Reactive oxygen species in plant development. **Development**, 145, n. 15, p. dev164376, 2018.

MICHALSKA, J.; ZAUBER, H.; BUCHANAN, B. B.; CEJUDO, F. J. *et al.* NTRC links built-in thioredoxin to light and sucrose in regulating starch synthesis in chloroplasts and amyloplasts. **Proceedings of the National Academy of Sciences**, 106, n. 24, p. 9908-9913, 2009.

MICHELET, L.; ZAFFAGNINI, M.; MORISSE, S.; SPARLA, F. *et al.* Redox regulation of the Calvin–Benson cycle: something old, something new. **Frontiers in plant science**, 4, p. 470, 2013.

MODDE, K.; TIMM, S.; FLORIAN, A.; MICHL, K. *et al.* High serine: glyoxylate aminotransferase activity lowers leaf daytime serine levels, inducing the phosphoserine pathway in Arabidopsis. **Journal of Experimental Botany**, 68, n. 3, p. 643-656, 2017.

MOHL, v. Welchen ursachen bewirken die erweiterung und verengung der spaltöffnungen? . **Botanische Zeitung**, 14, p. 679–704., 1856.

NAKANO, Y.; ASADA, K. Hydrogen peroxide is scavenged by ascorbate-specific peroxidase in spinach chloroplasts. **Plant and cell physiology**, 22, n. 5, p. 867-880, 1981.

NARANJO, B.; DIAZ-ESPEJO, A.; LINDAHL, M.; CEJUDO, F. J. Type-f thioredoxins have a role in the short-term activation of carbon metabolism and their loss affects growth under short-day conditions in Arabidopsis thaliana. **Journal of Experimental Botany**, 67, n. 6, p. 1951-1964, 2016.

NIKKANEN, L.; TOIVOLA, J.; RINTAMÄKI, E. Crosstalk between chloroplast thioredoxin systems in regulation of photosynthesis. **Plant, cell & environment**, 39, n. 8, p. 1691-1705, 2016.

NOCTOR, G.; MHAMDI, A.; FOYER, C. H. The roles of reactive oxygen metabolism in drought: not so cut and dried. **Plant physiology**, 164, n. 4, p. 1636-1648, 2014.

OLAS, J. J.; FICHTNER, F.; APELT, F. All roads lead to growth: imaging-based and biochemical methods to measure plant growth. **Journal of Experimental Botany**, 71, n. 1, p. 11-21, 2020.

OUTLAW JR, W. H.; LOWRY, O. H. Organic acid and potassium accumulation in guard cells during stomatal opening. **Proceedings of the National Academy of Sciences**, 74, n. 10, p. 4434-4438, 1977.

OUTLAW JR, W. H.; MANCHESTER, J. Guard cell starch concentration quantitatively related to stomatal aperture. **Plant Physiology**, 64, n. 1, p. 79-82, 1979.

OUTLAW JR, W. H.; MAYNE, B. C.; ZENGER, V. E.; MANCHESTER, J. Presence of both photosystems in guard cells of Vicia faba L: implications for environmental signal processing. **Plant Physiology**, 67, n. 1, p. 12-16, 1981.

PÉREZ-RUIZ, J. M.; CEJUDO, F. J. A proposed reaction mechanism for rice NADPH thioredoxin reductase C, an enzyme with protein disulfide reductase activity. **FEBS letters**, 583, n. 9, p. 1399-1402, 2009.

PÉREZ-RUIZ, J. M.; NARANJO, B.; OJEDA, V.; GUINEA, M. *et al.* NTRC-dependent redox balance of 2-Cys peroxiredoxins is needed for optimal function of the photosynthetic apparatus. **Proceedings of the National Academy of Sciences**, 114, n. 45, p. 12069-12074, 2017.

PEREZ-RUIZ, J. M.; SPÍNOLA, M. C.; KIRCHSTEIGER, K.; MORENO, J. *et al.* Rice NTRC is a high-efficiency redox system for chloroplast protection against oxidative damage. **The Plant Cell**, 18, n. 9, p. 2356-2368, 2006.

PLAXTON, W. C. The organization and regulation of plant glycolysis. **Annual review of plant biology**, 47, n. 1, p. 185-214, 1996.

PULIDO, P.; SPÍNOLA, M. C.; KIRCHSTEIGER, K.; GUINEA, M. *et al.* Functional analysis of the pathways for 2-Cys peroxiredoxin reduction in Arabidopsis thaliana chloroplasts. **Journal of experimental botany**, 61, n. 14, p. 4043-4054, 2010.

RAI, A.; SAITO, K.; YAMAZAKI, M. Integrated omics analysis of specialized metabolism in medicinal plants. : Wiley Online Library. 90**:** 764-787 p. 2017.

RASCHKE, K.; SCHNABL, H. Availability of chloride affects the balance between potassium chloride and potassium malate in guard cells of Vicia faba L. **Plant Physiology**, 62, n. 1, p. 84-87, 1978.

REICHHELD, J.-P.; KHAFIF, M.; RIONDET, C.; DROUX, M. *et al.* Inactivation of thioredoxin reductases reveals a complex interplay between thioredoxin and glutathione pathways in Arabidopsis development. **The Plant Cell**, 19, n. 6, p. 1851-1865, 2007.

REICHHELD, J.-P.; MEYER, E.; KHAFIF, M.; BONNARD, G. *et al.* AtNTRB is the major mitochondrial thioredoxin reductase in Arabidopsis thaliana. **FEBS letters**, 579, n. 2, p. 337-342, 2005.

REISSIG, G. N.; OLIVEIRA, T. F. d. C.; OLIVEIRA, R. P. d.; POSSO, D. A. *et al.* Fruit herbivory alters plant electrome: evidence for fruit-shoot long-distance electrical signaling in tomato plants. **Frontiers in Sustainable Food Systems**, 5, p. 657401, 2021.

RIBEIRO, R. V.; MACHADO, E. C.; HABERMANN, G.; SANTOS, M. G. *et al.* Seasonal effects on the relationship between photosynthesis and leaf carbohydrates in orange trees. **Functional Plant Biology**, 39, n. 6, p. 471-480, 2012.

RICHTER, A. S.; PÉREZ-RUIZ, J. M.; CEJUDO, F. J.; GRIMM, B. Redox-control of chlorophyll biosynthesis mainly depends on thioredoxins. **FEBS letters**, 592, n. 18, p. 3111-3115, 2018.

RICHTER, A. S.; PETER, E.; ROTHBART, M.; SCHLICKE, H. *et al.* Posttranslational influence of NADPH-dependent thioredoxin reductase C on enzymes in tetrapyrrole synthesis. **Plant physiology**, 162, n. 1, p. 63-73, 2013.

RINALDUCCI, S.; MURGIANO, L.; ZOLLA, L. Redox proteomics: basic principles and future perspectives for the detection of protein oxidation in plants. **Journal of Experimental Botany**, 59, n. 14, p. 3781-3801, 2008.

RIVERO, R. M.; MITTLER, R.; BLUMWALD, E.; ZANDALINAS, S. I. Developing climate-resilient crops: improving plant tolerance to stress combination. **The Plant Journal**, 109, n. 2, p. 373-389, 2022.

SAITO, K.; YONEKURA-SAKAKIBARA, K.; NAKABAYASHI, R.; HIGASHI, Y. *et al.* The flavonoid biosynthetic pathway in Arabidopsis: structural and genetic diversity. **Plant Physiology and Biochemistry**, 72, p. 21-34, 2013.

SCHWENDER, J.; OHLROGGE, J.; SHACHAR-HILL, Y. Understanding flux in plant metabolic networks. **Current opinion in plant biology**, 7, n. 3, p. 309-317, 2004.

SERRATO, A. J.; PÉREZ-RUIZ, J. M.; SPÍNOLA, M. C.; CEJUDO, F. J. A novel NADPH thioredoxin reductase, localized in the chloroplast, which deficiency causes hypersensitivity to abiotic stress in Arabidopsis thaliana. **Journal of Biological Chemistry**, 279, n. 42, p. 43821-43827, 2004.

SHABBIR, R.; SINGHAL, R. K.; MISHRA, U. N.; CHAUHAN, J. *et al.* Combined abiotic stresses: challenges and potential for crop improvement. **Agronomy**, 12, n. 11, p. 2795, 2022.

SHIMAZAKI, K.; IINO, M.; ZEIGER, E. Blue light-dependent proton extrusion by guard-cell protoplasts of Vicia faba. **Nature**, 319, n. 6051, p. 324-326, 1986.

SILVA, A. J. d.; MAGALHÃES FILHO, J. R.; SALES, C. R. G.; PIRES, R. C. d. M. *et al.* Source-sink relationships in two soybean cultivars with indeterminate growth under water deficit. **Bragantia**, 77, p. 23-35, 2018.

SIN'KEVICH, M.; SELIVANOV, A.; ANTIPINA, O.; KROPOCHEVA, E. *et al.* Activities of antioxidant enzymes of Arabidopsis thaliana plants during cold hardening to hypothermia. **Russian Journal of Plant Physiology**, 63, p. 749-753, 2016.

SMITH, E. N.; SCHWARZLÄNDER, M.; RATCLIFFE, R. G.; KRUGER, N. J. Shining a light on NAD-and NADP-based metabolism in plants. **Trends in Plant Science**, 26, n. 10, p. 1072-1086, 2021.

SOUZA, P. V.; HOU, L. y.; SUN, H.; POEKER, L. *et al.* Plant NADPH-dependent thioredoxin reductases are crucial for the metabolism of sink leaves and plant acclimation to elevated CO2. **Plant, Cell & Environment**, 2023.

SOUZA, P. V.; LIMA-MELO, Y.; CARVALHO, F. E.; REICHHELD, J.-P. *et al.* Function and compensatory mechanisms among the components of the chloroplastic redox network. **Critical Reviews in Plant Sciences**, 38, n. 1, p. 1-28, 2019.

SPÍNOLA, M. C.; PÉREZ-RUIZ, J. M.; PULIDO, P.; KIRCHSTEIGER, K. *et al.* NTRC new ways of using NADPH in the chloroplast. **Physiologia Plantarum**, 133, n. 3, p. 516-524, 2008.

STENBAEK, A.; HANSSON, A.; WULFF, R. P.; HANSSON, M. *et al.* NADPH-dependent thioredoxin reductase and 2-Cys peroxiredoxins are needed for the protection of Mg–protoporphyrin monomethyl ester cyclase. **FEBS letters**, 582, n. 18, p. 2773-2778, 2008.

SWEETLOVE, L. J.; FERNIE, A. R. Regulation of metabolic networks: understanding metabolic complexity in the systems biology era. **New Phytologist**, 168, n. 1, p. 9-24, 2005.

SWEETLOVE, L. J.; FERNIE, A. R. The spatial organization of metabolism within the plant cell. **Annual Review of Plant Biology**, 64, p. 723-746, 2013.

SWEETLOVE, L. J.; RATCLIFFE, R. G. Flux-balance modeling of plant metabolism. **Frontiers in plant science**, 2, p. 38, 2011.

TA, T.; JOY, K. Metabolism of some amino acids in relation to the photorespiratory nitrogen cycle of pea leaves. **Planta**, 169, p. 117-122, 1986.

TAIZ, L.; ALKON, D.; DRAGUHN, A.; MURPHY, A. *et al.* Plants neither possess nor require consciousness. **Trends in plant science**, 24, n. 8, p. 677-687, 2019.

TEH, J. T.; LEITZ, V.; HOLZER, V. J.; NEUSIUS, D. *et al.* NTRC regulates CP12 to activate Calvin–Benson cycle during cold acclimation. **Proceedings of the National Academy of Sciences**, 120, n. 33, p. e2306338120, 2023.

THIEME, C. J.; ROJAS-TRIANA, M.; STECYK, E.; SCHUDOMA, C. *et al.* Endogenous Arabidopsis messenger RNAs transported to distant tissues. **Nature Plants**, 1, n. 4, p. 1-9, 2015.

THORMAEHLEN, I.; RUBER, J.; VON ROEPENACK-LAHAYE, E.; EHRLICH, S. M. *et al.* Inactivation of thioredoxin f1 leads to decreased light activation of ADP-glucose pyrophosphorylase and altered diurnal starch turnover in leaves of Arabidopsis plants. **Plant, cell & environment**, 36, n. 1, p. 16-29, 2013.

THORMÄHLEN, I.; MEITZEL, T.; GROYSMAN, J.; ÖCHSNER, A. B. *et al.* Thioredoxin f 1 and NADPH-dependent thioredoxin reductase C have overlapping functions in regulating photosynthetic metabolism and plant growth in response to varying light conditions. **Plant physiology**, 169, n. 3, p. 1766-1786, 2015.

THORMÄHLEN, I.; ZUPOK, A.; RESCHER, J.; LEGER, J. *et al.* Thioredoxins play a crucial role in dynamic acclimation of photosynthesis in fluctuating light. **Molecular Plant**, 10, n. 1, p. 168-182, 2017.

TIMM, S.; FLORIAN, A.; ARRIVAULT, S.; STITT, M. *et al.* Glycine decarboxylase controls photosynthesis and plant growth. **FEBS letters**, 586, n. 20, p. 3692-3697, 2012.

TRETHEWEY, R. N.; RIESMEIER, J. W.; WILLMITZER, L.; STITT, M. *et al.* Tuber-specific expression of a yeast invertase and a bacterial glucokinase in potato leads to an activation of sucrose phosphate synthase and the creation of a sucrose futile cycle. **Planta**, 208, p. 227-238, 1999.

TROTTER, E. W.; GRANT, C. M. Overlapping roles of the cytoplasmic and mitochondrial redox regulatory systems in the yeast Saccharomyces cerevisiae. **Eukaryotic cell**, 4, n. 2, p. 392-400, 2005.

TSIONSKY, M.; CARDON, Z. G.; BARD, A. J.; JACKSON, R. B. Photosynthetic electron transport in single guard cells as measured by scanning electrochemical microscopy. **Plant Physiology**, 113, n. 3, p. 895-901, 1997.

TSUGAWA, H.; NAKABAYASHI, R.; MORI, T.; YAMADA, Y. *et al.* A cheminformatics approach to characterize metabolomes in stable-isotope-labeled organisms. **Nature methods**, 16, n. 4, p. 295-298, 2019.

VAVASSEUR, A.; RAGHAVENDRA, A. S. Guard cell metabolism and CO2 sensing. **New Phytologist**, 165, n. 3, p. 665-682, 2005.

VERPOORTE, R.; VAN DER HEIJDEN, R.; MEMELINK, J. Engineering the plant cell factory for secondary metabolite production. **Transgenic research**, 9, p. 323-343, 2000.

WENG, J. K. The evolutionary paths towards complexity: a metabolic perspective. **New Phytologist**, 201, n. 4, p. 1141-1149, 2014.

WILLMER, C.; FRICKER, M. **Stomata**. Springer Science & Business Media, 1996. 0412574306.

WONG, J. H.; BALMER, Y.; CAI, N.; TANAKA, C. K. *et al.* Unraveling thioredoxin-linked metabolic processes of cereal starchy endosperm using proteomics. **FEBS letters**, 547, n. 1-3, p. 151-156, 2003.

XIE, D.-L.; ZHENG, X.-L.; ZHOU, C.-Y.; KANWAR, M. K. *et al.* Functions of redox signaling in pollen development and stress response. **Antioxidants**, 11, n. 2, p. 287, 2022.

YERUSHALMI, S.; YAKIR, E.; GREEN, R. M. Circadian clocks and adaptation in Arabidopsis. **Molecular ecology**, 20, n. 6, p. 1155-1165, 2011.

YOSHIDA, K.; HISABORI, T. Two distinct redox cascades cooperatively regulate chloroplast functions and sustain plant viability. **Proceedings of the National Academy of Sciences**, 113, n. 27, p. E3967-E3976, 2016.

ZANDALINAS, S. I.; FICHMAN, Y.; DEVIREDDY, A. R.; SENGUPTA, S. *et al.* Systemic signaling during abiotic stress combination in plants. **Proceedings of the National Academy of Sciences**, 117, n. 24, p. 13810-13820, 2020.

ZLUHAN-MARTÍNEZ, E.; LÓPEZ-RUÍZ, B. A.; GARCÍA-GÓMEZ, M. L.; GARCÍA-PONCE, B. *et al.* Integrative roles of phytohormones on cell proliferation, elongation and differentiation in the Arabidopsis thaliana primary root. **Frontiers in Plant Science**, 12, p. 659155, 2021.